PNNL-24377, Rev. 0

Pacific Northwest NATIONAL LABORATORY

Proudly Operated by Battelle Since 1965

Component-Level Prognostics Health Management Framework for Passive Components

Advanced Reactor Technology Milestone: M2AT-15PN2301043

June 2015

P Ramuhalli
S Roy
EH Hirt
M Prowant
SG Pitman
JC Tucker
G Dib
AF Pardini

U.S. DEPARTMENT OF ENERGY

Prepared for the U.S. Department of Energy
under Contract DE-AC05-76RL01830

PACIFIC NORTHWEST NATIONAL LABORATORY
operated by
BATTELLE
for the
UNITED STATES DEPARTMENT OF ENERGY
under Contract DE-AC05-76RL01830

Printed in the United States of America

**Available to DOE and DOE contractors from the
Office of Scientific and Technical Information,
P.O. Box 62, Oak Ridge, TN 37831-0062;
ph: (865) 576-8401
fax: (865) 576-5728
email: reports@adonis.osti.gov**

**Available to the public from the National Technical Information Service,
U.S. Department of Commerce, 5285 Port Royal Rd., Springfield, VA 22161
ph: (800) 553-6847
fax: (703) 605-6900
email: orders@ntis.fedworld.gov
online ordering: http://www.ntis.gov/ordering.htm**

This document was printed on recycled paper.

(9/2003)

PNNL-24377, Rev. 0

Component-Level Prognostics Health Management Framework for Passive Components

Advanced Reactor Technology Milestone: M2AT-15PN2301043

P Ramuhalli
S Roy
EH Hirt
M Prowant
SG Pitman
JC Tucker
G Dib
AF Pardini

June 2015

Prepared for
the U.S. Department of Energy
under Contract DE-AC05-76RL01830

Pacific Northwest National Laboratory
Richland, Washington 99352

Abstract

Prognostic health management technologies are expected to play a vital role in the deployment and safe, cost-effective operation of advanced reactors by providing the technical means for lifetime management of significant passive components and reactor internals. This report describes a Bayesian methodology for the prediction of remaining life of materials and passive AR components. This approach, previously applied to predict time-to-failure of materials subjected to localized aging and degradation, is adapted for component-level prognostics. The Bayesian framework for component-level prognostics incorporates the ability to fuse information from multiple sources, including information on localized degradation and component-level condition indicators. The ability to switch between multiple models of degradation accumulation rate and/or multiple models of measurement physics becomes important in this context, and a reversible jump Markov chain Monte Carlo methodology has been developed for this purpose. Evaluations of the Bayesian framework and the model switching and selection methodology were performed using synthetic data as well as experimental measurements on a high-temperature creep testbed. Results to date indicate that the feasibility of the proposed Bayesian framework for prognostics, though an improvement over previous methods' accuracy, will require the ability to quantify sources of uncertainties within the various models used in the prognostic framework. Ongoing efforts are focused on sensing and measurement (particularly in-situ measurements) that would be applied as inputs to the prognostics framework, with the objective of identifying measurement methods that can provide early indicators of material degradation and quantifying the reliability and sensitivity of these measurement methods.

Executive Summary

Advanced reactors (ARs) and advanced small modular reactors (AdvSMRs; based on modularization of advanced reactor concepts) may provide a longer-term alternative to traditional light-water reactor concepts, given their passive safety features and the ability to incrementally add modules over time.

Information on component condition and failure probability is considered critical to maintaining adequate safety margins and avoiding unplanned shutdowns, both of which have regulatory and economic consequences. The relatively lower level of operational experience with AR concepts (when compared with light-water-cooled reactors), and the consequent limited knowledge of physics-of-failure mechanisms in AR environments, when combined with the potential for increased degradation rates, point to the need for enhanced situational awareness with respect to critical systems.

Prognostic health management (PHM) technologies provide one approach to overcoming these challenges. PHM is a proactive philosophy where operational decisions, maintenance, and repairs to systems, structures, and components are performed prior to failure based on diagnostic input on component condition and models that predict when failure is likely to occur given the present condition of the component. Diagnostics and prognostics provide the technical means for enhancing affordability and safe operation of ARs over their lifetime by enabling lifetime management of significant passive components and reactor internals.

The use of PHM technology is anticipated to be of particular importance in the management of degradation in passive components. A significant component of operations and maintenance (O&M) costs is associated with the management and mitigation of degradation of passive components because of their increased safety-significance in AR concepts (which increasingly rely on passive safety mechanisms), and the need to provide longer lead-times for maintenance planning as passive components constitute large capital expenditures. In particular, degradation (such as cracking, creep, or creep-fatigue damage) in passive components, if not addressed in a timely fashion, is likely to result in unplanned plant shutdowns. Traditional approaches to detecting and managing degradation such as periodic in-service nondestructive inspections are likely to have limited applicability to ARs, given the expectation of longer operating periods and potential difficulties with inspection access to critical components because of compact designs and submersion of primary-circuit components in pool-type designs.

To predict failure, PHM systems require some type of input (data) about the state of the component(s) of interest. These inputs could be in the form of information on stressors to which the system or component is exposed, or information on the condition of a specific system or component. Consequently, measurements and diagnostics, in addition to prognostics, are key elements to a PHM system.

Given the potential need to provide PHM for several systems within the hierarchy of an AR design, a hierarchy of PHM systems is being explored, with information at one or more levels of this hierarchy being supplied to a supervisory plant control system for optimizing plant operations with respect to O&M requirements. This hierarchy corresponds to PHM systems operating on localized measurements, PHM systems operating on component-wide measurements, and global PHM systems that integrate diagnostics and prognostics information across multiple components. For example, component-level PHM systems may be applied to assess the condition of components or sub-systems, such as the intermediate heat exchanger. The use of multiple PHM modules provides increased opportunity to monitor the health of critical sub-systems within the plant. However, it increases the amount of information that must be aggregated prior to use with risk monitors and in plant supervisory control actions. Figure ES.1 shows a possible scenario for the aggregation, where each PHM module is associated with a risk monitor resulting in predictive estimates of the subsystem health and the associated risk metrics. This information is used to augment data for supervisory control and plant-wide coordination of multiple modules by providing the incremental risk incurred from aging and demands placed on components that support mission requirements.

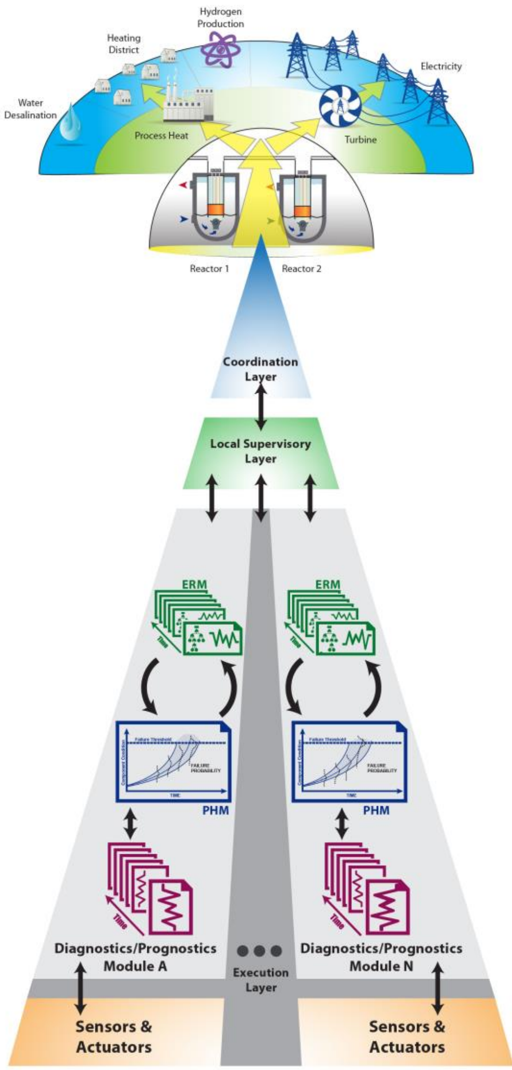

Figure ES.1. Schematic Showing the Integration of PHM Systems with Enhanced Risk Monitors, and Their Location within the Hierarchy of Supervisory Control Algorithms for ARs

This report describes research results to date in support of the integration and demonstration of diagnostics technologies for prototypical AR passive components (to establish condition indices for monitoring) with model-based prognostics methods. Achieving this objective will necessitate addressing several of the research gaps and technical needs described in previous technical reports in this series.

The focus of the PHM methodology and algorithm development described in this report is at the component scale. Multiple localized measurements of material condition (using advanced nondestructive measurement methods), along with available measurements of the stressor environment are expected to be used to enhance the performance of localized diagnostics and prognostics of passive AR components and systems.

A Bayesian methodology for prognostics is described for the prediction of remaining life of materials and components. Bayesian methods for prognostics have many advantages, including the ability to update the prognostic result as new information (for instance, measurement data) becomes available, and the ability to inherently provide confidence bounds on the prognostic result. While this approach has been previously applied to predict time-to-failure of materials subjected to aging and degradation, a similar approach may be applied to component-level prognostics. For component-level prognostics, appropriate models of component degradation growth and measurement physics will be needed, and these models are likely to describe performance degradation.

The Bayesian framework for component-level prognostics incorporates the ability to fuse information from multiple sources, including information on localized degradation, and component-level condition indicators. The ability to switch between multiple Degradation Rate models and/or multiple Measurement Physics models becomes important in this context, and a reversible jump Markov chain Monte Carlo (RJMCMC) approach has been developed for this purpose.

Evaluations of the Bayesian framework and the RJMCMC model switching/model selection were done using synthetic data as well as experimental measurements on a high-temperature creep testbed. Results to date using this data indicate that the proposed Bayesian framework can be used to identify distinct stages of creep progression.

Ongoing efforts are beginning to focus the research on sensing and measurements (particularly in-situ measurements) that would be applied as inputs to the prognostics framework. This renewed focus on measurements and sensing is with a view to identifying measurement approaches that are most likely to provide indicators of materials and component degradation that are applicable within the prognostics framework. The research will also address the need for quantitative nondestructive evaluation (NDE) analysis tools by examining the sensitivity of selected advanced NDE methods to relevant degradation mechanisms, and leverage other recent results in this area. Degradation condition indices (along with any associated uncertainties) calculated from these measurements will be integrated with models of material or component failure to enable estimation of remaining life of passive components with detected degradation. Gaps with respect to deployment of sensors and instrumentation, and integration with plant control algorithms, exist and will be addressed as this research progresses. The outcomes of these next steps in this research will enable the development of methods for supporting emerging needs within other Technical Areas in the Advanced Reactor Technologies (ART) program, particularly the Materials and Fuels areas.

The research described in this report, as well as in the previous reports in this series, provides some of the essential instrumentation and control (I&C) technologies that are vital to safe, cost-effective operation of nuclear power plants. Innovative use of advanced technology can have a significant impact on achieving safe and efficient operability, optimizing plant staffing, and controlling O&M costs. While the cited areas of impact for these technologies are beneficial for all ARs, the latter two outcomes are essential for the economic viability of ARs. The research, development, and demonstration described in this report (and related reports) resolves gaps in technology capabilities, and enables these advanced technologies to be matured to the appropriate readiness level in a timely manner while ensuring the associated capabilities can be incorporated into reactor designs at an appropriate early stage.

.

Acknowledgments

The work described in this report was sponsored by the Advanced Reactor Technologies research program of the U.S. Department of Energy's Office of Nuclear Energy. The authors gratefully acknowledge Ms. Kay Hass for her invaluable assistance in the technical editing and formatting of this report. The authors also acknowledge Dr. Ryan Meyer's contributions to the experimental design, Mr. Eric Berglin and Dr. David Wootan's contributions to summarizing advanced reactor concepts, and Mr. Royce Mathews and Mr. Trenton Hartman for their help in the measurements. The authors also thank the technical peer reviewers for their feedback and assistance in improving this report.

Acronyms

AdvSMR	Advanced small modular reactor
AR	Advanced reactors
ART	Advanced Rector Technologies
ASME	American Society of Mechanal Engineers
CDF	Core damage frequency
CSNI	Committee on the Safety of Nuclear Installations
Code	ASME Boiler and Pressure Vessel Code
GCR	Gas-cooled reactors
HTGR	High-temperature gas reactor(s)
I&C	Instrumentation and control
IAEA	International Atomic Energy Agency
ISI	In-service inspection
LWR	Light-water-cooled reactor
MCMC	Markov chain Monte Carlo
NDE	Nondestructive evaluation/examination
NEA	Nuclear Energy Agency
NLU	Non-linear ultrasonics
O&M	Operations and maintenance
OECD	Organization for Economic Co-Operations and Development
PDF	Probability density function
PHM	Prognostic health management
POF	Probability of failure
PRA	Probabilistic risk assessment
R&D	Research and development
RI-ISI	Risk-informed in-service inspection
RISMET	Risk-Informed In-Service Inspection Methodologies
RJMCMC	Reversible jump Markov chain Monte Carlo
RUL	Remaining useful life
SCC	Stress corrosion cracking
SFR	Sodium-cooled fast reactor
SG	Steam generator
SIR	Sampling important resampling
SSC	Systems, structures, and components
VHTR	Very-high-temperature gas reactor

Contents

Figures

Tables

1.0 Introduction

Prognostic health management (PHM) is a proactive philosophy where operational decisions, maintenance, and repairs to systems, structures, and components (SSC) are performed prior to failure based on diagnostic input on component condition and models that predict when failure is likely to occur given the present condition of the component.

PHM technologies are expected to play a vital role in the deployment and safe, cost-effective operation of advanced reactors (ARs). Diagnostics and prognostics provide the technical means for enhancing affordability and safe operation of ARs over their lifetime by enabling lifetime management of significant passive components and reactor internals.

A key characteristic of AR concepts, which include sodium-cooled fast reactors (SFRs) and high-temperature gas reactors (HTGRs) (Abram and Ion 2008), are the harsh environments within the primary and intermediate loops, and include high temperatures (in excess of 500°C), potential for fast spectrum neutrons, and corrosive coolant chemistry. These environments in proposed advanced reactor concepts increase the possibility of degradation of safety-critical components and therefore pose a particular challenge for deployment and extended operation of these concepts. The relatively lower level of operational experience with AR concepts (when compared with LWRs), and the consequent limited knowledge of physics-of-failure mechanisms of materials and components in AR environments, when combined with the potential for increased degradation rates, point to the need for enhanced situational awareness with respect to critical systems. Information on component condition and failure probability is considered critical to maintaining adequate safety margins and avoiding unplanned shutdowns, both of which have regulatory and economic consequences.

Under these conditions, PHM is a key enabling technology for providing dependable, high-fidelity assessments of component conditions and incipient failure detection in AR SSCs. Periodic in-service inspection (ISI) technologies already exist and are used in operating nuclear power plants to provide an assessment of passive component condition, including whether significant cracking exists that could compromise structural integrity. However, the applicability of existing technologies may be limited in ARs, because of their compact design, restricted access to key in-vessel and in-containment components, and extended periods between inspection and maintenance opportunities. PHM systems, with their emphasis on increased in-situ structural health monitoring and prognostics to assess remaining service life (also referred to as remaining useful life or RUL) provide a mechanism to address the limitations of current ISI approaches for use with ARs. PHM technologies provide improved awareness of system condition, and when integrated during design of AR, can provide the tools necessary for quantifying the operational envelope for safe economic O&M of the AR, and in coordination with supervisory control algorithms, enable these reactors to stay within the operational envelope while maintaining adequate safety margins.

ARs are expected to benefit by the use of PHM systems through:

- Providing early warning of potential degradation in inaccessible passive components leading to failure in AR environments. Such early warning can inform operational planning and maintenance scheduling decisions during infrequent refueling outages;
- Reducing risks by providing enhanced situational awareness of plant equipment and component conditions and margins to failure, particularly in conditions where knowledge of physics-of-failure in the AR environment is limited;

- Enhanced affordability and safe operation during their lifetime by enabling lifetime management of significant passive components and reactor internals (especially for critical passive safety components) in harsh environments (high-temperature, fast flux, and corrosive coolant chemistry);
- Relieving the cost and labor burden of currently required periodic ISI during refueling outages, especially for components in hard-to-access areas such as those in-vessel/in-containment; and
- Supporting a science-based justification for extended plant lifetime by ensuring reliable component operation.

To predict failure, PHM systems require some type of input (data) about the state of the component(s) of interest. These inputs could be in the form of information on stressors to which the system or component is exposed, or information on the condition of a specific system or component. Consequently, measurements and diagnostics, in addition to prognostics, are key elements to a PHM system.

This report documents research towards developing and deploying prototypical PHM systems that, if integrated with supervisory plant control systems and enhanced risk monitors, can provide the capability requirements listed and meet the goals of controlling O&M costs.

1.1 Research Objectives

This report describes research results to date in support of the integration and demonstration of diagnostics technologies for prototypical AR passive components (to establish condition indices for monitoring) with model-based prognostics methods. Achieving this objective will necessitate addressing several of the research gaps and technical needs described in Meyer et al. (2013a).

Given the potential need to provide PHM for several systems within the hierarchy of an AR design (Meyer et al. 2013a; Meyer et al. 2013d), a hierarchy of PHM systems was proposed (Meyer et al. 2013c), with information at one or more levels of this hierarchy being supplied to a supervisory plant control system for optimizing plant operations with respect to O&M requirements. This hierarchy corresponds to PHM systems operating on localized measurements; PHM systems operating on component-wide measurements, and global PHM systems that integrate diagnostics and prognostics information across multiple components.

Previous research in this project performed a gap assessment, and focused on the development of a framework for PHM at the localized scale. Meyer et al. (2013a) discussed a number of technical gaps that limit the applicability of current PHM systems in ARs. The major limiting factors identified were: (i) advanced sensor technology for operating under harsh environments; (ii) accurate models for material degradation accumulation and subsequent progression; (iii) prognostics under different sources of uncertainty such as measurements noise, temperature variations, fluctuations in pressure and loading profiles, and model uncertainties; (iv) sensor data fusion; and (v) verification and validation of the PHM systems. A number of technical requirements for PHM systems in ARs were identified based on these gaps, and technologies were developed to address several of these requirements. These technologies are documented in several previous reports in this series (Ramuhalli et al. 2014b; Meyer et al. 2013a; Meyer et al. 2013d).

The focus of the PHM methodology and algorithm development described in this report is at the component scale. Multiple localized measurements of material condition (using advanced nondestructive measurement methods) along with available measurements of the stressor environment are expected to be used to enhance the performance of localized diagnostics and prognostics of passive AR components and systems.

The research described in this report, as well as in the previous reports in this series, provides some of the essential I&C technologies that are vital to safe, cost-effective operation of nuclear power plants. Innovative use of advanced technology can have a significant impact on achieving safe and efficient operability, optimizing plant staffing, and controlling O&M costs. While the cited areas of impact for these technologies are beneficial for all ARs, the latter two outcomes are essential for the economic viability of AdvSMRs. The research, development, and demonstration described in this report (and related reports) resolves gaps in technology capabilities, and enables these advanced technologies to be matured to the appropriate readiness level in a timely manner while ensuring the associated capabilities can be incorporated into reactor designs at an appropriate early stage.

1.2 Organization of Report

This technical report is organized as follows. Section 2 includes background information on AR concepts and characteristics, PHM for ARs, and requirements and assumptions for PHM methodology (framework) development for ARs. Section 3 describes the benefits of prognostics for ARs. Section 4 describes the comploent-level PHM framework for passive components. Section 5 provides an assessment of the PHM framework for passive components. Section 6 summarizes the status of research to date. Finally, Section 7 briefly outlines planned research and opportunities going forward.

2.0 Background

ARs generally encompass all non–LWR concepts, and are being considered as a longer-term option for meeting electrical generation and process heat needs in the United States (Abram and Ion 2008). Among the concepts being considered are SFRs and HTGRs, both of which have some operational history in the United States and elsewhere. A detailed description of these concepts is available in previous reports in this series (Meyer et al. 2013a). Additional details of AR concepts as they apply to AdvSMRs and likely O&M approaches are provided in the previous reports in this series associated with AdvSMR prognostics and ERM research (Coble et al. 2013b; Meyer et al. 2013a; Ramuhalli et al. 2013; Ramuhalli et al. 2014a).

Degradation and failure of materials that make up passive components in ARs are likely to be key factors impacting safety and economics of ARs. The challenges associated with materials operating under conditions likely to be encountered in SFR and VHTR (very-high-temperature gas reactor) reactors (Appendix A) include degradation mechanisms not encountered in LWRs, and potentially unexpected materials performance under the expected complex loading conditions in ARs. The limited knowledge of physics-of-failure mechanisms of materials used in structural components in AR environments (high temperatures, fast neutron fluxes, potentially corrosive chemistry due to the coolant), and longer exposure times due to extended periods between maintenance and refueling outages are likely to challenge available inspection and maintenance technologies.

Material damage accumulation in structural components of ARs can be monitored by employing a combination of several nondestructive evaluation (NDE) techniques (Bond et al. 2008) such as eddy current inspection, ultrasound, acoustic emission, magnetic Barkhausen noise measurements, etc., with the selection of specific techniques dependent on the material, degradation mechanism, and location within the reactor system. Meyer et al. (2013a) discussed a number of technical gaps that limit the applicability of current inspection and predictive maintenance approaches in AR. Among the major limiting factors identified were:

- advanced sensor technology for operating under harsh environments;
- accurate models for material degradation accumulation and subsequent progression;
- predictive maintenance under different sources of uncertainty such as measurements noise, temperature variations, fluctuations in pressure and loading profiles, and model uncertainties; and
- sensor data fusion to assess material degradation state.

2.1 Prognostic Health Management for Advanced Reactors

PHM is a proactive maintenance philosophy where maintenance or repairs to systems or components are performed prior to failure based on models that estimate (predict) when failure is likely to occur. To estimate time-to-failure, PHM systems require some type of input (measurement data) about the state of the component(s) of interest. These inputs could be in the form of information on stressors to which the system or component is exposed, or information on the condition of a specific system or component, or both. Keys to effective PHM are the ability to detect incipient failure through increased monitoring, application of advanced in-situ diagnostics tools for degradation severity assessment, and the reliable estimation of remaining service life (also often referred to as RUL) (see Meyer et al. 2013a).

All PHM systems have several elements including: (1) sensors for performing measurements of both process parameters as well as indicators of degradation; (2) diagnostic algorithms that use the sensor measurements to estimate the condition of the component; (3) prognostics algorithms to calculate the RUL of the component with degradation; and (4) interfaces to decision and control systems that are used to make O&M decisions.

Given the potential need to provide PHM for several systems within the hierarchy of an AR design (Meyer et al. 2013a; Meyer et al. 2013d), a hierarchy of PHM systems is being explored (Meyer et al. 2013c), with information at one or more levels of this hierarchy being supplied to a supervisory plant control system for optimizing plant operations with respect to O&M requirements. This hierarchy corresponds to PHM systems operating on localized measurements, PHM systems operating on component-wide measurements, and global PHM systems that integrate diagnostics and prognostics information across multiple components.

Research conducted to date on PHM systems in ARs and AdvSMRs was previously documented in a series of technical reports (Ramuhalli et al. 2014b; Meyer et al. 2013a; Meyer et al. 2013d). Meyer et al. (2013a) discussed a number of technical gaps that limit the applicability of current PHM systems in ARs. The major limiting factors identified were: (i) advanced sensor technology for operating under harsh environments; (ii) accurate models for material degradation accumulation and subsequent progression; (iii) prognostics under different sources of uncertainty such as measurements noise, temperature variations, fluctuations in pressure and loading profiles, and model uncertainties; (iv) sensor data fusion; and (v) verification and validation of the PHM systems. A number of technical requirements for PHM systems in ARs were identified based on these gaps, and technologies were developed to address several of these requirements. These technologies are documented in other reports in this series (Ramuhalli et al. 2014b; Meyer et al. 2013a; Meyer et al. 2013d).

2.1.1 Prototypic Prognostic Methodology

The overall approach to PHM that is taken in this research is a system-of-systems approach. As shown in Figure 2.1, individual systems are expected to be needed to address the prognostics requirements for each component or subsystem; higher levels in the hierarchy are used to mediate the information flow and integration from these lower-level PHM systems.

The specific details of these interfaces are not yet determined. In this research, the focus is on further developing the framework for the lower-level PHM systems. This framework, and a potential approach to performing prognostics, is described in Ramuhalli et al. (2014b). Figure 2.1 illustrates a system-of-systems approach, with individual PHM systems monitoring the different SSCs, with additional systems in the hierarchy integrating the output from the individual PHM systems and providing the necessary interfaces to plant supervisory control systems, operational risk monitors, and O&M decision making.

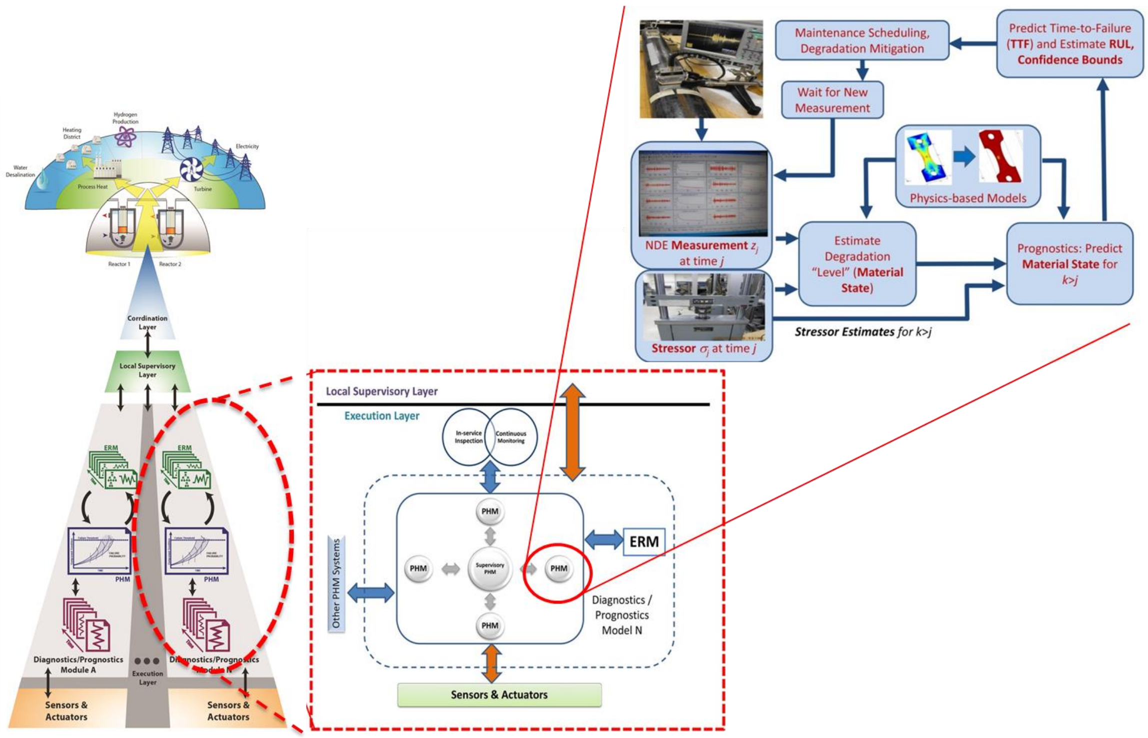

Figure 2.1. Proposed Hierarchy of PHM Systems

The representative drill-down into an individual PHM system shown within Figure 2.1 illustrates the process flow from measurement to diagnostics, prognostics, and decision making. The hierarchy within this system-of-systems approach may be developed in many ways. The approach taken in this research is to largely map the PHM system hierarchy to the measurement location hierarchy, resulting in: PHM systems operating on localized measurements, PHM systems operating on component-wide measurements, and global PHM systems that integrate diagnostics and prognostics information across multiple components.

2.1.2 Bayesian PHM Systems – Overview

An initial methodology for estimating RUL from spatially localized NDE measurements was previously described (Meyer et al. 2013b; Ramuhalli et al. 2014b; Roy et al. 2015). This methodology for PHM uses Bayesian approaches and multiple filtering algorithms to diagnose and predict the RUL of materials. Applying this type of "tracking" filter to the problem of predicting degradation accumulation in materials from NDE measurements requires two models—one (Degradation Rate model) that captures the progressive accumulation of degradation in the material from one or more stressors, and the second (Measurement model) that relates the level of material degradation to one or more measurements. This approach provides a relatively simple Bayesian mechanism for updating the predictions when additional measurements are available. Modifications to these algorithms to account for model selection and uncertainty quantification are described in detail in this present document in Section 4.0.

Specifically, we developed a particle filtering algorithm integrated with a RJMCMC method for this purpose.

Figure 2.2 shows the schematic of this Bayesian prognostic framework using the automatic RJMCMC method (Green 1995; Hastie and Green 2012) and particle filtering algorithm (Ristic et al. 2004) to enable model selection while accounting for uncertainty from various sources. The approach requires a predefined set of models that capture the different stages of degradation growth. For the specific example of creep damage, we begin with a set of damage progression models that capture the three distinctive stages of creep growth; namely, primary stage, secondary stage, and tertiary stage. The objective is then to infer the present state of material degradation from the measured sensor response, select an appropriate damage growth model as well as the parameters of the model, and predict the RUL of the component.

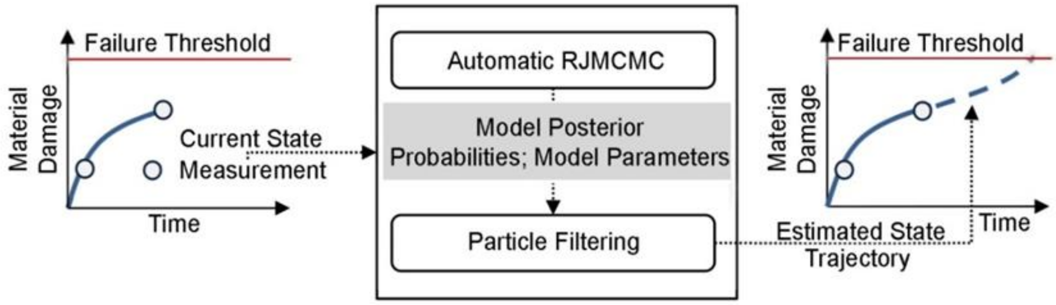

Figure 2.2. Automated Model Selection Methodology During Prognostics

2.1.3 Risk-informed In-service Inspection and Monitoring

Risk-informed ISI (RI-ISI), as used by the U.S. Nuclear Regulatory Commission, implies that decisions on component selection for periodic inspections are based on risk insights along with deterministic and licensing basis information (Phillips 2005). The concept of RI-ISI has been successfully implemented in several countries, as reported in the Committee on the Safety of Nuclear Installations (CSNI) state-of-the-art report (OECD/NEA 2005). Current practice for in-service degradation detection in passive components in the nuclear industry is generally geared towards the detection of macroscopic degradation (such as cracking or material loss). Given the likely impracticality of inspecting every component in a power plant, recommended practice in the nuclear industry is to follow RI-ISI (Atkinson and Kytömaa 1992) to identify risk-significant components and prioritize inspection activities.

The Benchmark Study on Risk-Informed In-Service Inspection Methodologies (RISMET) project (OECD/NEA 2010) compared qualitative and quantitative RI-ISI with traditional in-service inspection programs, and augmented programs developed in response to a particular issue (e.g., break exclusion regions, flow assisted corrosion, localized corrosion). This comparative study was aimed at identifying the impact of such methodologies on reactor safety and how the main differences influence the final result (i.e., the definition of the risk-informed inspection program). Included was the recognition that the next challenge facing the industry is the development of RI-ISI programs for new reactor designs, that could include AR designs. Conclusions of the RISMET project supported further RI-ISI research efforts in the field of risk-informed selection of components for inspection. Among the questions reported for future RI-ISI research and development (R&D) efforts to provide answers were the following relevant to this PHM effort:

- Consistent criteria are needed to determine the potential for a certain damage mechanism.
- Better information regarding the efficacy of various NDE methods.
- The use of probabilistic methods to determine inspection intervals.
- Methods enabling reliable probabilistic analyses for some damage mechanisms.

Along these lines, Unwin et al. propose a semi-Markov model for integrating information on passive component degradation with conventional risk models (Unwin et al. 2012; Unwin et al. 2011). This approach provides a cost-effective solution to integrating degradation-growth information (such as crack growth rates) with risk calculation. This approach is now being incorporated into newer models for risk assessment in LWRs (Guler et al. 2014).

In Ramuhalli et al. (2014b) it was noted that for ARs an assessment of risk-significance may not be the sole deciding factor for deployment of PHM systems as degradation growth may occur fastest in locations that are not considered to be high-risk. Further, taking a plant offline for unplanned maintenance or repairs (even on non-risk-significant components) will impact the economics of operation. Thus, achieving reliability and integrity goals for passive components will require careful choices in design, fabrication, operation, and maintenance, with PHM systems forming the final level of defense-in-depth for selected components.

2.2 Role of PHM in Advanced Reactor Control and Coordination

PHM systems (Figure 2.3) can potentially contribute to the affordability of ARs by providing greater awareness of in-vessel and in-containment component and system conditions. In turn, such increased awareness can help inform O&M decisions to target maintenance activities that reduce risks associated with safety and investment protection through a greater understanding of precise plant component conditions and margins to failure.

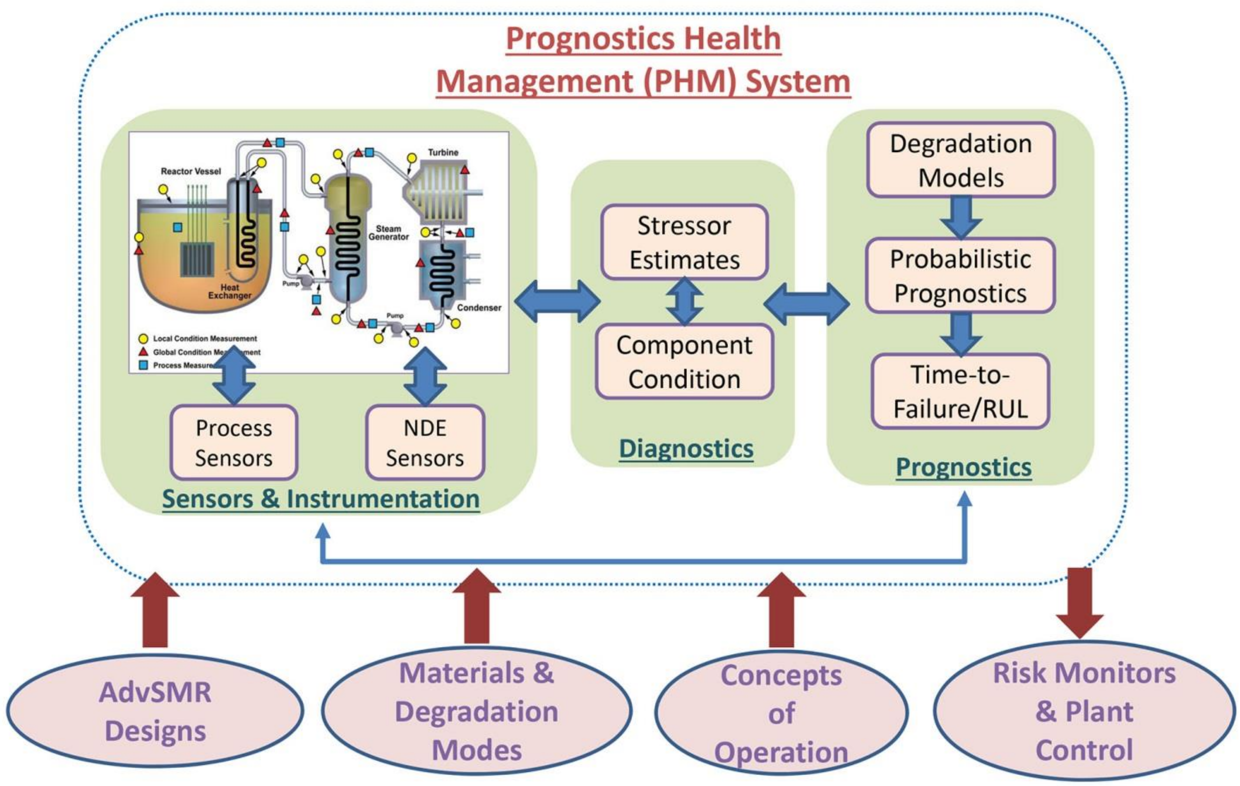

Figure 2.3. Overview of a Typical Prognostics Health Management System

Available information from AR design concepts, expected operational characteristics, and relevant operating experience may be used to both define requirements for the various elements of the PHM system, as well as bound estimates of RUL with high confidence. Interfaces with plant supervisory control systems ensure that the information about component RUL and system conditions are utilized as a basis for planning maintenance activities. In particular, the ability to estimate remaining life provides a basis for determining whether continued safe operation (over some pre-determined interval) is possible, or whether operating conditions need to be changed to limit further degradation growth until a convenient maintenance opportunity presents itself.

The basis of the overall approach for PHM, risk monitors, and plant control technologies used in this research (Ramuhalli et al. 2014b) takes into account the PHM system hierarchy and its relationship with an AR supervisory control architecture that has resulted in the prototypic prognostic methodology that follows.

2.3 Requirements and Assumptions for PHM Methodology (Framework) Development

2.3.1 Requirements for Prototypic Prognostics Health Management Systems

Based on an assessment of the drivers for PHM in ARs (including AdvSMRs), Meyer et al. (2013a) described the initial requirements for PHM systems for passive components in ARs. These are summarized below:

- Sensors and instrumentation for condition assessment of AR passive components
- Fusion of measurement data from diverse sources, such as NDE and stressor information
- Address coupling between components or systems, and across modules
- Incorporate lifecycle prognostics
- Integrate with risk monitors for real-time risk assessment
- Interface with plant supervisory control system

2.3.2 Assumptions

Several assumptions are made in the development of the prototypic prognostic methodology for PHMs for use in ARs that use time-dependent stressor information with measurements of material or component condition:

- Information about representative materials and conditions in AR concepts, and concepts of operations for these designs, is available.
- Research is focused on detection of early stages of degradation in selected safety-critical passive components (such as heat-exchanger tubing and major structural elements such as vessel and key piping), and the assessment of the RUL of these components. Specifically, the PHM will be on inaccessible passive components key to the safe operation of AR concepts, such as liquid-SFRs or HTGRs.
- Laboratory-scale testbed for degradation assessment and prognostics for a prototypical AR (including AdvSMRs) passive component will only simulate conditions and features necessary for proof-of-principle demonstration for target degradation mechanism.

- High-temperature creep will be the focus of measurements and prognostics in this stage of the research effort as it is a damage mechanism of concern in several AR concepts. Specifically, the goal will be to examine primary and secondary stages of creep damage. The material of choice is austenitic stainless steel because of its anticipated wide use in several AR concepts.
- NDE methods that provide measurements sensitive to creep damage in austenitic stainless steel are available and may be readily applied. Localized NDE measurements of material condition, along with measurements of temperature and mechanical load, are assumed sufficient to detect creep damage and predict its progression.
- Measurements will be taken periodically (interrupted testing); such testing is assumed to not impact the progression of creep degradation in the material.
- Accelerated creep testing is assumed to result in measurements and damage accumulation that is representative of creep damage that occurs during the lifetime of components in ARs.

- Harsh-environment sensors for measurement/monitoring of safety-critical AR passive components are assumed to be available and provide measurement sensitivity similar to those obtained from sensors in a laboratory setting.

The choice of degradation mode, measurements, and prognostic models are based on a state-of-the-art summary included in requirements, research gaps, and technical needs analysis documented in Meyer et al. (2013a).

2.4 Assessment Approach: High-Temperature Creep as Prototypic Mechanism

To provide context to the description of PHM requirements and research developments, we are exploring the example of high-temperature creep degradation in passive components. Creep degradation is the plastic deformation that occurs in materials under stress at high temperatures, and is a relevant mechanism for materials damage in AR environments. Creep damage accumulation in structural components of ARs can be monitored by employing a combination of several NDE techniques (Sposito et al. 2010) such as eddy current inspection, ultrasound, acoustic emission, magnetic Barkhausen noise measurements, etc., with the selection of specific techniques dependent on the material, degradation mechanism, and location within the reactor system.

Interim research results were reported in Ramuhalli et al. (2014b) supporting the integration and demonstration of diagnostics technologies for prototypical AR passive components (to establish condition indices for monitoring) with model-based prognostics methods. These results also addressed the need for quantitative NDE analysis tools by examining the sensitivity of advanced NDE methods to relevant degradation mechanisms.

3.0 Benefits of Prognostics Technologies for Advanced Reactors

PHM systems are expected to play a vital role in the safe and economic operation of ARs by ensuring early warning of material damage accumulation in structural components. This will pave the way for condition-based maintenance activities with a positive impact on safety and operating economics of ARs.

3.1 PHM as a Tool for Advanced Reactors Design, Deployment, O&M

A primary challenge to wide deployment of ARs is the relatively lower level of operational experience with AR concepts (when compared with LWRs), and the consequent limited knowledge of physics-of-failure mechanisms in advanced reactor environments. This is especially the case with structural materials that are used in passive components (e.g., components that are internal to the reactor vessel as well as components such as heat-exchanger tubing or Class 1 piping that is external to the vessel), given the desire to increase operating temperatures, refueling intervals, and the increased dependence on passive safety systems. The resulting stresses on the materials may result in failure mechanisms that are not experienced in the current fleet.

Information on AR passive component condition and failure probability is considered critical to maintaining adequate safety margins and avoiding unplanned shutdowns (which have regulatory and economic consequences), and for providing sufficient lead-time for planning O&M activities. Technologies that provide improved awareness of system condition, when integrated during design of the AR, can provide the tools necessary for quantifying and maintaining the operational envelope for safe economic O&M.

PHM systems that use in-service nondestructive inspections and online structural condition monitoring are one such class of technologies that (Ramuhalli et al. 2014b):

- Enhance affordability and safe operation of AR over their lifetime by enabling lifetime management of significant passive components and reactor internals (especially for critical passive safety components) in harsh environments (high-temperature, fast flux, and corrosive coolant chemistry);
- Relieve the cost and labor burden of currently required periodic ISI during refueling outages, especially for components in hard-to-access areas such as those in-vessel/in-containment;
- Reduce risks by providing increased understanding of plant equipment conditions and margins to failure, particularly in conditions where knowledge of physics-of-failure is limited;
- Inform O&M decisions to target maintenance activities during infrequent refueling outages; and
- Support a science-based justification for extended plant lifetime by ensuring reliable component operation.

Ironically, PHM systems are seldom considered as a part of a component design process and are deployed only at the very later stages of its operational/service life. This often puts constraints on the optimal design of sensor configuration, affecting structural condition monitoring and diagnostics of critical plant components, and thereby reducing the overall effectiveness of a PHM system.

However, if PHM systems are designed concurrently as a part of the overall system design, then they will help optimize the performance of the entire plant. There is a wide consensus that damage initiation and rate of damage accumulation in a structural component is dependent on the initial loading conditions.

Gathering this information and making appropriate use in AR O&M requires appropriate sensors and diagnostic/prognostic systems to be integrated during the design process for ARs. The deployment of PHM systems earlier in the lifecycle of the components will also provide vital clues about degradation and performance from the very early stages of service life; this in turn will reduce the uncertainties associated with lifecycle prediction and RUL estimation.

3.2 PHM as an Enabling Tool for Research

Fundamental challenges with PHM for AR passive components include the potential for detecting and managing degradation mechanisms not common to the existing LWR fleet, and the potential for changing plant conditions as new operating regimes and diverse missions are being proposed. Degradation mechanisms in materials used in passive components are expected to be significant in the harsher operating environments in ARs and are expected to challenge NDE technologies currently used in ISI for detecting macroscopic cracking. At the same time, the introduction of modularity in some designs can introduce interconnections or dependencies between SSCs in reactor modules and generation blocks (multiple reactor modules connected to common balance-of-plant systems, such as the power-blocks proposed for the Power Reactor Innovative Small Module [PRISM] reactor). Such interconnections can impact overall degradation accumulation rates in ways that are very different from current operating nuclear power reactors, and challenge approaches to estimating RUL of these components (Meyer et al. 2013a).

Given that materials being considered for AR components need to be able to handle such requirements, a considerable amount of research is being conducted to better understand materials performance in such environments and ascertain their limits. PHM systems are expected to be valuable in this endeavor as first-of-a-kind reactors can be instrumented with these types of systems to provide the necessary data that form the basis for increasing confidence in materials performance. Such data will need to be backed up with appropriate experimental data from laboratory and other smaller-scale testbeds, so as to provide the necessary technical basis for qualification and licensing.

However, for AR components, PHM systems will also need to account for uncertainty, be able to change models of degradation growth as needed, accommodate redundancies in information, update current state and projections as new information becomes available, and be able to handle a modest amount of missing information (ambiguity) (Meyer et al. 2013b).

Note that the needs for monitoring and performance assessment of novel components planned for use in AR systems are similar and may be addressed using similar technologies.

3.3 Technologies for Augmenting Information

The need for deploying PHM systems for ARs would require advances in the following key thrust areas:

- In-situ NDE sensing techniques under harsh environments: An increased and sustained effort is currently required for near real-time, online diagnostics of passive structural components. The behavior of both the sensors and the substrate material under extreme temperature, pressure, and radiation environments needs to be investigated to interpret the sensor data and relate them with the structural changes associated with damage accumulation and growth.
- Data interpretation and fusion strategies: There is a need to understand and investigate the role of varying environmental conditions on the sensor signals to be able to accurately interpret the structural changes from the sensor data. There is also need to relate sensor measurements with the microstructural changes in the structure, known as damage precursors, before actual irreversible

damage initiates and starts accumulating inside the material. Furthermore, no single measurement technique would be sufficient to capture the onset of different damage types, which calls for fusion of information from different sensor types and locations.

- PHM as a design tool for next-generation structures: As mentioned earlier, there is a need for concurrent design of PHM systems and the structural components in order to optimize the design performance criteria for both of them. Furthermore, integration of PHM systems in the initial prototypes would give reliable and accurate estimates of the in-situ strength and material characterization. Thus, PHM systems can be used as an efficient design tool for the next-generation structures to be more economical by moving away from the traditional factor-of-safety–based designs allowing lighter, thinner walled and lower cost structures.

3.4 PHM Integration with Emerging Technologies

3.4.1 High-Temperature Sensing

As discussed earlier, in-situ NDE sensing in harsh environments will require sensors capable of tolerating high temperatures and/or high neutron flux levels. Recent developments in this area may be leveraged for a subset of NDE measurement techniques that rely on the interaction of stress waves with materials. High-temperature piezoelectric sensors that are radiation tolerant are being investigated (Daw et al. 2014; Turner et al. 1994; Daw et al. 2015; Sinding et al. 2014b; Sinding et al. 2014a) at a number of institutions. Further, techniques for field fabrication/application of these sensors are also being investigated (Sinding et al. 2014b; Sinding et al. 2014a; Veilleux et al. 2013; Kobayashi et al. 2002). These technologies are being examined within this project to determine if they can be integrated into ongoing experimental studies for degradation monitoring.

3.4.2 Enhanced Risk Monitors

ERMs incorporate real-time component condition into the calculation of plant risk [usually measured in terms of core damage frequency (CDF) or some other safety-related risk metric (Coble et al. 2013a; Ramuhalli et al. 2014a)]. In their use of real-time component condition, ERM technologies differ from conventional risk monitors (Wu and Apostolakis 1992; Kafka 2008) that use a static estimate for event probability and probability of failure (POF), typically based on historical observations and engineering judgment. More recently, time-based POF values derived from operating experience and traditional reliability analysis have been used (Vesely and Wolford 1988; Arjas and Holmberg 1995); however, these are usually not specific to the component.

Critical to the ERMs is a predictive estimate of POF of the component, which is precisely what PHM provides (Coble et al. 2012b). As a result, PHM technologies are likely to be applicable to achieving enhanced risk monitoring to obtain a realistic assessment of dynamic risk that is unit-specific and accounts for the operational history of the component (Ramuhalli et al. 2013).

3.4.3 Automated Plant Control Systems

It is likely that PHM technologies can also support higher-level I&C functions, such as plant supervisory control systems. In SMR/ICHMI/ORNL/TR-2013/03, Cetiner et al. (2012) describe the rationale for designing a supervisory control system for AdvSMR plants, based on the financial incentive to reduce staffing requirements and to enhance plant availability, and on the more complex operating regime expected for AdvSMR plants. This rationale also holds for AR plants, as supervisory control can simplify the operator’s workload in managing startup, load changes, and shut down of individual reactors within a multi-reactor power-block. Beyond operations, the supervisory control can provide for automated diagnosis of failed/failing components and automated plant response to isolate the failure, and monitor condition of equipment to allow O&M personnel to avoid overloading failing equipment and to make preparations for repair. Under these conditions, technologies for determining component condition become important, and PHM technologies play a vital role in this regard. A possible scenario for the aggregation of multiple PHM modules and ERMs was shown previously in Figure 2.1 (Ramuhalli et al. 2014a); where each PHM module is associated with a risk monitor, resulting in predictive estimates of the subsystem health and the associated risk metrics. This information is used to augment data used for supervisory control and plant-wide coordination of multiple modules by providing the incremental risk incurred because of aging components and demands placed on those components to support mission requirements.

4.0 Component-Level Prognostics Health Management Framework for Passive Components

In general, a PHM system for passive components will consist of the elements described earlier—sensors, diagnostic and prognostic algorithms, and interfaces to other elements of plant operations and control. The process of applying the various stages in the PHM system is iterative, and is illustrated in Figure 4.1.

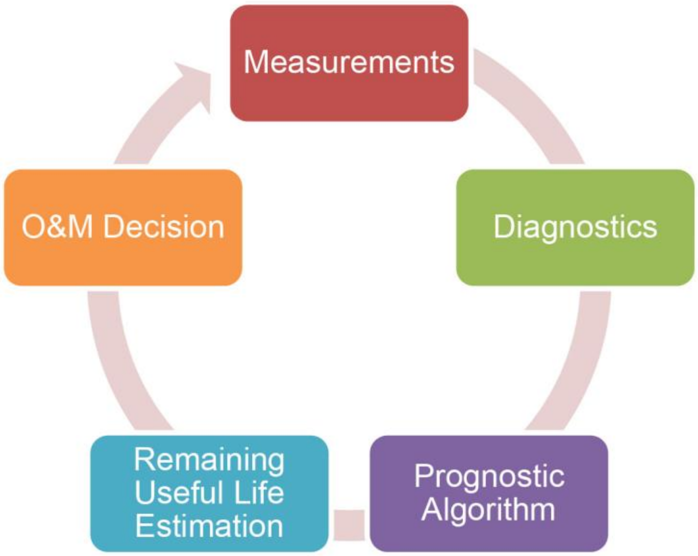

Figure 4.1. Elements of a PHM System for Passive AR Components

In proposed AR concepts, a number of passive components may be identified (see Appendix A for examples) that may benefit from the use of PHM.

In this section, we describe an overview of the Bayesian approach and its applicability to localized and component-level PHM. Bayesian methods for prognostics have many advantages, including the ability to update the prognostic result as new information (for instance, measurement data) becomes available, and the ability to inherently provide confidence bounds on the prognostic result.

4.1 Bayesian Approach to Prognostics

Damage accumulates in materials over time from one or more stressors and may be monitored using one or more of NDE measurements (Appendix B). These measurements, when combined with a model that defines the relationship between the measurement and the underlying material condition or state, are used to assess the underlying material condition. Given the assessment of the current material condition, the RUL can be determined by using a model of degradation accumulation and growth. As additional measurements become available, the current material state estimate and RUL may be updated using the same process.

Mathematically, the process is described through two models. The Degradation Rate model defines the relationship between degradation levels x_k and x_j ($k > j$) and is a representation of the evolution of damage in the material or component with time. The model may also include information on stressor history; that is,

$$x_k = f\left(x_j, \sigma_k, \sigma_{k-1}, ...\sigma_j, \eta_k\right) \quad (4.1)$$

where $\sigma_k, \sigma_{k-1}, ..., \sigma_j$ are the stressor values at times $k, k–1, \ldots, j$, with $j < k$. In this Degradation Rate model (Eq. 4.1), η_k represents the uncertainty in the state transition model and is a measure of the amount of knowledge available regarding the damage accumulation process. Typically, this is represented by a probability density function (PDF). For the moment, we postpone the discussion of how the material state is defined. This is addressed in Section 5, where the evaluation approach and results to date are described.

The second (Measurement Physics) model relates the degradation level to the measurements z_k at the present time instant:

$$z_k = h\left(x_k, v_k\right) \quad (4.2)$$

with the quantity v_k representing the level of uncertainty in the relationship between the degradation condition and the measurement. As with η_k, v_k is generally represented by means of a PDF.

The problem of prognostics (estimating the RUL from the measurements) is decomposed into the two related problems discussed above—estimation of x_k from z_k (i.e., determining the current degradation state from the measurements) and the estimation of the corresponding time-to-failure and the RUL.

Mathematically, the problem of estimating x_k from z_k using these two models is identical to the formulation of a tracking problem (Ristic et al. 2004; Arulampalam et al. 2002; Khan and Ramuhalli 2008), and therefore, solutions to the tracking problem can also be applied to the material state prognostics problem. If the functions $f(\bullet)$ and $h(\bullet)$ are linear (Horn and Johnson 1985), and η_k and v_k are independent and Gaussian-distributed, the optimal solution to the tracking problem can be shown to be the Kalman filter (Ristic et al. 2004). However, when the functions are non-linear and/or the noise terms are non-Gaussian (as is likely in the early degradation estimation problem), then more general solutions to the tracking problem are necessary, and include algorithms such as the extended Kalman filter, unscented Kalman filter, and the particle filter. In this study, we use the particle filter because of its applicability to non-linear, non-Gaussian models. A detailed description of the particle filter is given elsewhere (Ristic et al. 2004; Arulampalam et al. 2002), and its applicability to material state prognostics is discussed in Ramuhalli et al. (2012) and Meyer et al. (2013d).

Below, we describe the particle filter's use for component-level prognostics, and discuss some of the advances in model selection. These advances are currently being studied for localized prognostics, but are equally applicable (with appropriate Degradation Rate and Measurement Physics models) to component-level prognostics.

4.2 Overview of Component-Level Prognostics Framework

Demonstrating a prototypic PHM system to manage degradation of passive AR components necessitates addressing several of the research gaps and technical needs described in previous reports (Meyer et al. 2013a). Specific concepts needed are:

- The use of multiple condition and stressor measurements to enhance the performance of diagnostics and prognostics of passive components and systems in AR.
- Ability to quantitatively account for uncertainties and to propagate uncertainties in RUL predictions.

- A lifecycle prognostics framework that can enable updating of models. This includes the ability to perform accurate RUL prediction on a passive component subject to changing or time varying stressors.
- Ability to account for coupling effects between passive components in performing diagnostics and prognostics.

The component level of the PHM system consists of the measurements and algorithms used to diagnose and predict failure of a component. Measurements of stressor variables will be one key source of information for component-level diagnostics and prognostics. Other potential sources of information include global condition measurements such as vibration measurements or acoustic emission measurements. These measurements provide an indirect assessment of component degradation, which will introduce significant uncertainty into diagnostics and prognostics. The uncertainty can be reduced and the PHM performance can be enhanced by fusing component-level measurements with relevant local-level information. In addition to reducing uncertainty, the fusion of global and local information also potentially provides the opportunity to detect failures that might occur at non-weld locations (weldments have been the traditional focus of ISI). The fusion of global condition, local NDE, and process (stressor) information to enhance PHM of a passive AR component is notionally illustrated in Figure 4.2.

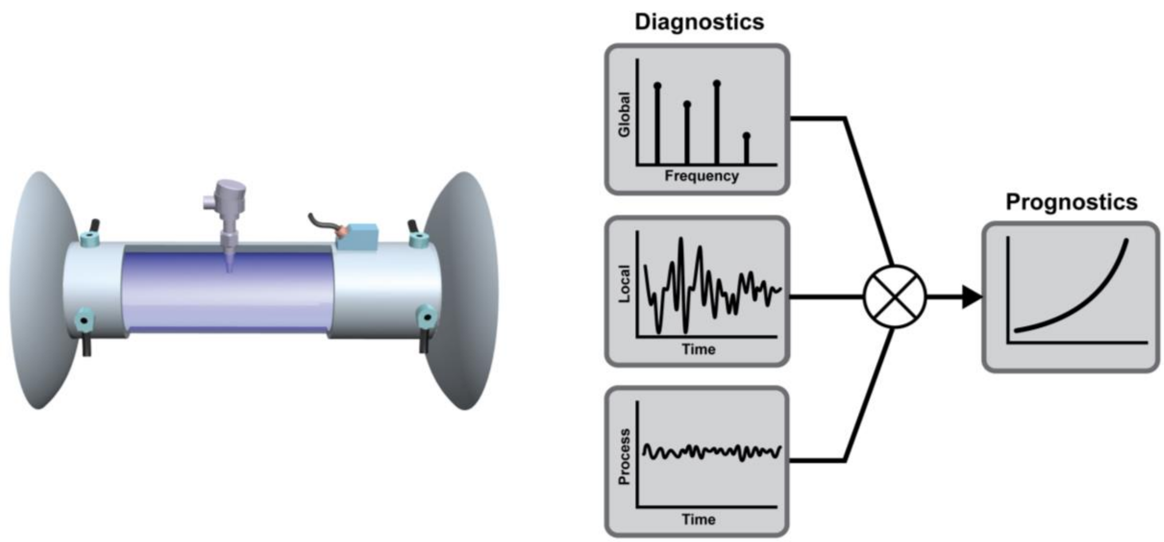

Figure 4.2. Notional Illustration of Enhanced Component-Level PHM Performed by Fusing Data from Global Condition, Local NDE, and Process (stressor) Measurements

4.2.1 Fusion of Information from Multiple Locations

For component-level prognostics, the Bayesian approach described in Section 4.1 may be effectively adapted by choosing appropriate models of component degradation-growth and measurement physics. At the (passive) component level, a simplified approach to prognostics would be to determine the time-to-failure at one or more locations on the component based on local measurements of material degradation (localized PHM), and use the smallest time-to-failure as the component time-to-failure. This approach has a couple of drawbacks. First, this requires measuring material degradation at many locations, increasing overall cost and. Also, the probability of over-estimating the time-to-failure increases from degradation that was missed at one or more locations due to these locations not being inspected/monitored. Second, the approach fails to take into account the possibility of multiple, individually small-scale, degraded locations that collectively may impact the ability of the component to provide the necessary functionality.

Finally, this approach is entirely reliant on the reliability of the localized measurements for detecting degradation onset and growth. However, the reliability of localized measurements (using NDE methods) can be variable and depend on the size, shape, location, and type of degradation (Singh 2000).

An alternate approach is to specify, at the component level, degradation in terms of loss of performance or functionality. In this case, measurements (at the global and local levels) are treated as observables that provide some insight into the state of the component and its ability to meet its performance metrics. This approach also raises the possibility of fusing information from global and local scales, as well as integrating information on stressors.

As a consequence, the appropriate degradation models are likely to describe performance degradation and not the accumulation of damage in the material that forms the component.

Using this approach, degradation states x_k and x_j ($k > j$) are then simply representations of the state of the component relative to its inability to meet its functional requirements. For instance, an appropriate state description might use two possible states that the component may be in: Normal (i.e., capable of meeting its functional requirements) and Degraded (incapable of meeting its functional requirements). Alternatively, the state may be a suitably normalized metric quantifying the inability to meet functional requirements. An example here may be the reduction in the amount of flow possible in heat-exchanger tubing in the presence of fouling, normalized with respect to its nominal value. The Degradation Rate model (Eq. 4.1) is a representation of the change in the component functionality with time. The model may also include information on stressor history as shown in Eq. (4.1).

A key challenge with this approach to component degradation prognostics is the possibility of information from multiple sources/locations. For example, in the degradation monitoring of steam generator (SG) tubing, vibration data may be available to monitor the overall vibrational profile of the SG tube, while crack length information from the NDE inspection of individual tubes in the SG bundle provides a local view of degradation. For component-level prognostics, it is clear that this disparate information (at different scales) will need to be merged properly to provide a holistic view of the component condition and RUL.

This challenge may be met by adapting the Bayesian prognostic approach to incorporate information from these diverse sources. To achieve this, we utilize the common definition of component-state described above to underlie the prognostic process. Two sets of Measurement Physics models are then defined: a set of Measurement Physics models that relate the localized measurement to the component-state, and a set of global condition measurements that are linked to the global-state.

Given these models, the prognostic approach follows the multisensor fusion method described in Khan (2009) and Khan et al. (2011). Specifically, we assume that Q measurements $z_k^q, 1 \le q \le Q$ are available. Define $\underline{z}_k = \left[z_k^1, z_k^2, ..., z_k^q, .z_k^Q \right]$. The Bayesian approach then reduces to evaluating the posterior density $p(x_k \mid \underline{z}_k) = p(x_k \mid \underline{z}_k, \underline{z}_{1:k-1})$. As described in Appendix C, the Bayesian tracking filter method utilizes samples and associated weights for each possible state, where the weights are computed using the likelihood function $p(z_k \mid x_k^i)$, the transitional prior density $p(x_k^i \mid x_{k-1}^i)$, and an importance density $q(x_k^i \mid x_{k-1}^i, z_k)$, and the superscript i in the state variable represents the i-th sample.

For multisensor fusion, Khan (2009) adapts the the weight assignment process to utilize multiple likelihood functions $p(z_k^q \mid x_k^i)$, and under assumptions of independence of the measurement modes, the weight w_k^i assigned to the ith sample x_k^i may be derived as:

$$w_k^i \propto \prod_{q=1}^{Q} p\left(z_k^q \mid x_k^i\right) \tag{4.3}$$

When the measurements cannot be considered to be independent, the weight assignment calculation will need to account for the covariance between the various measurement modes.

4.2.2 Component Degradation Models and Model Selection

A critical necessity for component-level prognostics is an appropriate Degradation Rate model that operates over the degradation state for the component. Such models are difficult to obtain, as they deal with macroscopic systems that are impacted by changes (damage accumulation) at microscopic scales. As described earlier, to overcome this issue, we use a degradation state description wherein the degradation state is a coarse representation of the inability of the component to meet its functional requirements. A Degradation Rate model is then defined where the component condition evolves over time under the influence of stressors.

The component condition may be defined over a continuum of states, or over a discrete set of states depending on the needs of the problem. In either case, the component may exist in only one degradation state at a given time. However, the Degradation Rate model may be dependent on the condition the component experiences as well as the degradation state that the component is in. For instance, the rate of component degradation change over time may be substantially higher as the component experiences more and more degradation. Clearly, in this case, the ability to choose the correct model at any instant in time becomes important. For this aspect, we use the model selection approach that is described in greater detail in Section 4.3.2, in the context of local-level prognostics.

4.2.3 Integration of Stressor Information

The incorporation of stressor information in the component-level PHM framework is complicated by the fact that stressors, such as mechanical, thermal, or chemical stresses over time, generally result in the localization of degradation and the formation of microcracking that, if left unchecked, will result in failure of the component. For this reason, we focus on the incorporation of stressor information predominantly in local-level Degradation Rate models.

The incorporation of stressor information occurs through the use of an appropriate local-level Degradation Rate model (Equation 4.1 in Section 4.1). For instance, during the course of this study, high-temperature creep has been explored as a prototypic degradation mechanism of relevance to AR components. Thermal creep has several likely underlying mechanisms of which dislocation-creep, also known as power-law creep, is likely to be the creep mechanism of most significance to consequential aging in AR components (Ashby and Jones 2012). The rate of dislocation-creep depends on the movement of dislocations within a material, which is affected by intrinsic lattice resistance and resistance caused by obstacles such as precipitates, solute atoms, or other dislocations. Ultimately, the rate of dislocation-creep, $\dot{\varepsilon}$, is dependent on the diffusion processes in a given material (Ashby and Jones 2012), and is a function of both atomic diffusion as well as stress effects that result in dislocation movement:

$$\dot{\varepsilon} = A\sigma^n Exp\left(-\frac{Q}{RT}\right) \tag{4.4}$$

where R is the ideal gas constant, σ represents the applied stress, t represents time, T is the temperature, and Q is the activation energy representing the height of the energy barrier atoms must overcome in a given diffusion process. It should be noted that the stressors, applied stress σ, and temperature *T*, may vary as a function of time and the information can be incorporated in the Degradation Rate model for estimating RUL of the structural components using prognostic algorithms.

4.3 Local-level Prognostics

4.3.1 Bayesian Local-level Prognostics

As described previously, the local level of the PHM system refers primarily to direct measurements of material condition performed by the application of NDE technologies during an outage or possibly online. This is illustrated in Figure 4.3, with details of the PHM process outlined in Figure 4.4. As shown in these two figures, the localized PHM process utilizes the NDE measurements at one location, and estimates RUL of the material based on the degradation level at this location. As discussed earlier, this may also be viewed as component remaining life assessment with a single set of measurements at one location, with the component failure occurring when the degradation at this location reaches a level that results in material failure.

At the localized level, the PHM system can be thought of as several individual units that could be defined as a single measurement location (for instance, a portion of a weldment or other small region of a component). In addition to the condition measurements, it is possible to combine stressor measurements with the condition measurements for local diagnosis and prognosis. Either the measurement data and/or the processed prognosis data may be transferred up to the component level for use in component health assessment.

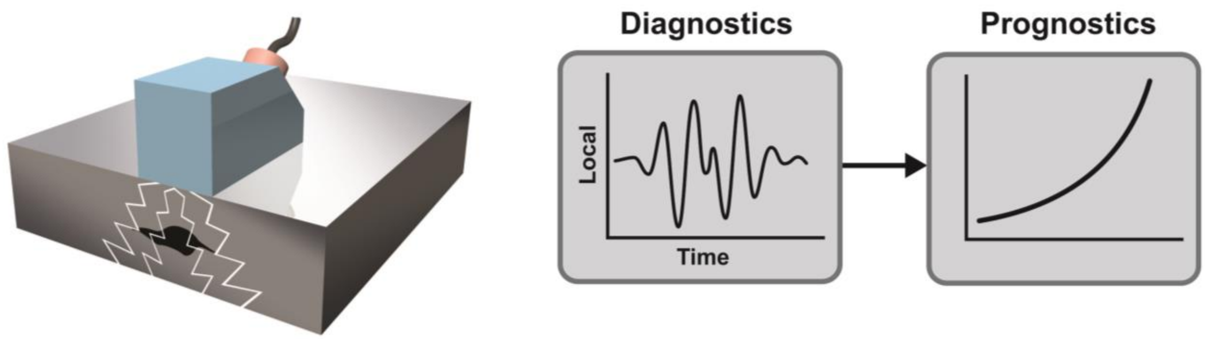

Figure 4.3. Depiction of Local PHM Based on Local NDE Measurements

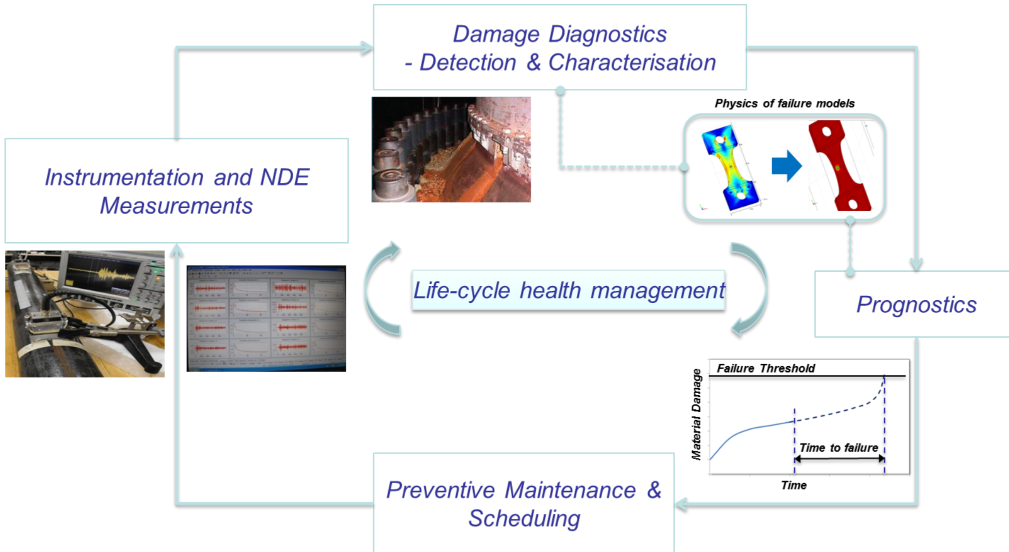

Figure 4.4. Local Prognostics Health Management Framework

4.3.2 Prognostic Model Selection

The Bayesian prognostics framework, as described earlier, is readily applicable if the material degradation phenomenon is well understood and the degradation rate model is defined. Quite often it is difficult to quantify all the stressors that exist in real-world operating conditions. Material degradation under such conditions can be highly non-linear, making it difficult for a single Degradation Rate model to track evolution of damage in a material with time. Thus, a combination of different Degradation Rate models that capture changes in different physical properties of the material may be needed for accurate and reliable prognostics.

To provide context for the development of mode-selection approaches, high-temperature creep damage is selected as the prototypic degradation mechanism for structural materials in ARs. Creep degradation is the plastic deformation that occurs in materials under stress at high temperatures. Deformation from creep is a function of time, temperature, and stress (Ashby and Jones 2012):

$$\varepsilon = f\left(\sigma, t, T\right) \tag{4.5}$$

where ε represents the strain, σ represents the applied stress, *t* represents time, and *T* is the temperature. In this case, high temperature is roughly defined as temperatures greater than $0.3T_m$ where T_m is the melting temperature of the material. Different mechanisms for thermal creep are dominant depending on the applied mechanical and thermal stresses that will result in different Degradation Rate models (Figure 4.5). Furthermore, Degradation Rate models can also transition from one level of complexity to another until the point of material failure due to creep progression as shown in Figure 4.6.

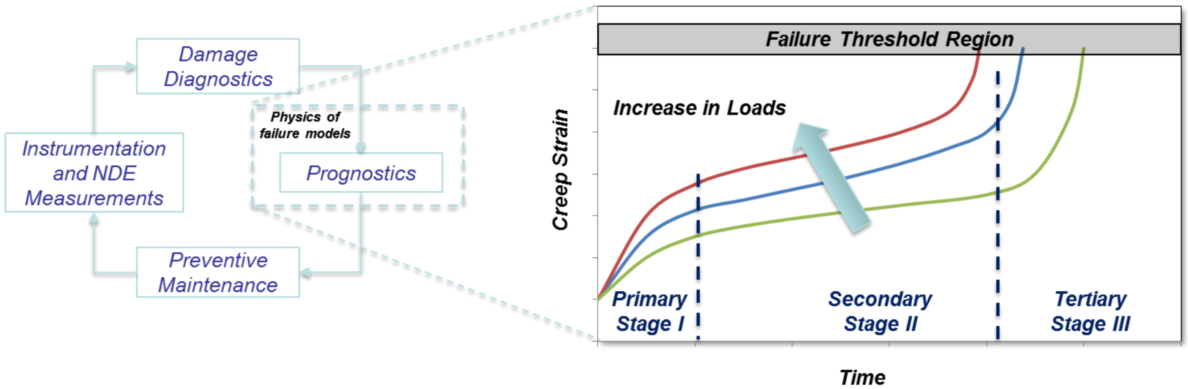

Figure 4.5. Prognostic Model Selection

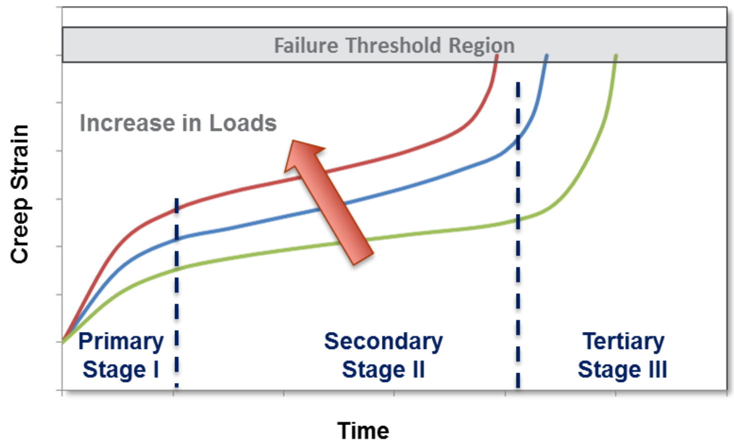

Figure 4.6. Schematic Showing Variation in Creep Rates as a Function of Applied Load (mechanical and thermal)

The Bayesian material state estimation and prognostics framework, as described earlier, is readily applicable if the material degradation phenomenon is well understood and the degradation rate model is defined. Quite often it is difficult to quantify all the stressors that exist in real-world operating conditions. Material degradation under such conditions can be highly non-linear, making it difficult for a single Degradation Rate model to track evolution of damage in a material with time. Thus, a combination of different Degradation Rate models that capture changes in different physical properties of the material may be needed for accurate and reliable prognostics.

Given multiple possible material Degradation Rate models, it will be imperative for any prognostics algorithm to select the appropriate model before estimating the remaining life. As discussed earlier, this is especially important if the appropriate model changes over the lifecycle of the material or component. The selection of the appropriate model will require the prognostics algorithm to calculate posterior probabilities for each model based on the evidence (likelihood) at each measurement update. In this section, we briefly describe an algorithm that provides these model posterior probabilities, and is integrated into the particle filter-based Bayesian framework. This algorithm acts as a wrapper (or outer loop) to the particle filter. Appendix C contains additional details of this approach.

Let $\mathrm{M}_{\mathrm{I}}^{(\mathrm{k})}$ represents I-th model being considered at time index *k* from a finite set of material degradation models $\boldsymbol{M}:\{M_1, M_2, \ldots M_{Nmodels}\}$ (Guan et al. 2011). *Nmodels* is the total number of models under consideration. Let $\theta_I^{(k)}$ represent the model parameters for the I-th model at time index *k*. Let $p\left(z_k, \theta_I^{(k)}, M_I^{(k)}\right)$ be defined as the joint probability distribution of model $M_I^{(k)}$, model parameters $\theta_I^{(k)}$, and observed state z_k at time index *k*, which can be expressed as

$$p\left(z_k, \theta_I^{(k)}, M_I^{(k)}\right) = P\left(M_I^{(k)}\right) p\left(\theta_I^{(k)} \mid M_I^{(k)}\right) p(z_k \mid \theta_I^{(k)}, M_I^{(k)}) \tag{4.6}$$

where $P\left(M_i^{(k)}\right)$ is the probability of $M_I^{(k)}$; $p\left(\theta_I^{(k)} \mid M_i^{(k)}\right)$ is the prior density for the parameter set for $M_i^{(k)}$; and $p\left(z_k \mid \theta_I^{(k)}, M_I^{(k)}\right)$ is the posterior distribution of observed state z_k given model $M_I^{(k)}$, and model parameters $\theta_I^{(k)}$, at time *k*.

Identifying the appropriate model (and model parameters) at each time index *k* may be done in one of two approaches (Guan et al. 2011; Newton and Raftery 1994b).The first approach is to evaluate the marginal likelihood of the observed data z_k under each model $M_I^{(k)} \in \mathcal{M}$ using Monte Carlo-based importance sampling schemes (Newton and Raftery 1994b). However, the marginal likelihood estimate has to be obtained for each model at each measurement update. This may become computationally expensive as the size of $\mathcal{M}$ increases (*Nmodels* >> 1).

An alternate approach to calculate posterior model probabilities is to consider model itself as a variable (Guan et al. 2011). Eq. (4.6) can be re-expressed as:

$$p\left(\theta_I^{(k)}, M_I^{(k)} \mid z_k\right) = \frac{p\left(z_k \mid \theta_I^{(k)}, M_I^{(k)}\right) p\left(\theta_I^{(k)} \mid M_I^{(k)}\right)}{P\left(z_k\right)} \tag{4.7}$$

A standard Markov chain Monte Carlo (MCMC) simulation using Metropolis-Hastings (M-H) algorithm (Hastings 1970) can be used to obtain samples of $p\left(\theta_I^{(k)}, M_I^{(k)} \mid z_k\right)$ if all models in set $\mathcal{M}$ have their parameters belonging to the same dimensional space. In the case where model parameters span different dimensional spaces, a reversible jump MCMC (RJMCMC) approach is necessary (Green 1995).

In this study, we use an automatic RJMCMC, as described in Guan et al. (2011) and Hastie and Green (2012), to evaluate posterior Degradation Rate model probabilities at each measurement update. This approach allows for transition from one model to the other using a pre-defined set of model transition probabilities. Material state estimation is obtained using particle filtering algorithm as discussed earlier. In addition, a model averaging procedure is incorporated wherein the state trajectory estimation is obtained using the weighted average of each model in the set $\mathcal{M}$, the weights are the model posterior probabilities obtained using the automatic RJMCMC algorithm at the latest measurement update time index. A schematic representation of this approach is shown in Figure 4.7.

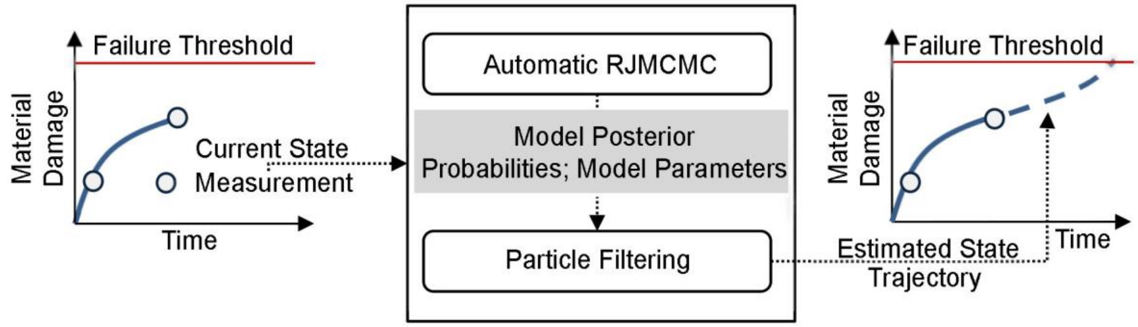

Figure 4.7. Schematic of Material State Estimation Using Automatic RJMCMC and Particle Filtering Method

At the end of the single simulation instance of the RJMCMC chain, posterior model probabilities can be calculated as (Guan et al. 2011):

$$P\left(M_I^{(k)} \mid z_k\right) = \frac{N_I}{N_{total} - N_{burn}} \tag{4.8}$$

where N_I is the number of samples in the RJMCMC chain under I-th model, N_{burn} is the number of burn-in samples used in the RJMCMC chain, and the total number of samples is represented by N_{total}. Burn-in samples are used to initialize the RJMCMC chain and are discarded once the RJMCMC chain converges. Given the posterior model probabilities at time index k, the mean state trajectory estimation at time k is calculated by taking the weighted average of the trajectories obtained under each model:

$$\bar{x}_{mean,k} = \frac{1}{N_S} \sum_{I=1}^{Nmodels} P\left(M_I^{(k)} \mid z_k\right) \sum_{i=1}^{N_S} x_k^i \tag{4.9}$$

To summarize, the problem of Degradation Rate model selection for lifecycle prognostics may be addressed using the following process:

- At a given time step, obtain relevant measurement data that is sensitive to the degradation.
- Determine the appropriate current phase of degradation (for instance, primary, secondary, or tertiary creep) by using information from available measurements.
- Determine the likelihood of each Degradation Rate model (from many possible models) and the model parameters for the current phase of degradation.
- Project the degradation growth to future time instants over a given time horizon using the each of the Degradation Rate models.
- Using the likelihood information as weights, compute the weighted average of the projected degradation-growth trajectories.
- As the material or component ages, repeating the steps above to update the lifecycle prognostics Degradation Rate model and parameter selection as more measurements become available.

Uncertainty in this context can arise from many sources. In the case of creep damage, the strain rate in each stage of creep depends on the applied load and environmental conditions (e.g., temperature). Consequently, Degradation Rate model parameters will vary as a function of the load (mechanical and thermal) (Figure 4.8). The variation introduces uncertainties in Degradation Rate model parameters that prognostics algorithms use for RUL prediction. Further, the dependence of creep rates on the material microstructure (which may not always be known in practice) indicates that a source of uncertainty is the set of creep model parameters. Finally, the measurements themselves are noisy and do not provide a unique mapping back to the material condition domain. Consequently, the available measurements add to the uncertainty in diagnostics and prognostics.

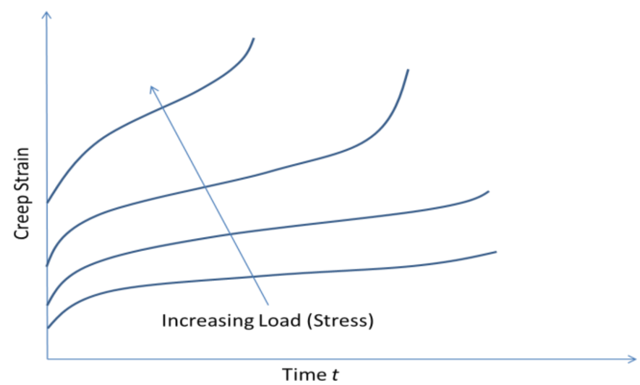

Figure 4.8. Schematic Showing Variation of Creep Strain with Load. Adapted from Li and Dasgupta (1993).

5.0 Assessment of PHM Framework for Passive Components

An effective PHM system for ARs should be able to adapt or adjust its prognostics methodology to the stage the component or degradation is in its lifecycle (Hines et al. 2009). For passive components, this requirement may be posed in terms of degradation growth lifecycle and is fundamentally one of Degradation Rate (reference Section 4.0) model selection based on available data. This formulation is particularly useful where classical population-statistics–based approaches for prognostics may not be viable, as the volume of historical failure data necessary to develop reliability models may not be available for long-lived passive structures such as reactor vessels or piping. Indeed, different models may be more appropriate (e.g., more accurate, more precise, or suitable to runtime requirements) during different stages of component degradation (Nam et al. 2012). The issue of lifecycle prognostics for passive components is addressed by formulating the problem as one of model selection (Section 4.3.2) within the context of a Bayesian prognostic algorithm.

As discussed earlier, to provide context to research described here, high-temperature creep damage is used as the prototypic degradation mechanism for structural materials in ARs.

Creep degradation is the plastic deformation that occurs in materials under stress at high temperatures. Unlike the deformation of materials under stress at low temperatures, which is independent of time, deformation from creep is a function of time, temperature, and stress (Ashby and Jones 2012). In general, the evolution of creep appears over three distinct phases (Li and Dasgupta 1993; Hosford 2005) from fault onset to rupture: primary, secondary, and tertiary. In the primary (or transient) phase, the rate of creep strain decreases with time. In the secondary phase, the strain rate is approximately constant. The strain rate increases rapidly in the tertiary phase until material rupture or failure.

A combination of synthetic and measurement data is being used in the evaluation process. These are described below, followed by a summary of the results to date on the evaluation.

5.1 Assessment Using Synthetic Data

Several models have been proposed to describe the primary, secondary, or tertiary phase of creep (Naumenko and Altenbach 2007). Some of these models have been proposed to describe two phases in a unified model (Brear and Aplin 1994). The most appropriate model for each phase of creep depends on the material properties and environmental conditions.

To assess the PHM framework, we used synthetic data generated using three different models (Table 5.1), one for each stage of creep progression; that is, primary, secondary, and tertiary. We assume that the material state is defined as the level of creep strain experienced by the material, and that measurements are of the creep strain itself. A zero-mean Gaussian process is used to generate noise $\mathrm{N}\left(0,1e-2\right)$ that is added to each data point to simulate measurements under noisy environments. The resulting data is shown in Figure 5.1 where the creep strain is in percent strain while time is represented using arbitrary units. The relevant parameters for the Degradation Rate models used for generating the data in Figure 5.1 are provided in Table 5.1; the resulting creep progression curves are consistent with the creep-rupture curves of welds (Manjoine 1985).

Table 5.1. Example: Thermal-Creep Prognostics from Synthetic Data for Degradation Rate Model

Creep Stage	Model	Duration (time units)	a_0	a_1	a_2	a_3
Primary (I)	$\dot{\varepsilon} = a_0\left[1 - \exp\left(-a_1 k\right)\right]$	$k < 6$	0.40	1.00	-	-
Secondary (II)	$\dot{\varepsilon} = a_1 k - a_0$	$6 < k < 24$	0.75	0.07	-	-
Tertiary (III)	$\dot{\varepsilon} = a_3 k^3 + a_2 k^2 + a_1 k + a_0$	$k > 24$	12.93	−0.63	−1e-5	3.53e-4

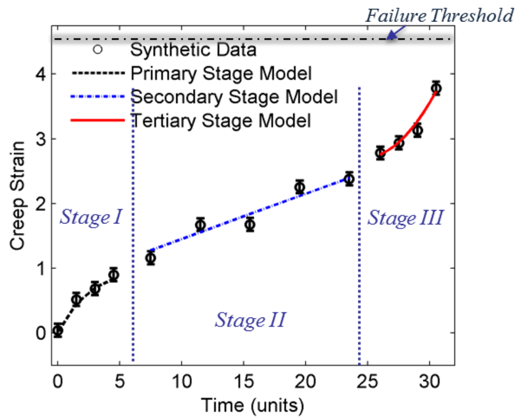

Figure 5.1. Synthetic Measurements from Table 5.1 Data Using Three Different Models for Thermal-Creep Progression

The results of applying the prognostics algorithm for model selection and RUL prediction using this data are summarized here; additional details may be found in Roy et al. (2015). A key finding of model selection (Figure 5.2) is that the improved RUL estimates are obtained through dynamic selection of models. Figure 5.2(a) shows the predicted creep strain using a sequence of measurements, and the updates to these predictions as subsequent measurements become available. As each measurement becomes available, the need is to determine if the material is in the primary, secondary, or tertiary stage. To this end, the model selection algorithm is applied to identify the most likely model (out of the three models – primary, secondary and tertiary – shown in Table 5.1); the probabilities of each model being selected are shown in Figure 5.2(b). Finally, Figure 5.2(c) presents the remaining life of the material with and without the model selection process. The RUL data are only shown as the material transitions into the tertiary stage of damage, to simplify the calculation process.

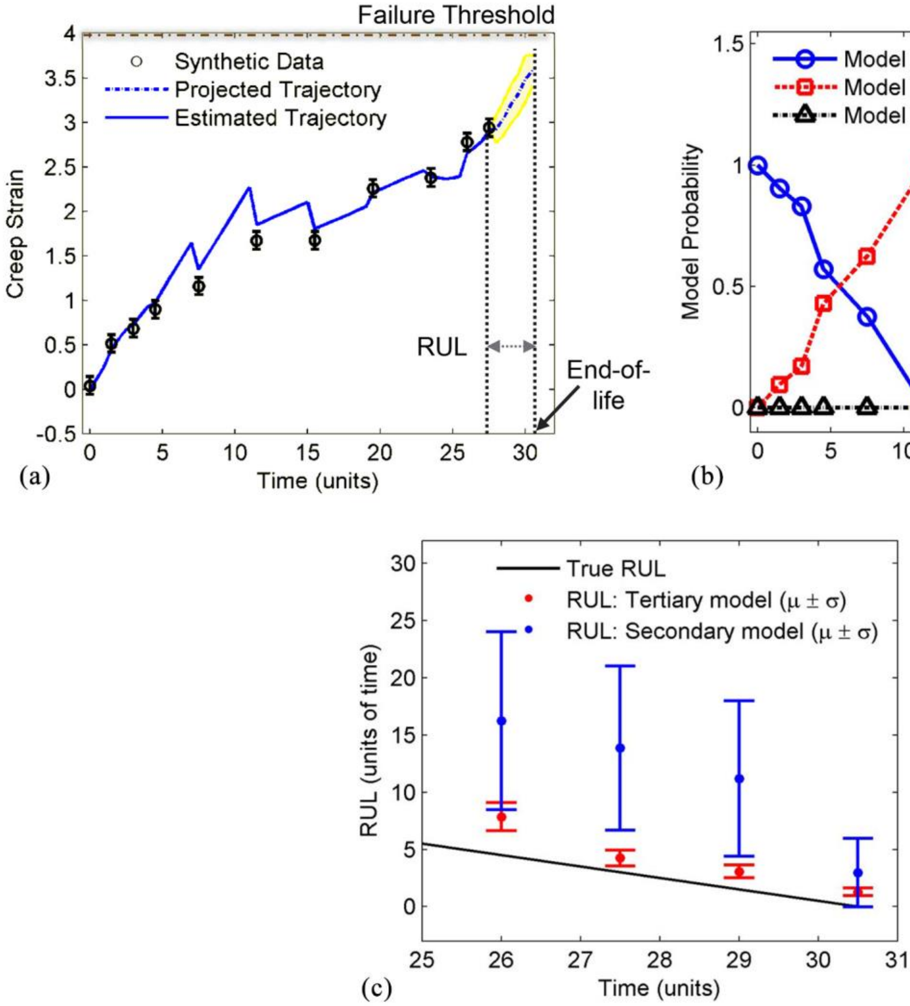

Figure 5.2. Example Results: Model Selection

These results, and other similar results to date using alternate noise levels, indicate the feasibility of the model selection approach and show that the use of model selection can improve the accuracy of the prognostic result for AR passive components. The results also indicate that within the Bayesian prognostic framework, the accuracy of the model selection may be impacted by the noise levels assumed in the process and measurement models.

5.2 Assessment Using Experimental Data

Experimental evaluations to date have relied on the use of data from purpose-built testbeds for inducing creep damage, and quantifying the level of degradation using destructive and nondestructive measurements. These are described briefly next, with details provided in Appendix C.

5.2.1 Testbed Concepts for Prognostics

5.2.1.1 Laboratory-scale Testbed for Ex-situ Measurements

To perform initial validation of the prognostic algorithms, a laboratory-scale creep degradation testbed was designed and built (Figure 5.3) to allow ex-situ NDE measurements. Using this testbed ("ex-situ testbed"), specimens are removed after a defined amount of time and measured using advanced NDE techniques, and can be re-inserted for inducing additional creep damage if needed. Measurements include ultrasonic, eddy current, magnetic Barkhausen, and creep-strain measurements that provide the true state (level of accumulated creep strain). Details of these measurement methods are provided in Appendix B.

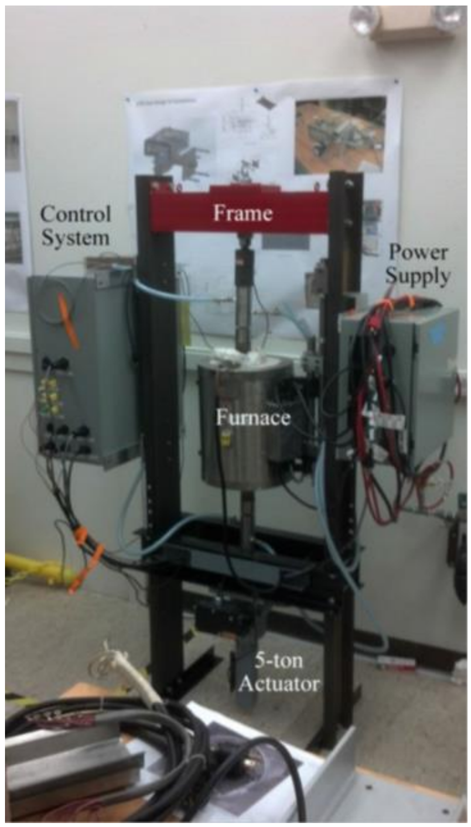

Figure 5.3. Creep-Test System for Validating Prognostic Algorithms

The ex-situ creep testbed (Figure 5.3) consists of a mechanical load frame, furnace, 5-ton actuator, power supply enclosure, and control system enclosure. The control system enclosure houses the electronics that run the system, including the motor drive for the stepper motor that is used in conjunction with the 5-ton actuator. The load frame is the base that all components are mounted to, and is based off a 20-ton shop press. The furnace, actuator, and both electrical boxes mount to the load frame. The machine allows the user to specify a force to be applied to the specimen, as well as a temperature for testing. During a test, the machine logs the date, stepper position, sensor position, temperatures, and force applied to a file for future analysis.

A programmable logic controller is used to control the operation of the testbed, and enables independent control of temperature and load. Heating is controlled by means of three control circuits for the heater, with a 5-point thermocouple to control the heat independently in each of the three heater circuits. The load is controlled by means of a 5-ton actuator with a 24:1 gear reduction ball screw, which allows the system to apply a force of 5 tons to the specimen. A stepper motor with a 100:1 gear reduction allows for very precise control of the actuator. A separate position sensor is mounted to the actuator to monitor the position of the actuator.

5.2.1.2 Laboratory-scale Testbed for In-situ Measurements

A second creep-test system (with similar capabilities as the one described in Section 5.2.1.1) that was available at Pacific Northwest National Laboratory (PNNL) was repurposed for use as a testbed facilitating in-situ measurements (“in-situ testbed”). Figures 5.4 and 5.5 show this testbed. Within this testbed, specimens are instrumented with ultrasonic probes at either end (Figure 5.5) and enable ultrasonic measurements as the specimen is experiencing creep damage. The specifications for this in-situ testbed, including the load frame, furnace, actuator, and control system, are identical to the ex-situ testbed. The primary difference is that the specimen grips have been modified to accommodate the ultrasonic sensors at either end of the specimen, and the grips are cooled using chilled water to keep the probes within their temperature limits. Measurement data is automatically acquired (on a set schedule) using an automated data acquisition system. Figure 5.6 shows the user interface for this automated data acquisition system.

Figure 5.4. In-Situ Creep-Test Frame

Figure 5.5. In-Situ Creep-Test Frame Specimen Chamber

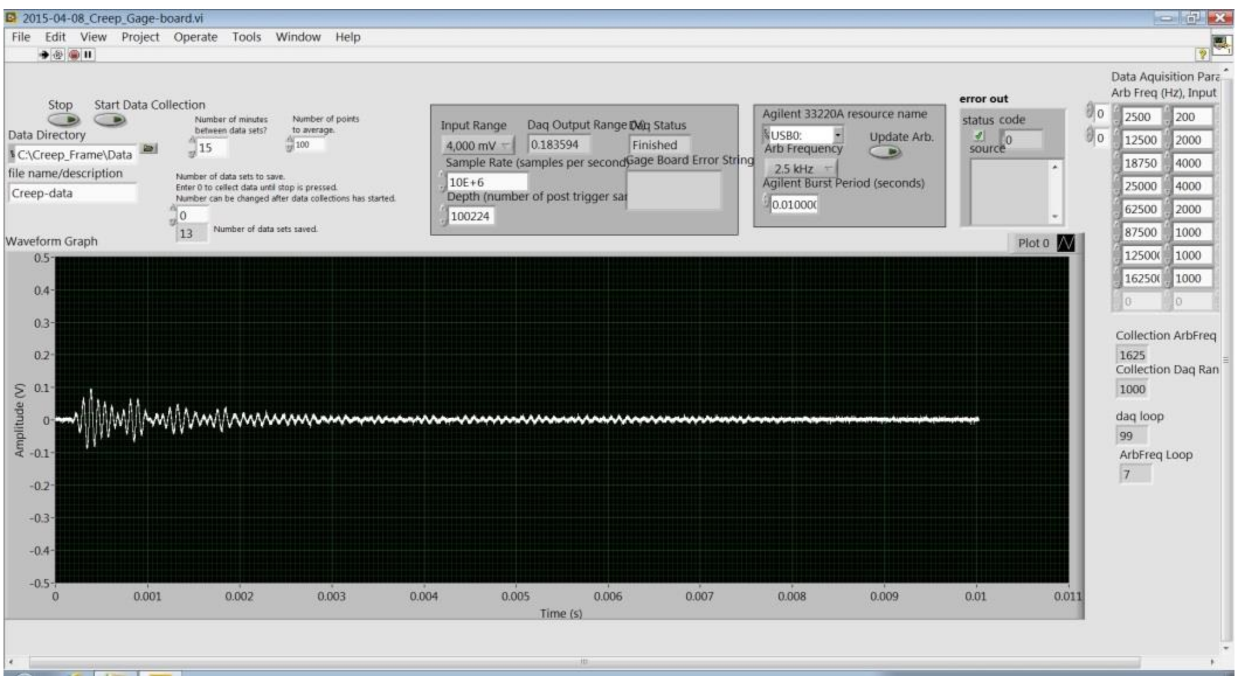

Figure 5.6. Interface for In-situ Creep Testbed Automated Measurement Data Acquisition System

5.2.1.3 Laboratory-scale Testbed for Component-Level Measurements

A concept design for a component-level testbed, that utilizes passive components such as tubes and piping, was developed based on the ex-situ and in-situ testbeds. This concept is shown in Figure 5.7, where mechanical and thermal loading is applied to the component to induce degradation (thermal aging, mechanical degradation, or creep damage) while facilitating in-situ measurements such as vibration, guided ultrasonic waves, or other NDE methods. Details of this concept are in Appendix D.

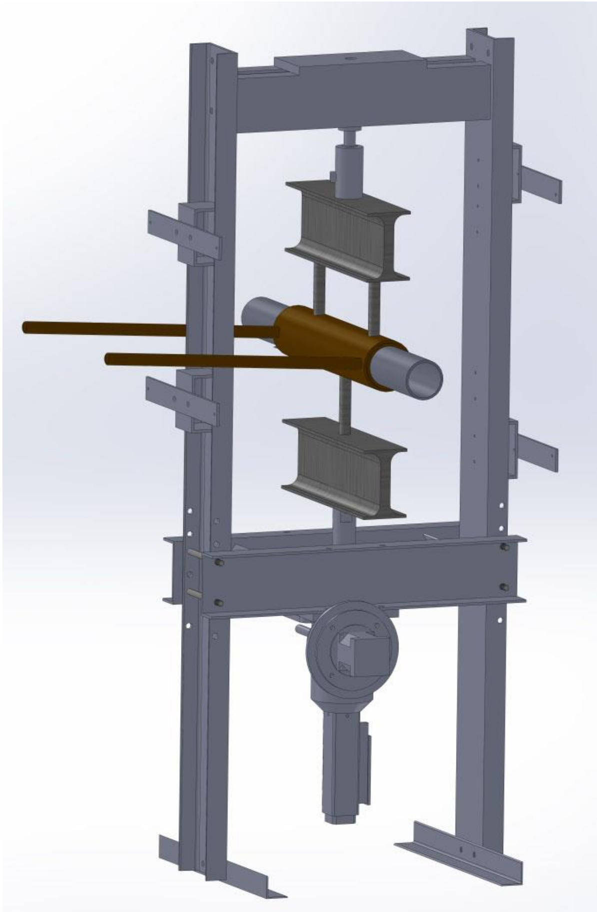

Figure 5.7. Concept Drawing, Showing a Potential Modification to Creep Testbed, to Enable Testing of Scaled Versions of Components

5.2.2 Creep Test Specimens

A number of stainless steel coupons (specimens) were fabricated to facilitate measurements in both the in-situ and ex-situ testbeds.

5.2.2.1 Specimens for Ex-situ Measurements

Early in the research lifecycle, a preliminary test specimen geometry was utilized (Figures 5.8 and 5.9) for conducting the accelerated thermal-creep experiment using the ex-situ testbed. The specimens were designed to determine the constraints associated with the NDE measurements and with attempting timely thermal-creep aging of specimens at high temperature. The specimens are also marked with scribe lines in the gage section to facilitate a redundant and potentially more accurate measurement of creep strain, in addition to the displacement measurements.

The gage section in these specimens is approximately 12.5 cm (5 in.) long, 1.0 cm (0.4 in.) wide, and 0.1 cm (0.04 in.) thick. The initial simulation analysis (using the ANSYS program) of these specimens is documented in Ramuhalli et al. (2014b).

Measurements (such as conventional through-thickness pulse-echo ultrasound measurements) were obtained at several measurement locations along the specimen. Creep damage causes localized microstructural changes in the specimens due to plastic deformation, which is expected to affect ultrasonic wave propagation velocity, electrical conductivity, and magnetic permeability. Measurements obtained to date on these specimens indicate that the variation in the measurements within each region was low (on the order of a few hundredths of a percent).

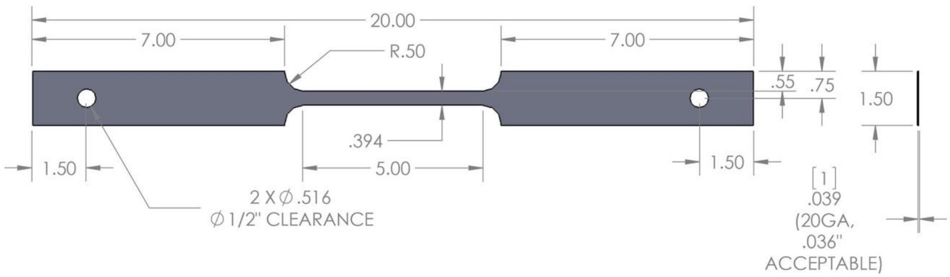

Figure 5.8. Creep Test Preliminary Specimen Geometry

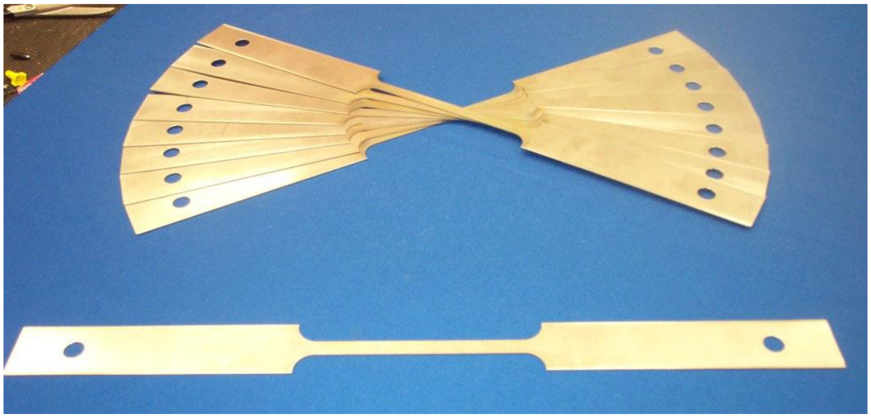

Figure 5.9. Initial Flat Stainless Steel Specimens for Creep Testing to Validate Prognostic Algorithms

Based on information regarding measurement constraints gathered during the initial shake-down tests, a new specimen design was developed and specimens fabricated, to ensure repeatable measurements. The new design for ex-situ creep specimens is shown in Figure 5.10. In addition to re-designing the specimens, the ex-situ testbed was also modified to better constrain the specimen during the creep test to stabilize the specimen during testing.

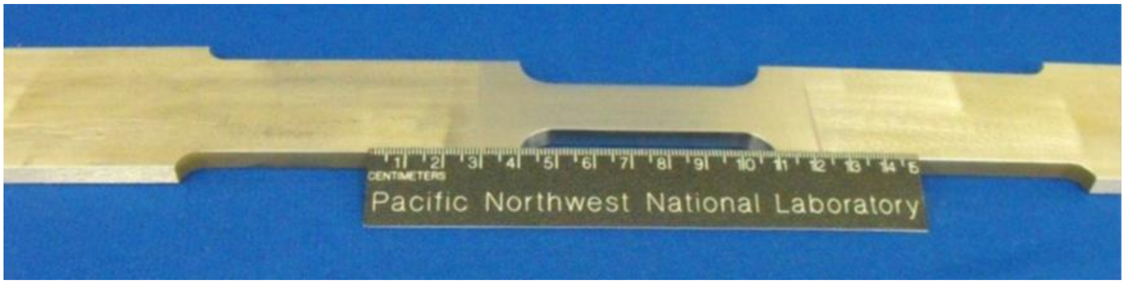

Figure 5.10. New Specimen Design for Creep Tests and NDE Measurements

5.2.2.2 Specimens for In-situ Measurements

Given the knowledge gained from the ex-situ specimen design with respect to measurement constraints, a set of specimens for use in the in-situ testbed were designed and fabricated (Figures 5.11 and 5.12). These specimens are cylindrical in nature to simplify the attachment of the ultrasonic probe for in-situ measurements, as well as to simplify the assessment of ultrasonic wave propagation for waves that are guided along this structure. The specimen is threaded at either end to enhance heat loss and keep the ultrasonic probes (attached at either end) cool. As described in Section 5.2.1.2, the cooling is further enhanced using chilled water circulating around this region.

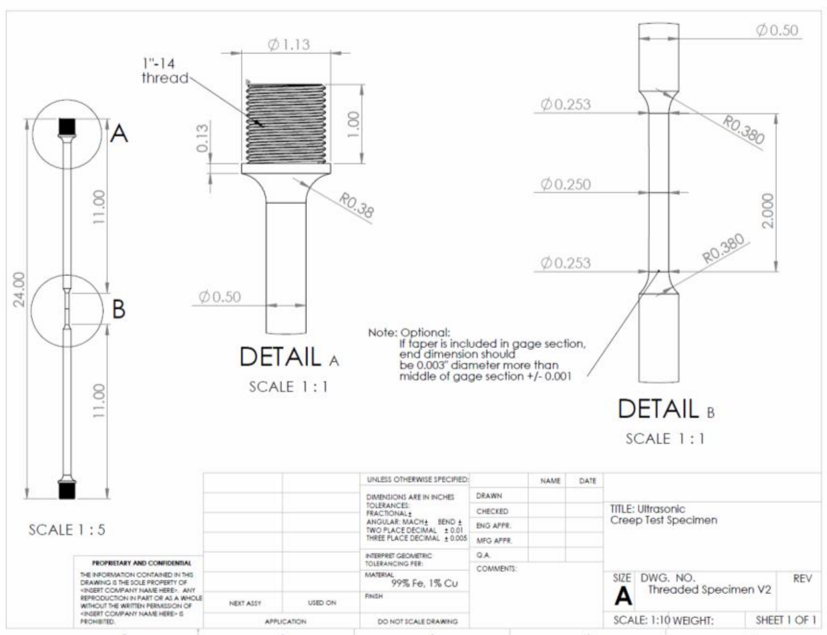

Figure 5.11. In-situ Testbed Creep Specimen Design

Figure 5.12. Specimen Design for Creep Testing with In-situ Test-frame

5.2.3 Measurement Methods

A number of NDE measurements are being used with both the ex-situ and in-situ testbeds, and include magnetic Barkhausen, linear and non-linear ultrasonics, and eddy currents (Figure 5.13). Magnetic Barkhausen noise measurements are sensitive to the presence of dislocations and precipitates that form during the aging process (Jiles 2000, 2011). These act as pinning sites for magnetic domains and their effect may be inferred by applying a low-frequency (generally < 100 Hz) sinusoidal magnetic field to the specimen and measuring the potential energy released as magnetic domains overcome the pinning. Effectively, these interactions lead to changes in the magnetic hysteresis of the material, which manifests itself as a change in magnetic permeability. Eddy current measurements, usually conducted at higher frequencies up to about 10 MHz, rely on changes in the electrical conductivity (in addition to magnetic permeability changes) due to similar microstructural changes. Ultrasonic measurements, on the other hand, rely on the interaction of elastic or stress waves with the material. This interaction is governed by the elastic properties of the material, which in turn is affected by the presence of microstructural changes such as dislocation loops, precipitates, and slip planes. Higher order changes to the elastic constants due to such damage result in the generation of harmonics, which may be used to compute a non-linear ultrasonic parameter. Details of these methods are provided in Appendix B.

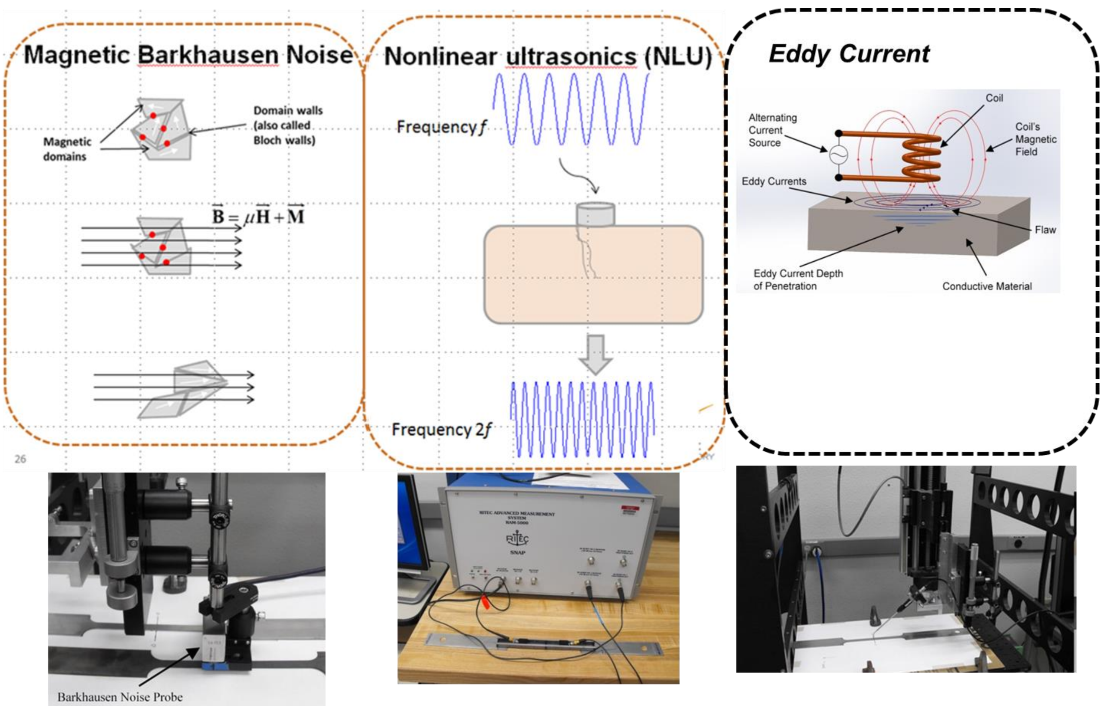

Figure 5.13. Schematic Description of NDE Measurements Used for Evaluating Prototypic Prognostic Methods

5.2.4 Results

Initial (or baseline) measurements using multiple NDE methods were completed on several creep specimens, including on a specimen set aside as a reference or verification standard. The relative change in the measurements provides an understanding of the sensitivity of the NDE technique, and can be related back to the level of accumulated creep strain in the specimen. Note that inferring the present state of material degradation from the measured sensor response is equivalent, in the case of creep damage, to estimating the level of accumulated creep strain in the specimen.

For this reason, we used the creep-strain measurements directly for the purposes of validating the prognostics algorithms. Follow-up assessments using ultrasonic data are ongoing (given the longer-than-anticipated timelines for the creep testing), and analysis status using the ultrasonic data will be presented in subsequent reports.

Figure 5.14(a) shows an example of the experimental strain measurements obtained from accelerated thermal aging of a stainless steel specimen (described in the previous section) at 625°C and 110 MPa in the ex-situ testbed. The measured strains were observed to rise quite rapidly during the first two hours of testing as the specimen temperature and applied load increased to their final values, and the specimen was exposed to steady temperatures and loads. Data from this time period was discarded for the prognostic analysis in this study. After this stage, natural creep progression follows, with the primary and secondary stages of creep damage seen in the data. Specifically, it can be observed from Figure 5.14(a) that there are two distinct stages of creep progression—a rapid increase in creep strain until about 4 hours into the test, followed by a somewhat linear increase in strain after that until the end of the data set at 15 hours. For the purposes of this validation, the creep strain after 15 hours is assumed to indicate end-of-life, based on this test duration (additional studies beyond this limit are ongoing).

The end-of-life threshold for creep strain at t = 15 hours is shown in Figure 5.14(b). Figure 5.14(b) also shows strain measurements selected at an interval of one hour, which will be used as the intermittent measurements for updating Degradation Model predictions. The figure also shows the model-fits from two distinct Degradation Models for characterizing primary and secondary stages of creep progression (Li and Dasgupta 1993; Evans et al. 1992). Model parameters are fitted with the experimental strain measurements and can be mathematically described as:

- Primary stage (Degradation Model 1):
  $\dot{\varepsilon} = a_1\left[1-\exp\left(-a_0 k\right)\right]; \quad t<6; \quad a_1 = 0.0012; \quad a_0 = 0.7936.$
- Secondary stage (Degradation Model 2):
  $\dot{\varepsilon} = a_1 k + a_0; \quad 4<t; \quad a_1 = 0.0756e-3; \quad a_0 = 0.9757e-3.$

It should be mentioned that the experiments were not carried out until failure of the specimen. As a result, the tertiary stage of creep damage (rapid accumulation of creep strain leading to failure) is not observed from the experimental data.

To validate the algorithms, we examined the process uncertainty by varying the model parameters for both primary and secondary stages of creep progression. The shaded regions in Figure 5.14(c) and Figure 5.14(d) are obtained by random sampling from the following assumed distribution of the model parameters.

- Primary stage (Degradation Rate Model 1):
  $\{a_1, a_0\} \in \mathrm{N}\left(0, \sigma^2_{primary}\right); \quad \sigma_{primary} = 1.5\times 10^{-3}.$
- Secondary stage (Degradation Rate Model 2):
  $\{a_1, a_0\} \in \mathrm{N}\left(0, \sigma^2_{secondary}\right); \quad \sigma_{secondary} = 5\times 10^{-4}.$

As can be observed, most of the experimental data (>95%) lies within these shaded regions. Thus, these distributions may be used to characterize process uncertainty in the primary and secondary stages of creep progression. The automatic RJMCMC algorithm developed within this project is used to obtain posterior probabilities of two different models based on the experimental measurements.

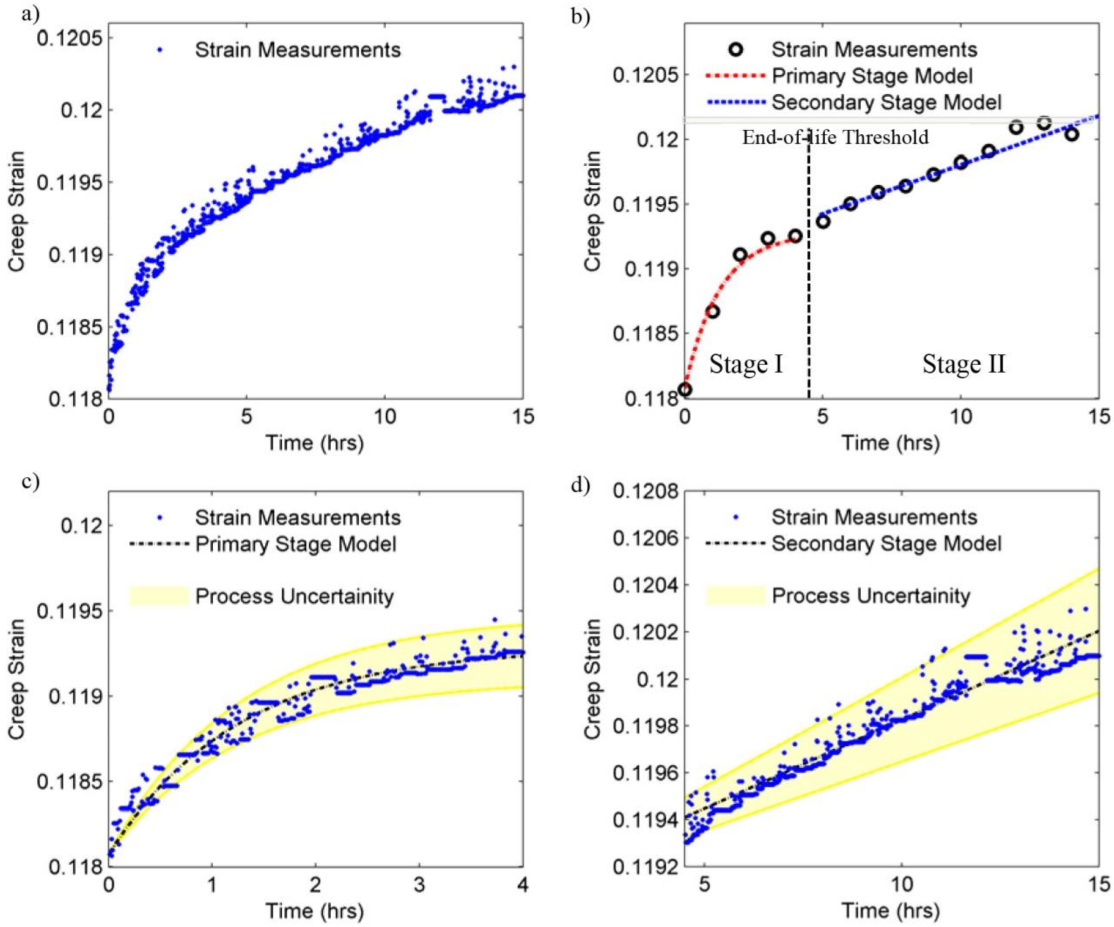

Figure 5.14 Comparison of Strain Measurements. (a) experimental strain measurements on stainless steel specimen under accelerated thermal creep; (b) strain measurements for model prediction update and identified creep models; process uncertainty quantification for (c) primary stage, and (d) secondary stage

Assuming that transitions are equally likely from any model to any other model, and assuming that prior probabilities of each of the Degradation Rate models are equally likely, the posterior probabilities of primary and secondary stage Degradation Rate models after a measurement update is shown in Figure 5.15(a). The posterior probabilities are shown for two different process and measurement noise levels (Figure 5.15(a) and (b)), to determine the sensitivity of the model selection procedure to various uncertainties. Also shown (Figure 5.15(c) and (d)) are the corresponding RUL values, which are estimated by taking the difference between the time index corresponding to the current measurement and the time index when the creep strain is estimated to reach the end-of-life threshold.

The posterior probabilities show the ability of the approach developed within this project to identify the appropriate model, and account for various uncertainty levels. Because the true time-to-failure is known (15 hours, in this example), the error in the estimated RUL may be used as an indicator of the performance of the algorithm. Results from the present data set indicate that the algorithm overestimates the RUL somewhat (as seen in Figure 5.15(c) and (d)); however, the error in RUL appears to be a function of the amount of uncertainty in the data, with higher levels of noise (uncertainty) introducing higher uncertainty into the estimated RUL). Thus, accurate characterization of process uncertainties and measurement noise is important for reliable and robust performance of prognostics algorithms.

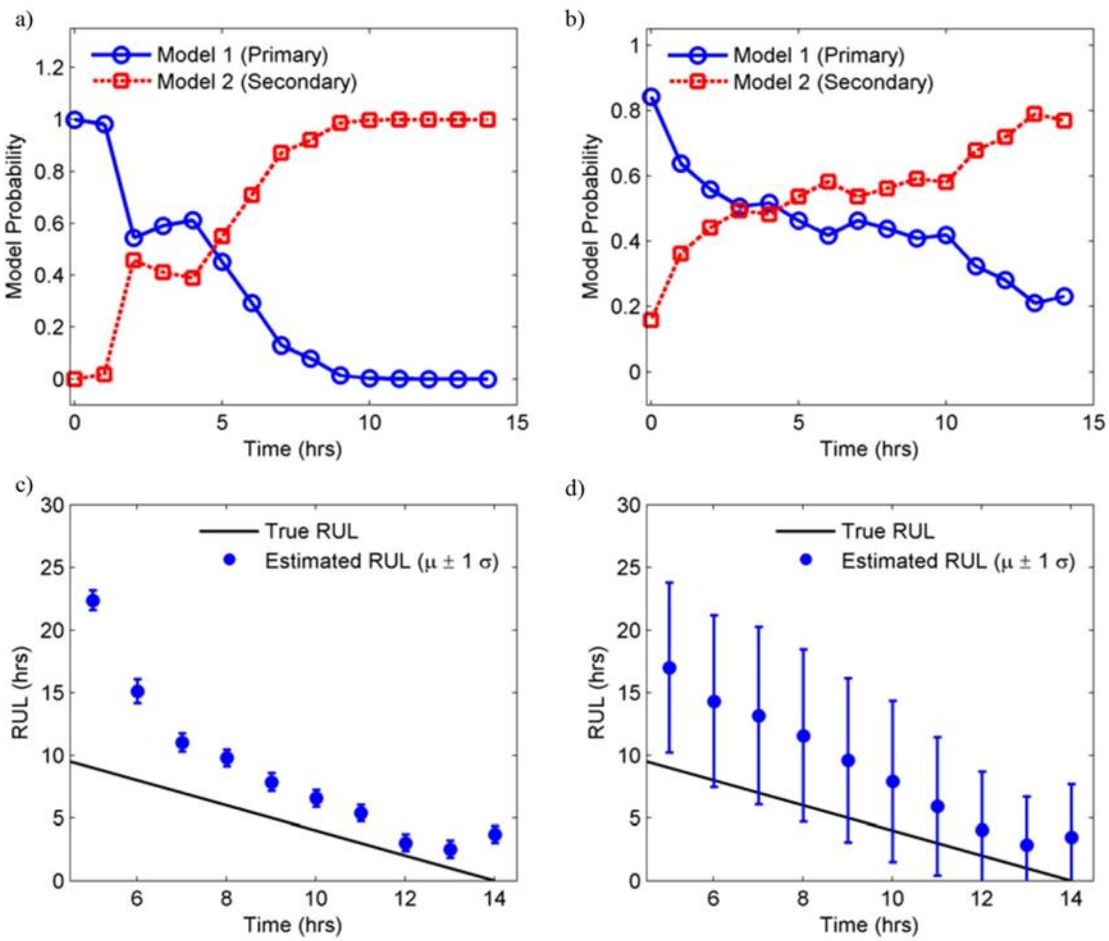

Figure 5.15. Model Posterior Probabilities for Two Models. 'Model 1': Primary Stage, 'Model 2': Secondary Stage and RUL Estimation for Different Process and Measurement Noise Terms;
(a) and (c) Process Noise: $\mathrm{N}\left(0,\sigma^2_{process}\right); \sigma_{process} = 1e-4$,
Measurement Noise: $\mathrm{N}\left(0,\sigma^2_{measurement}\right); \sigma_{measurement} = 5e-5$;
(b) and (d) Process Noise: $\mathrm{N}\left(0,\sigma^2_{process}\right); \sigma_{process} = 1e-4$,
Measurement Noise: $\mathrm{N}\left(0,\sigma^2_{measurement}\right); \sigma_{measurement} = 5e-5$.

5.2.5 Status of Ongoing Experiments for Local and Component-Level PHM

Several experiments are ongoing with a view to generating additional measurements for evaluating the algorithms, as well as to support anticipated future emphasis on measurements and sensing approaches that provide indicators of degradation early in the component lifecycle. In addition to several specimens being tested using the ex-situ testbed, experiments have been initiated in the in-situ testbed. Figure 5.16 shows an example of the measurements obtained during a shake-down test. In particular, measurements of applied load were made, with periodic ultrasonic measurements also taken using the automated data acquisition system. Measurements at several times are shown in the figure, and indicate a gradual change in the shape of the of the measured signal (indicating a change in overall specimen dimensions, resulting in a change in propagating modes in the stress wave). In addition, the non-linear parameter was computed and shows a gradual increase with time (indicative of slowly accumulating damage).

These results are preliminary and additional specimens are being tested within this setup as well, with follow-on studies planned on microstructural characterization, to quantify relationships between the microstructural changes and the observed measurement changes.

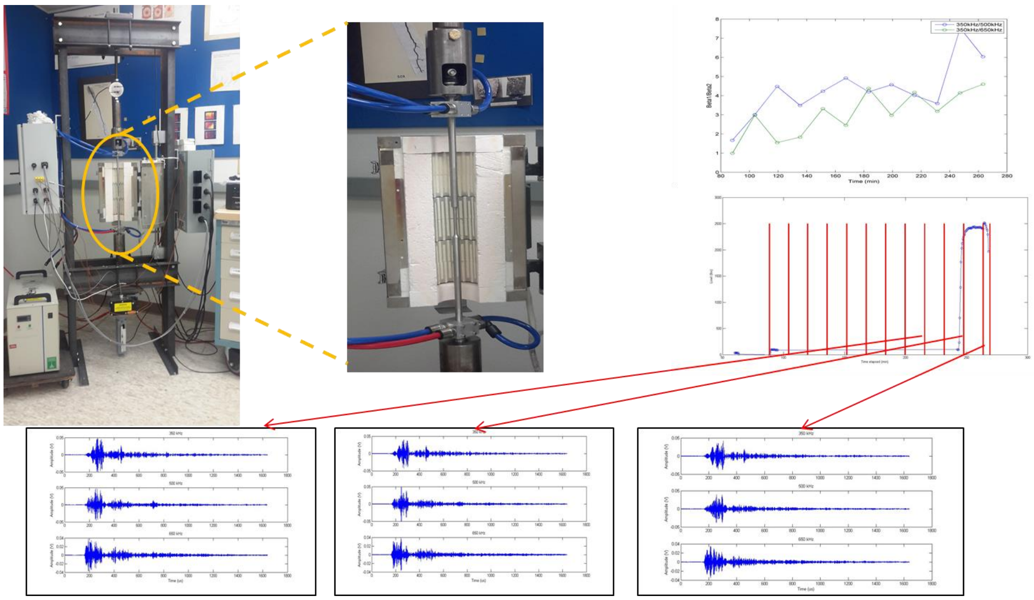

Figure 5.16. Ongoing Testing: In-situ Creep Monitoring

5.3 Discussion

Two laboratory-scale testbeds (ex-situ and in-situ) havebeen built for obtaining data for evaluating (and eventually validating) prognostic algorithms. Results to date using ex-situ testbed data indicate that the proposed Bayesian framework can be used to identify distinct stages of creep progression. However, the accuracy of the prognostic result is dependent on the ability to quantify the sources of uncertainties within the Measurement model and Degradation Rate model used within the Bayesian prognostic methodology.

NDE measurements using the various testbeds also show promising results, with respect to the ability to track degradation in materials and components. These studies will be continued with a view to determining reliability and sensitivity of these measurement approaches, and the applicability of these approaches to use in prognostics for passive components in ARs.

6.0 Summary

PHM technologies are expected to play a vital role in the deployment and safe, cost-effective operation of ARs. Diagnostics and prognostics provide the technical means for enhancing affordability and safe operation of ARs over their lifetime by enabling lifetime management of significant passive components and reactor internals. PHM technologies provide one approach to overcoming challenges due to relatively lower levels of operational experience with AR concepts (when compared with LWRs), and the consequent limited knowledge of physics-of-failure mechanisms of materials and components in AR environments, and can enhance situational awareness with respect to critical systems.

A Bayesian methodology for prognostics has been described for the prediction of remaining life (also know as RUL) of materials and components. Bayesian methods for prognostics have many advantages, including the ability to update the prognostic result as new information (for instance, measurement data) becomes available, and the ability to inherently provide confidence bounds on the prognostic result. While this approach has been previously applied to predict time-to-failure of materials subjected to aging and degradation, a similar approach may be applied to component-level prognostics. For component-level prognostics, appropriate models of component degradation-growth and measurement physics will be needed, and these models are likely to describe performance degradation.

The Bayesian framework for component-level prognostics incorporates the ability to fuse information from multiple sources, including information on localized degradation, and component-level condition indicators. The ability to switch between multiple Degradation Rate models and/or multiple Measurement Physics models becomes important in this context, and an RJMCMC approach has been developed for this purpose.

Evaluations of the Bayesian framework and the RJMCMC model switching/model selection were done using synthetic data as well as experimental measurements on a high-temperature creep testbed. Results to date using this data indicate that the proposed Bayesian framework can be used to identify distinct stages of creep progression. However, the accuracy of the prognostic result is dependent on the ability to quantify the sources of uncertainties within the Measurement model and Degradation Rate model used within the Bayesian prognostic methodology. The use of an explicit model selection method appears to improve the accuracy and error bounds of the prediction, though this needs further evaluation.

7.0 Path Forward

As described in Section 5.0, a set of testbeds (ex-situ and in-situ) are being used to develop the data sets for validation of the prognostic algorithms. Going forward, this effort is going to be used to increase the focus of this work on sensing and measurements (particularly in-situ measurements). This renewed focus on measurements and sensing is with a view to identifying measurement approaches that are most likely to provide indicators of materials and component degradation that are applicable within the prognostics framework. Specifically, the research will address the need for quantitative nondestructive examination analysis tools by examining the sensitivity of advanced NDE methods to relevant degradation mechanisms. Degradation condition indices (along with any associated uncertainties) calculated from these measurements will be integrated with models of material or component failure to enable estimation of remaining life of passive components with detected degradation. The outcomes of these next steps in this research will enable the development of methods for supporting emerging needs within other Technical Areas in the program, particularly the Materials and Fuels areas.

Gaps with respect to deployment of sensors and instrumentation, and integration with plant control algorithms, exist and will be addressed as this research progresses. A key element in the sensing and measurement activities will be the development of approaches for in-situ monitoring that are likely to be applicable in the operational environments of ARs. A critical need for in-situ monitoring is sensors and sensor materials that can withstand the harsh environments. Recent research has led to the development of high-temperature-resistant sensor materials as well as methods for field deployment. These techniques and sensors will be leveraged to enable in-situ monitoring of materials and components.

The testbeds will be further leveraged to generate additional measurement data sets for validation of the prognostic methodology. In addition, opportunities to use other test setups for generating supporting data of relevance to ongoing research within other Technical Areas in the Advanced Reactor Technologies (ART) program will be explored. Results of these efforts will be presented in future reports.

8.0 References

Abram T, and S Ion. 2008. "Generation-IV Nuclear Power: A Review of the State of the Science." *Energy Policy* 36(12):4323-30. 10.1016/j.enpol.2008.09.059.

Arie K, and T Grenci. 2009. "*4s Reactor: Super-Safe, Small and Simple*." Toshiba Corporation.

Arjas E, and J Holmberg. 1995. "Marked Point Process Framework for Living Probabilistic Safety Assessment and Risk Follow-Up." *Reliability Engineering & System Safety* 49(1):59-73. http://www.sciencedirect.com/science/article/pii/0951832095000306. 10.1016/0951-8320(95)00030-6.

Arulampalam MS, S Maskell, N Gordon, and T Clapp. 2002. "A Tutorial on Particle Filters for Online Nonlinear/Non-Gaussian Bayesian Tracking." *IEEE Transactions on Signal Processing* 50(2):174-88. 10.1109/78.978374.

Ashby MF, and DRH Jones. 2012. *Engineering Materials 1, an Introduction to Properties, Applications, and Design, Fourth Edition*. Elsevier Ltd., Waltham, Massachusetts.

ASNT. 2004. *Nondestructive Testing Handbook, Third Edition: Volume 5, Electromagnetic Testing*. American Society for Nondestructive Testing, Columbus, Ohio.

Atkinson CM, and HK Kytömaa. 1992. "Acoustic Wave Speed and Attenuation in Suspensions." *International Journal of Multiphase Flow* 18(4):577-92. http://www.sciencedirect.com/science/article/pii/030193229290053J. 10.1016/0301-9322(92)90053-j.

Bermes C, J-Y Kim, J Qu, and LJ Jacobs. 2008. "Nonlinear Lamb Waves for the Detection of Material Nonlinearity." *Mechanical Systems and Signal Processing* 22(3):638-46. http://www.sciencedirect.com/science/article/pii/S0888327007001872. 10.1016/j.ymssp.2007.09.006.

Bond LJ, SR Doctor, and TT Taylor. 2008. *Proactive Management of Materials Degradation - A Review of Principles and Programs*. Report No. PNNL-17779, Pacific Northwest National Laboratory, Richland, Washington.

Brear JM, and PF Aplin. 1994. Predictive Modelling of Long Term Creep Performance of Critical Plant Components. In *Proceedings of Proceedings of the International Conference on Life Management of Power Plants,* 108-13 pp. IEE, Stevenage, United Kingdom,

Cantrell JH, and WT Yost. 2001. "Nonlinear Ultrasonic Characterization of Fatigue Microstructures." *International Journal of Fatigue* 23:487-90.

Cetiner SM, DL Fugate, RA Kisner, and RT Wood. 2012. *Functional Requirements for Supervisory Control of Advanced Small Modular Reactors*. Report No. SMR/ICHMI/ORNL/TR-2013/03, Oak Ridge National Laboratory, Oak Ridge, Tennessee.

Coble JB, GA Coles, RM Meyer, and P Ramuhalli. 2013a. "Incorporating Equipment Condition Assessment in Risk Monitors for Advanced Small Modular Reactors." *Chemical Engineering Transactions* 33:913-18. 10.3303/CET1333153.

Coble JB, GA Coles, P Ramuhalli, RM Meyer, EJ Berglin, DW Wootan, and MR Mitchell. 2013b. *Technical Needs for Enhancing Risk Monitors with Equipment Condition Assessment for Advanced Small Modular Reactors*. Report No. PNNL-22377 Rev. 0; SMR/ICHMI/PNNL/TR-2013/02, Pacific Northwest National Laboratory, Richland, Washington.

Coble JB, RM Meyer, P Ramuhalli, LJ Bond, HM Hashemian, BD Shumaker, and DS Cummins. 2012a. *A Review of Sensor Calibration Monitoring for Calibration Interval Extension in Nuclear Power Plants*. Report No. PNNL-21687, Pacific Northwest National Laboratory, Richland, Washington.

Coble JB, P Ramuhalli, LJ Bond, JW Hines, and BR Upadhyaya. 2012b. *Prognostics and Health Management in Nuclear Power Plants: A Review of Technologies and Applications*. Report No. PNNL-21515, Pacific Northwest National Laboratory, Richland, Washington.

Csikor FF, C Motz, D Weygand, M Zaiser, and S Zapperi. 2007. "Dislocation Avalanches, Strain Bursts, and the Problem of Plastic Forming at the Micrometer Scale." *Science* 318(5848):251-54. http://www.sciencemag.org/content/318/5848/251.abstract. 10.1126/science.1143719.

Daw J, J Palmer, P Ramuhalli, PE Keller, RO Montgomery, HT Chien, B Tittman, B Reinhardt, GE Kohse, and J Rempe. 2015. *Ultrasonic Transducer Irradiation Test Results*. Presented at ANS Topical Meeting on Nuclear Plant Instrumentation, Control and Human-Machine Interface Technologies (NPIC-HMIT) 2015, Charlotte, North Carolina, American Nuclear Society, La Grange Park, Illinois,

Daw J, J Rempe, J Palmer, P Ramuhalli, PE Keller, RO Montgomery, HT Chien, B Tittman, and B Reinhardt. 2014. *Neet In-Pile Ultrasonic Sensor Enablement-Final Report*. Report No. INL/EXT-14-32505; PNNL-23746, Idaho National Laboratory, Idaho Falls, Idaho.

Daw J, J Rempe, J Palmer, P Ramuhalli, RO Montgomery, HT Chien, B Tittman, B Reinhardt, and GE Kohse. 2013. *Neet In-Pile Ultrasonic Sensor Enablement-FY 2013 Status Report*. Report No. PNNL-22801; INL/EXT-13-29144 Rev. 0, Idaho National Laboratory, Idaho Falls, Idaho.

Daw J, J Rempe, P Ramuhalli, R Montgomery, HT Chien, B Tittmann, and B Reinhardt. 2012. *Neet In-Pile Ultrasonic Sensor Enablement-FY 2012 Status Report*. Report No. INL/EXT-12-27233, PNNL-21835, Idaho National Laboratory, Idaho Falls, Idaho.

De S, S Palit Sagar, S Dey, A Prakash, and I Chattoraj. 2010. "Quantification of Pitting in Two Tempers of 7075 Aluminium Alloy by Non-Destructive Evaluation." *Corrosion Science* 52(5):1818-23. http://www.sciencedirect.com/science/article/pii/S0010938X10000284. 10.1016/j.corsci.2010.01.023.

Doctor SR. 2008. *The History and Future of Nde in the Management of Nuclear Power Plant Materials Degradation*. Presented at Proceedings of the ASME 2008 Pressure Vessels and Piping Division Conference, Chicago, Illinois, 197-207 pp. American Society of Mechanical Engineers, New York,

Doctor SR, SM Bruemmer, MS Good, LA Charlot, TT Taylor, DM Boyd, JD Deffenbaugh, and LD Reid. 1989. *Utilization of Ultrasonic Measurements to Quantify Aging-Induced Material Microstructure and Property Changes*. Presented at Nondestructive Monitoring of Materials Properties Symposium, Boston, Massachusetts, 143-49 pp. Materials Research Society, Pittsburgh, Pennsylvania, Donoghue JE, JN Donohew, GR Golub, RM Kenneally, PB Moore, SP Sands, ED Throm, and BA Wetzel. 1994. *Preapplication Safety Evaluation Report for the Power Reactor Innovative Small Module (Prism) Liquid-Metal Reactor. Final Report*. Report No. NUREG-1368, U.S. Nuclear Regulatory Commission, Washington, D.C. http://www.osti.gov/energycitations/servlets/purl/10133164-2ZfTJr/native/.

Doucet A, S Godsill, and C Andrieu. 2000. "On Sequential Monte Carlo Sampling Methods for Bayesian Filtering." *Statistics and Computing* 10:197-208. 10.1023/A:1008935410038.

Ensminger D, and LJ Bond. 2011. *Ultrasonics: Fundamentals, Technology and Applications, Third Edition (Revised and Expanded)*. CRC Press, Boca Raton, Florida.

Evans RW, JD Parker, and B Wilshire. 1992. "The Θ Projection Concept—A Model-Based Approach to Design and Life Extension of Engineering Plant." *International Journal of Pressure Vessels and Piping* 50(1–3):147-60. http://www.sciencedirect.com/science/article/pii/030801619290035E. http://dx.doi.org/10.1016/0308-0161(92)90035-E.

General Atomics. 1996. *Gas Turbine-Modular Helium Reactor (Gt-Mhr): Conceptual Design Description Report*. Report No. Report No. 910720, Rev. 1, General Atomics, San Diego, California.

Goebbels K. 1994. *Materials Characterization for Process Control and Product Conformity*. CRC Press, Boca Raton, Florida.

Gorkunov ES, YN Dragoshanskii, and M Mikhovski. 2000. "Barkhausen Noise and Its Utilization in Structural Analysis of Ferromagnetic Materials (Review Article V-Effects of Volume and Surface Thermal Processing)." *Russian Journal of NDT* 36(6):389-417.

Green PJ. 1995. "Reversible Jump Markov Chain Monte Carlo Computation and Bayesian Model Determination." *Biometrika* 82(4):711-32.

Guan X, R Jha, and Y Liu. 2011. "Model Selection, Updating, and Averaging for Probabilistic Fatigue Damage Prognosis." *Structural Safety* 33(3):242-49. 10.1016/j.strusafe.2011.03.006.

Guler A, D Mandelli, A Alfonsi, J Cogliati, C Rabiti, and T Aldemir. 2014. *Methodology for the Incorporation of Passive Component Aging into the Raven/Relap-7 Environment*. Presented at Proceedings of the 2014 ANS Winter Meeting and Technology Expo, Anaheim, California, American Nuclear Society, La Grange, Illinois,

Hakan Gur C, and I Cam. 2007. "Comparison of Magnetic Barkhausen Noise and Ultrasonic Velocity Measurements for Microstructure Evaluation of Sae 1040 and Sae 4140 Steels." *Materials Characterization* 58(5):447-54.

Hastie DI, and PJ Green. 2012. "Model Choice Using Reversible Jump Markov Chain Monte Carlo." *Statistica Neerlandica* 66(3):309-38. http://dx.doi.org/10.1111/j.1467-9574.2012.00516.x. 10.1111/j.1467-9574.2012.00516.x.

Hastings WK. 1970. "Monte Carlo Sampling Methods Using Markov Chains and Their Applications." *Biometrika* 57(1):97-109. http://biomet.oxfordjournals.org/content/57/1/97.abstract. 10.1093/biomet/57.1.97.

Hines JW, J Garvey, J Preston, and A Usynin. 2009. *Tutorial: Empirical Methods for Process and Equipment Prognostics*. Presented at Annual Reliability and Maintainability Symposium (RAMS), 2009 Proceedings, Ft. Worth, Texas, Institute of Electrical and Electronics Engineers Inc., Piscataway, New Jersey,

Hoffman EA, WS Yang, and RN Hill. 2006. *Preliminary Core Design Studies for the Advanced Burner Reactor over a Wide Range of Conversion Ratios*. Report No. ANL-AFCI-177, Argonne National Laboratory, Argonne, Illinois. http://www.osti.gov/energycitations/servlets/purl/973480-o1tvNg/.

Horn RA, and CR Johnson. 1985. *Matrix Analysis*. Cambridge University Press, Cambridge, Massachusetts.

Hosford WF. 2005. *Mechanical Behavior of Materials*. Cambridge University Press.

IAEA. 2011. *Status Report 96 - High Temperature Gas Cooled Reactor - Pebble-Bed Module (Htr-Pm)*. Report, International Atomic Energy Agency (IAEA), Vienna, Austria.

Jiles DC. 2000. "Dynamics of Domain Magnetization and the Barkhausen Effect." *Czechoslovak Journal of Physics* 50(8):893-988.

Jiles DC. 2011. *Theory and Practice: Making Use of the Barkhausen Effect*. Presented at The Workshop on Large Fluctuations and Collective Phenomena in Disordered Materials, Champaign-Urbana, IL, 26 pp. Institute for Condensed Matter Theory & Materials Computation Center, University of Illinois at Urbana-Champaign, Champaign-Urbana, IL.

Kafka P. 2008. "Probabilistic Risk Assessment for Nuclear Power Plants." In *Handbook of Performability Engineering,* ed. KB Misra, pp. 1179-92. Springer, London.

Kameda J, and R Ranjan. 1987. "Nondestructive Evaluation of Steels Using Acoustic and Magnetic Barkhausen Signals – I. Effect of Carbide Precipitation and Hardness." *Acta Metallurgica* 35(7):1515-26.

Khan T. 2009. "A Sequential Monte Carlo Based Recursive Technique for Solving Nde Inverse Problems." Michigan State University, East Lansing, Michigan: Ph.D.

Khan T, and P Ramuhalli. 2008. "A Recursive Bayesian Estimation Method for Solving Electromagnetic Nde Inverse Problems." *IEEE Transactions on Magnetics* 44(7):1845-55.

Khan T, P Ramuhalli, and S Dass. 2011. "Particle-Filter Based Multisensor Fusion for Solving Low-Frequency Electromagnetic Nde Inverse Problems." *IEEE Transactions on Instrumentation and Measurement* 60(6):2142-53.

Kobayashi M, TR Olding, M Sayer, and CK Jen. 2002. "Piezoelectric Thick Film Ultrasonic Transducers Fabricated by a Sol–Gel Spray Technique." *Ultrasonics* 39:675-80.

Krause TW, L Clapham, and DL Atherton. 1994. "Characterization of the Magnetic Easy Axis in Pipeline Steel Using Magnetic Barkhausen Noise." *Journal of Applied Physics* 75(12):7983-88.

Krause TW, A Pattantyus, and DL Atherton. 1995. "Investigation of Strain Dependent Magnetic Barkhausen Noise in Steel." *IEEE Transactions on Magnetics* 31(6):3376-78.

Krautkrämer J, and H Krautkrämer. 1990. *Ultrasonic Testing of Materials, 4th Fully Revised Edition*. Springer-Verlag, New York.

Kyung-Young J. 2000. "Applications of Nonlinear Ultrasonics to the Nde of Material Degradation." *IEEE Transactions on Ultrasonics, Ferroelectrics and Frequency Control* 47(3):540-48. 10.1109/58.842040.

Li J, and A Dasgupta. 1993. "Failure-Mechanism Models for Creep and Creep Rupture." *IEEE Transactions on Reliability* 42(3):339-53. http://ieeexplore.ieee.org/ielx1/24/6538/00257816.pdf?tp=&arnumber=257816&isnumber=6538. 10.1109/24.257816.

Libby HL. 1971. *Introduction to Electromagnetic Nondestructive Test Methods*. Wiley-Interscience, New York.

Lindgren M, and T Lepistö. 2001. "Effect of Prestraining on Barkhausen Noise Vs. Stress Relation." *NDT & E International* 34(5):337-44. http://www.sciencedirect.com/science/article/pii/S0963869500000736. 10.1016/s0963-8695(00)00073-6.

Manjoine MJ. 1985. "Creep-Rupture Characteristics of Type 304 Stainless Steel Weldments with Type 308 Stainless Steel Welds at 1100°F." *Welding Research Supplement*:171s-79s.

Matlack KH, JY Kim, LJ Jacobs, J Qu, and PM Singh. 2012a. "Nonlinear Rayleigh Waves to Detect Initial Damage Leading to Stress Corrosion Cracking in Carbon Steel." *AIP Conference Proceedings* 1430(1):1452-59. http://dx.doi.org/10.1063/1.4716387.

Matlack KH, JJ Wall, J-Y Kim, J Qu, LJ Jacobs, and W-W Viehrig. 2012b. "Evaluation of Radiation Damage Using Nonlinear Ultrasound." *Journal of Applied Physics* 111(5):054911-1 to 11-3.

McCloy JS, RO Montgomery, P Ramuhalli, RM Meyer, SY Hu, Y Li, CH Henager Jr., and BR Johnson. 2013. *Materials Degradation and Detection (Md2): Deep Dive Final Report*. Report No. PNNL-22309, Pacific Northwest National Laboratory, Richland, Washington.

Meyer RM, JB Coble, EH Hirt, P Ramuhalli, MR Mitchell, DW Wootan, EJ Berglin, LJ Bond, and CH Henager Jr. 2013a. *Technical Needs for Prototypic Prognostic Technique Demonstration for Advanced Small Modular Reactor Passive Components*. Report No. PNNL-22488 Rev. 0, SMR/ICHMI/PNNL/TR-2013/01, Pacific Northwest National Laboratory, Richland, Washington.

Meyer RM, JB Coble, and P Ramuhalli. 2013b. *Requirements for Prognostic Health Management of Passive Components in Advanced Small Modular Reactors*. Presented at 2013 IEEE Conference on Prognostics and Health Management (PHM), Gaithersburg, Maryland, 1-8 pp. IEEE,

Meyer RM, P Ramuhalli, JB Coble, MR Mitchell, DW Wootan, EH Hirt, EJ Berglin, LJ Bond, and CH Henager. 2013c. *Prognostics Health Management for Advanced Small Modular Reactor Passive Components*. Presented at Proceedings of the Annual Conference of the Prognostics and Health Management Society (PHM 2013), October 14-17, New Orleans, Louisiana, Rochester, NY, Paper No. 071 pp. Prognostics and Health Management Society,

Meyer RM, P Ramuhalli, EH Hirt, AF Pardini, AM Jones, JE Deibler, SG Pitman, JC Tucker, M Prowant, and JD Suter. 2013d. *Prototypic Prognostics Health Management Systems for Passive*

Advsmr Components. Report No. PNNL-22889 Rev. 0, SMR/ICHMI/PNNL/TR-2013/06, Pacific Northwest National Laboratory, Richland, Washington.

Minato A, and N Handa. 2000. *Advanced 4s (Super Safe, Small and Simple) Lmr*. Presented at Proceedings of an Advisory Group Meeting, Obninsk, Russian Federation, 157-76 pp. International Atomic Energy Agency, Vienna, Austria,

Moorthy V, S Vaidyanathan, T Jayakumar, and B Raj. 1997. "Microstructural Characterization of Quenched and Tempered 0.2% Carbon Steel Using Magnetic Barkhausen Noise Analysis." *Journal of Magnetism and Magnetic Materials* 171:179-89.

Nagy PB. 1998. "Fatigue Damage Assessment by Nonlinear Ultrasonic Materials Characterization." *Ultrasonics* 36(1–5):375-81. http://www.sciencedirect.com/science/article/pii/S0041624X97000401. http://dx.doi.org/10.1016/S0041-624X(97)00040-1.

Nam A, ME Sharp, JW Hines, and BR Upadhyaya. 2012. *Bayesian Methods for Successive Transitioning between Prognostic Types: Lifecycle Prognostics*. Presented at 8th International Topical Meeting on Nuclear Plant Instrumentation, Control and Human Machine Interface Technologies, NPIC&HMIT 2012, San Diego, California, American Nuclear Society,

Naumenko KD, and H Altenbach. 2007. *Modeling of Creep for Structural Analysis*. Springer.

Newton MA, and AE Raftery. 1994a. "Approximate Bayesian Inference with the Weighted Likelihood Bootstrap." *Journal of the Royal Statistical Society. Series B (Methodological)*:3-48.

Newton MA, and AE Raftery. 1994b. "Approximate Bayesian Inference with the Weighted Likelihood Bootstrap." *Journal of the Royal Statistical Society. Series B (Methodological)* 56:3-48.

O'Donnell WJ, AB Hull, and SN Malik. 2008. *Historical Context of Elevated Temperature Structural Integrity for Next Generation Plants: Regulatory Safety Issues in Structural Design Criteria of Asme Section III Subsection Nh*. Presented at 2008 ASME Pressure Vessel and Piping Division Conference (PVP2008), Chicago, Illinois, 729-38 pp.

OECD/NEA. 2005. *Status Report on Developments and Cooperation on Risk-Informed In-Servce Inspection and Non-Destructive Testing (Ndt) Qualification in Oecd/Nea Member Countries*. Report No. NEA/CSNI/R(2005)9, Organisation for Economic Co-Operations and Development (OECD)/Nuclear Energy Agency (NEA), Committee on the Safety of Nuclear Installations (CSNI), Paris, France.

OECD/NEA. 2010. *Ec-Jrc/Oecd-Nea Benchmark Study on Risk Informed In Service Inspection Methodologies (Rismet)*. Report No. NEA/CSNI/R(2010)13, Organisation for Economic Co-Operations and Development (OECD)/Nuclear Energy Agency (NEA), Committee on the Safety of Nuclear Installations, Paris, France. http://www.oecd-nea.org/nsd/docs/2010/csni-r2010-13.pdf.

Parakka AP, J Batey, DC Jiles, M Zang, and H Gupta. 1997. "Effect of Surface Mechanical Changes on Magnetic Barkhausen Emissions." *IEEE Transactions on Magnetics* 33(5):ES-09.

Parks D, and BR Tittmann. 2011. *Ultrasonic Nde in a Reactor Core*. Presented at 38th Annual Review of Progress in Quantitative NDE, Burlington, Vermont, Parks DA, BR Tittmann, and MM Kropf. 2010. *Aluminum Nitride as a High Temperature Transducer*. Presented at Review of Progress in Quantitative Nondestructive Evaluation, Vol. 29, Kingston, Rhode Island, 1029-34 pp. American Institute of Physics, Melville, New York,

Perez-Benitez JA, J Capo-Sanchez, J Anglada-Rivera, and LR Padovese. 2005. "A Model for the Influence of Microstructural Defects on Magnetic Barkhausen Noise in Plain Steels." *Journal of Magnetism and Magnetic Materials* 288:433-42.

Phillips JH. 2005. "*Risk-Informed Inspection of Nuclear Power Plants.*" Idaho National Laaboratory, Lake Buena Vista, Florida.

Raj B, A Kumar, and T Jayakumar. 2000. "Ultrasonic Spectral Analysis for Microstructural Characterization of Austenitic and Ferritic Steels." *Philosophical Magazine A (UK)* 80(11):2469-87.

Ramuhalli P, GA Coles, JB Coble, and EH Hirt. 2013. *Technical Report on Preliminary Methodology for Enhancing Risk Monitors with Integrated Equipment Condition Assessment*. Report No. PNNL-22752, Rev. 0; SMR/ICHMI/PNNL/TR-2013/05, Pacific Northwest National Laboratory, Richland, Washington.

Ramuhalli P, JW Griffin, JM Fricke, and LJ Bond. 2012. An Assessment of Uncertainty in Remaining Life Estimation for Nuclear Structural Materials. In *Proceedings of 8th International Topical Meeting on Nuclear Plant Instrumentation, Control, and Human-Machine Interface Technologies 2012, NPIC and HMIT 2012: Enabling the Future of Nuclear Energy, July 22-25, 2012, San Diego, California,* 1325-37 pp. American Nuclear Society,

Ramuhalli P, EH Hirt, GA Coles, CA Bonebrake, BJ Ivans, DW Wootan, and MR Mitchell. 2014a. *An Updated Methodology for Enhancing Risk Monitors with Integrated Equipment Condition Assessment*. Report No. PNNL-23478, Rev. 0; SMR/ICHMI/PNNL/TR-2014/01, Pacific Northwest National Laboratory, Richland, Washington.

Ramuhalli P, S Roy, EH Hirt, AF Pardini, AM Jones, JE Deibler, SG Pitman, JC Tucker, M Prowant, and JD Suter. 2014b. *Local-Level Prognostics Health Management Systems Framework for Passive Advsmr Components - Interim Report*. Report No. PNNL-23625 Rev. 0; SMR/ICHMI/PNNL-TR-2014/02, Pacific Northwest National Laboratory, Richland, Washington.

Ranjan R, O Buck, and RB Thompson. 1987a. "A Study on the Effect of Dislocation on the Magnetic Properties of Nickel Using Magnetic Nde Methods." *Journal of Applied Physics* 61(8):3196-98.

Ranjan R, DC Jiles, O Buck, and RB Thompson. 1987b. "Grain Size Measurement Using Magnetic and Acoustic Barkhausen Noise." *Journal of Applied Physics* 61(8):3199-201. http://link.aip.org/link/?JAP/61/3199/1

http://dx.doi.org/10.1063/1.338900.

Ristic B, S Arulampalam, and N Gordon. 2004. *Beyond the Kalman Filter: Particle Filters for Tracking Applications*. Artech House.

Roy S, P Ramuhalli, EH Hirt, MS Prowant, AF Pardini, and SG Pitman. 2015. *Probabilistic Model Selection for Prognostics of Thermal Creep in Advanced Reactors*. Presented at ANS Topical Meeting on Nuclear Plant Instrumentation, Control and Human-Machine Interface Technologies

(NPIC-HMIT) 2015, Charlotte, North Carolina, American Nuclear Society, La Grange Park, Illinois,

Sagar PS, N Parida, S Das, G Dobmann, and DK Bhattacharya. 2005. "Magnetic Barkhausen Emission to Evaluate Fatigue Damage in a Low Carbon Structural Steel." *International Journal of Fatigue* 27(3):317-22. 10.1016/j.ijfatigue.2004.06.015.

Shintaku Y, Y Ohara, M Hashimoto, S Horinouchi, and K Yamanaka. 2010. *Evaluation of Stress Corrosion Cracks in Metals by Linear and Nonlinear Ultrasound*. Presented at 20th International Congress on Acoustics (ICA 2010), Sydney, Australia, 473 pp.

Shui G, J-Y Kim, J Qu, Y-S Wang, and LJ Jacobs. 2008. "A New Technique for Measuring the Acoustic Nonlinearity of Materials Using Rayleigh Waves." *NDT & E International* 41(5):326-29. http://www.sciencedirect.com/science/article/pii/S096386950800008X. 10.1016/j.ndteint.2008.01.007.

Sinding K, A Orr, B Reinhardt, L Tien, N Malarich, and B Tittman. 2014a. *Spray-on Ferroelectrics for Fabrication of Custom Tailored Composite Transducers for Nde and Shm*. Presented at Proceedings of the Joint IEEE International Symposium on the Applications of Ferroelectrics, University Park, Pennsylvania, IEEE, Piscataway, New Jersey,

Sinding K, C Searfass, N Malarich, B Reinhardt, and BR Tittmann. 2014b. *High Temperature Ultrasonic Transducers for the Generation of Guided Waves for Non-Destructive Evaluation of Pipes*. Presented at Review of Progress in Quantitative Nondestructive Evaluation, Vol. 33, AIP Conference Proceedings Vol. 1581, Baltimore, Maryland, 302-07 pp. American Institute of Physics, Mellville, New York,

Singh R. 2000. *Three Decades of Ndi Reliability Assessment*. Report No. Karta-3510-99-01, Karta Technology, Inc., San Antonio, Texas.

Sposito G, C Ward, P Cawley, PB Nagy, and C Scruby. 2010. "A Review of Non-Destructive Techniques for the Detection of Creep Damage in Power Plant Steels." *NDT & E International* 43(7):555-67. <Go to ISI>://WOS:000281348000003. 10.1016/j.ndteint.2010.05.012.

Stupakov O, J Pal'a, V Yurchenko, I Tomáš, and J Bydžovský. 2008. "Measurement of Barkhausen Noise and Its Correlation with Magnetic Permeability." *Journal of Magnetism and Magnetic Materials* 320(3-4):204-09. 10.1016/j.jmmm.2007.05.022.

Sullivan DO, M Cotterell, DA Tanner, and I Meszaros. 2004. "Characterisation of Ferritic Stainless Steel by Barkhausen Techniques." *NDT & E International* 37(6):489-96.

TAREF. 2011. *Experimental Facilities for Sodium Fast Reactor Safety Studies*. Report No. NEA/CSNI/R(2010)12, Nuclear Enenrgy Agency (NEA), Organisation for Economic Co-operation and Develop (OECD), Task Group on Advanced Reactor Experimental Facilities (TAREF).

Toshiba. 2011. *Status Report 76 - Super-Safe, Small and Simple Reactor (4s)*. Report, International Atomic Energy Agency, Vienna, Austria.

Turner RC, PA Fuierer, RE Newnham, and TR Shrout. 1994. "Materials for High Temperature Acoustic and Vibration Sensors: A Review." *Applied Acoustics* 41:229-324.

Unwin SD, PP Lowry, RF Layton, Jr., PG Heasler, and MB Toloczko. 2011. *Multi-State Physics Models of Aging Passive Components in Probabilistic Risk Assessment*. Presented at Proceedings of ANS PSA 2011, International Topical Meeting on Probabilistic Safety Assessment and Analysis, Wilmington, North Carolina, American Nuclear Society, La Grange, Illinois,

Unwin SD, PP Lowry, and MY Toyooka. 2012. "Reliability Models of Aging Passive Components Informed by Materials Degradation Metrics to Support Long-Term Reactor Operations." *Nuclear Science and Engineering* 171(1):69-77. 10.13182/NSE11-18.

Veilleux J, SE Kruger, K-T Wu, and A Blouin. 2013. *Multi-Element, High-Temperature Integrated Ultrasonic Transducers for Structural Health Monitoring*. Presented at Proceedings of SPIE, Smart Sensor Phenomena, Technology, Networks, and Systems Integration 2013, Volume 8693, San Diego, California, 86930I to 30I-8 pp. Society of Photo-Optical Instrumentation Engineers, Bellingham, Washington,

Vesely WE, and AJ Wolford. 1988. "Risk Evaluations of Aging Phenomena: The Linear Aging Reliability Model and Its Extensions." *Nuclear Engineering and Design* 108:179-85.

Wilkowski G, R Tregoning, P Scott, and D Rudland. 2002. *Status of Efforts to Evaluate Loca Frequency Estimates Using Combined Pra and Pfm Approaches*. Presented at 28th MPA-Seminar, Universitaet Stuttgart, Germany, Materials Testing Institute,

Wu JS, and GE Apostolakis. 1992. "Experience with Probabilistic Risk Assessment in the Nuclear Power Industry." *Journal of Hazardous Materials* 29(3):313-45.

Zarembo LK, and VA Krasil'nikov. 1971. "Nonlinear Phenomena in the Propagation of Elastic Waves in Solids." *Soviet Physics Uspekhi* 13(6):778-97. 10.1070/PU1971v013n06ABEH004281.

Zhang S, X Jiang, M Lapsley, P Moses, and TR Shrout. 2010. "Piezoelectric Accelerometers for Ultrahigh Temperature Application." *Applied Physics Letters* 96(1):013506-3. http://dx.doi.org/10.1063/1.3290251.

Appendix A

Summary Description of Near-Term Advanced Reactor Concepts and Expected Environments

Appendix A

Summary Description of Near-Term Advanced Reactor Concepts and Expected Environments

A.1 Sodium Fast Reactors

The sodium-cooled fast reactor (SFR) features very high core power densities, high reactor outlet temperatures, low system pressure (atmospheric), and a fast neutron spectrum. An advantage of sodium coolant is its relatively high heat capacity, which enables very efficient heat transfer from the core. However, internal core and reactor vessel components are exposed to a significant fast neutron flux. While sodium has the advantage that it does not corrode steel components, it does react chemically with air and water so the design of SFR components must take this into consideration.

The primary coolant system can either be arranged in a pool layout (a common approach, where all primary system components are housed in a single vessel), or in a compact loop layout. Several domestic SFR designs (e.g., Power Reactor Innovative Small Module [PRISM], traveling-wave reactor [TWR]) use a pool-type reactor vessel design containing the reactor core, primary heat-exchanger, and mechanical or electromagnetic (EM) pumps. An inert cover gas system is required to maintain sodium purity and to prevent the sodium from reacting with moisture in the air. In general, penetrations into the reactor vessel occur at the top of the vessel. Further information regarding modularized SFR concepts is provided in Table A.1 (Meyer et al. 2013a).

Key passive components in SFRs that could benefit from PHM include:

- Heat exchangers
- Reactor vessel, reactor core, reactor shields / reflectors / absorber
- Piping
- Tanks

Table A.1. Summary of Typical Operating Parameters for SFRs (Meyer et al. 2013a)

Parameter	Typical Values		References
Temperatures (°C)	Coolant Max	704 with max ramp rate of 9°C/sec	Minato and Handa (2000) Donoghue et al. (1994)
	Sodium Coolant Boiling	980 @ 0.2 MPa	TAREF (2011)
	Fuel (Max.)	810; ~ 825 (peak bounding)	Minato and Handa (2000) Arie and Grenci (2009) Toshiba (2011) Donoghue et al. (1994)
	Reactor Vessel Wall (Operating)	426	Minato and Handa (2000) Arie and Grenci (2009) Toshiba (2011) Donoghue et al. (1994)
	Reactor Vessel Wall (Max)	705	Minato and Handa (2000) Arie and Grenci (2009) Toshiba (2011) Donoghue et al. (1994)
	Primary Loop (Inlet/Outlet)	338 / 485	Donoghue et al. (1994)
	Secondary Loop (Inlet/Outlet)	282 / 443	Donoghue et al. (1994)
	Steam Generator (water)	285	Donoghue et al. (1994)
Pressures (MPa)	Primary Coolant (normal operations)	Near ambient (enough to circulate sodium) to 0.2	
	Reactor Vessel Design	0.3	Arie and Grenci (2009)
	IHX	0.88	Minato and Handa (2000)
	Water/Steam	6.9–10.5	Minato and Handa (2000) Donoghue et al. (1994)
Flow Rates (PRISM)	Primary Loop (Sodium)	174,128 (l/min)	Donoghue et al. (1994)
	Secondary Loop (Sodium)	156,148 (l/min)	Donoghue et al. (1994)
	At Steam Generator		Donoghue et al. (1994)
	Sodium	8.30×10^6 (kg/hr)	
	Water	1.025×10^6 (kg/hr)	
	Steam	9.30×10^5 (kg/hr)	
Power Density	17 (4S)-210(PRISM) (MW/m^3 or kW/l)		
Neutron Fluence	Peak fast fluence limit	4.0×10^{23} n/cm^2	Hoffman et al. (2006)
	Reactor Vessel	6.8×10^{12} n/cm^2	Donoghue et al. (1994)

A.2 Very-High-Temperature Gas Reactors

The very-high-temperature gas reactor (VHTR) is an evolution of high-temperature gas-cooled reactor (HTGR) technology. VHTRs are distinguished by the intent to operate at greater temperatures (up to 1000°C) to facilitate hydrogen production, creating significantly greater materials challenges. The main characteristics of VHTRs include the use of helium gas for coolant, use of graphite for major core and in-vessel components, low power density, high operating temperature, use of coated fuel particles, and reliance on passive mechanisms for heat removal in the event of a loss-of-coolant accident (LOCA). These design characteristics help maintain the integrity of the fuel and prevent the release of radioactive materials in the event of severe accidents. Another significant advantage of the helium gas reactor designs is that they enable direct coupling to He-Brayton energy conversion cycles.

Two major VHTR design variants include the pebble bed and prismatic block reactors. In the pebble bed reactors, coated fuel particles are embedded in spherical graphite pebbles, which circulate through the core. Reactivity is controlled through the distribution of pebbles loaded with fuel and absorber materials. This reactor concept enables online refueling as individual pebbles can be removed from the core and fresh pebbles added continuously. In prismatic block reactors, the coated fuel particles are embedded in a graphite matrix that is formed into prismatic blocks, so that the reactor must be shut down for refueling and control rods are employed for reactivity control. Table A.2 contains further information about VHTR concepts, while Table A.3 contains additional information about gas-cooled reactor concepts (Meyer et al. 2013a).

Table A.2. Summary of Design Parameters for Several Recent GCR Concepts (Meyer et al. 2013a)

General GCR Design Features	Parameters
Coolant	He (most common); other: N_2, air
Thermal Capacity Range (MWth)	~5–600
Gross Electrical Capacity Range (MWe)	2–285
Refueling Frequency (years)	1.5; 5–10; 30 (continuous for pebble bed)
Fuel Cycle	Once through, breed and burn

Key passive components in gas-cooled reactors (GCRs) that could benefit from PHM include:

- Heat exchangers
- Reactor vessel, reactor core, reactor shields/reflectors
- Piping – connecting to and outside of reactor vessel

Table A.3. Summary of Typical Operating Parameters for GCRs (Meyer et al. 2013a)

Parameter	Value		Reference
Temperature Range (°C)	Core Inlet	250–587	
	Core Outlet	530–850	
	For Hydrogen Productions	900–1000	
	Fuel (max.)	1238 (limit 1600)	
Pressure Range (MPa)	5–~9		
He Mass Flow Rate (kg/s)	96–320		General Atomics (1996) IAEA (2011)
Power Density (MW/m^3 or kW/l)	4–6.5		

Appendix B

Nondestructive Evaluation (NDE) Techniques

Appendix B

Nondestructive Evaluation (NDE) Techniques

Current in-service inspection (ISI) practices for light-water-cooled reactors (LWRs) are based on requirements in the ASME Boiler and Pressure Vessel Code (Code), which were originally developed in the 1960s for the management of fatigue degradation (Doctor 2008). Current ISI requirements are challenged by the emergence of diverse and challenging degradation mechanisms in nuclear power plants, such as stress corrosion cracking (SCC). In addition, as plants continue to age, it can be anticipated that new degradation mechanisms will continue to manifest in components (Wilkowski et al. 2002). Advanced reactors, with their higher operating temperatures and corrosive coolant chemistry, can be expected to experience mechanisms not commonly seen in LWRs (O'Donnell et al. 2008). Mitigation of such degradation mechanisms will require early warning to ensure that appropriate actions can be taken before significant degradation accumulates to the point where the only possible mitigating action is to replace the component.

To address these issues, it is likely that a combination of online, in-situ monitoring with periodic offline measurements of component or material condition will be needed (Meyer et al. 2013a). Such monitoring of materials degradation is expected to provide a better understanding of the surface and volumetric material changes occurring during the early stages of the incubation and micro-damage accumulation. By detecting the presence of material degradation mechanisms early in the process, better insights are gained about the state of the material that can be used to understand the precise margins to failure. A brief state-of-the-art assessment for real-time monitoring of early degradation in materials used in the production of nuclear power, including creep measurement techniques is covered in McCloy et al. (2013).

A critical step in achieving this objective is to develop an appropriate means to detect minor changes in material microstructures at the onset of degradation. Measurement techniques to estimate creep degradation are intended to address the challenges associated with the ability to perform real-time monitoring of material degradation. However, the use of sensors for long-term condition monitoring in harsh environments is likely to result in a gradual change in the sensor response and sensitivity because of aging and degradation especially in regions of high temperatures and irradiation (neutron and gamma) according to Daw et al. (2012). While recent advances (Coble et al. 2012a) may be used to monitor sensor drift, techniques to compensate for decreasing sensitivity may be needed to maintain the ability to monitor the materials/components over the long term.

Several NDE technologies have emerged as potential candidates to meet the requirements for early material degradation measurement, especially for creep damage, including micromagnetic techniques such as magnetic Barkhausen noise, ultrasonic non-linear techniques that are sensitive to early-stage material degradation, and electromagnetic methods such as eddy currents, which evaluate changes in material conductivity. These are described in PNNL-22889R0 (Meyer et al. 2013a), and are summarized below.

B.1 Magnetic Barkhausen Noise

The magnetic Barkhausen effect is a result of the magnetic hysteresis of ferromagnetic materials (Jiles 2000; Stupakov et al. 2008). The magnetic flux density (B) in ferromagnetic materials placed in an external applied magnetic field is a function of the applied magnetic field *(H)* and the magnetic permeability (μ): $B = \mu H$, with larger numbers of magnetic domains within the material aligning with the applied field direction with increasing applied field strength. This realignment is, however, not a continuous process, because the presence of dislocations or other damage precursors results in domain wall pinning. Increasing the applied field strength results in abrupt realignment of some domains, and is accompanied by a release of energy that may be detected using a sensing coil (Figure B.1). Studies indicate that the magnetic Barkhausen effect in many materials is primarily from the motion of 180° domains, and its interactions with dislocation tangles (Ranjan et al. 1987a; Krause et al. 1994). The number of Barkhausen counts is given by Ranjan et al. (1987b).

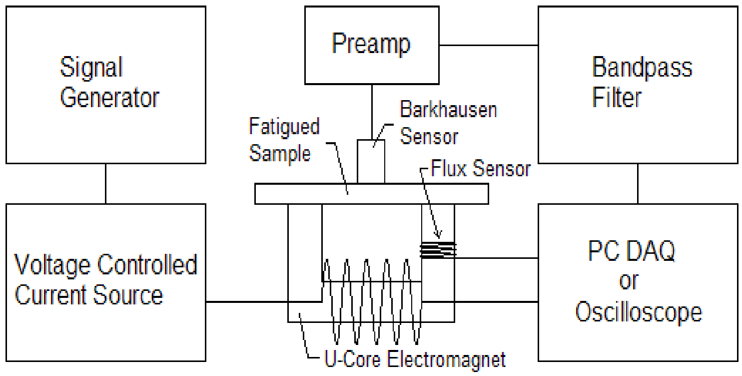

Figure B.1. Schematic of Magnetic Barkhausen Noise Measurement System

In general, two Barkhausen bursts are present—one for positive magnetization and the other for negative magnetization. Numerous models have been developed to predict Barkhausen response to microstructural defects in steels such as grain boundaries and second-phase precipitates (Perez-Benitez et al. 2005; Kameda and Ranjan 1987; Moorthy et al. 1997).

Like all electromagnetic methods, the magnetic Barkhausen method is predominantly a near-surface measurement, with the standard depth of penetration (the distance into the material where the induced current density decreases to 37% of its value at the surface) decreasing with increasing frequency (ASNT 2004). For non-ferritic steel (such as 304 or 316L), the skin depth at 1 kHz is about 13.1 mm.

In many stainless steels, the effect of increasing damage is an increase in dislocation density and/or a change in phase (from austenitic to ferritic). These phenomena combine to impact the Barkhausen noise measurement from steels subjected to aging and degradation. However, the correlation between the measured parameters and the amount of damage is not linear, and is a function of several other variables (such as hardness). The Barkhausen noise measurement method has been applied to determine residual stresses in ferritic steels, the amount of hardening or cold work, and other forms of mechanical damage in materials (Sullivan et al. 2004; Gorkunov et al. 2000; Hakan Gur and Cam 2007; Sagar et al. 2005; Parakka et al. 1997).

Sposito et al. (2010) summarize the results of several efforts to correlate the Barkhausen emission with level of creep damage in ferritic steels. The studies did indicate sensitivity to creep damage through changes in the amplitude of the peak in the Barkhausen emission signal and the value of the magnetic field at which this peak occurs. The Barkhausen response was attributed to several material phenomena such as the formation of precipitates and cavities, the coarsening of precipitates, and grains in the material. It is noted that the formation of oxides on the surface of the material can impact the magnetic Barkhausen response.

In spite of the documented sensitivity of this technique to many forms of degradation, there are multiple sources of uncertainty that impact the interpretation of the resulting measurement. Some of these sources of uncertainty include:

- Location of the measurement relative to the location and orientation of the external stressors.
- Orientation of tensile strain direction, relative to the applied external field direction and the magnetic easy axis (Krause et al. 1995).
- Specimen fabrication variability and residual stress in the specimen (Krause et al. 1995; Lindgren and Lepistö 2001).
- Number, location, and orientation of magnetic domains. In two-phase steels, the volume fraction and distribution of the ferromagnetic phase will affect the measurement (Csikor et al. 2007).
- Probe coupling, and tilt relative to the surface of the specimen. Changes in surface condition with degradation can result in improper probe contact with the specimen and lower the overall measurement.

All of these sources are likely to affect the measurement from high-temperature creep-damaged specimens.

B.2 Ultrasonic Measurements

Acoustic wave propagation in solids is a function of the mechanical properties of the solid (such as density) and is affected by the macro and microstructure. Details of wave propagation in solids, and the impacts of microstructural changes on the measured parameters, are given elsewhere (for instance, Ensminger and Bond 2011; Krautkrämer and Krautkrämer 1990; Goebbels 1994; Doctor et al. 1989; Raj et al. 2000). Traditionally, changes in bulk or guided wave ultrasonic velocity and attenuation have been correlated with microstructural changes from various forms of degradation. Measurement of non-linear elastic wave responses can provide improved sensitivity to accumulated damage. Techniques included in this method can employ:

- Bulk measurements (Cantrell and Yost 2001)
- Rayleigh wave measurements (Shui et al. 2008)
- Guided wave measurements (Bermes et al. 2008).

Non-linear ultrasonics (NLU) techniques are significantly more sensitive to early stages of material damage than conventional linear ultrasonic measurements (Nagy 1998). Conventional ultrasonic methods apply high-frequency (in excess of 500 kHz, typically between 2.25 MHz and 10 MHz) energy and measure the resulting response from scattering and reflection of the energy at interfaces such as crack faces or grain boundaries. The presence of cracking is detected by means of a reflection from the crack surface, or diffraction from crack tips. Other forms of damage (such as creep damage) may be detected by making use of velocity and attenuation measurements through one or more measurement configurations. However, such measurements are not as sensitive to earlier stages of damage. NLU methods rely on the generation of harmonics from a monochromatic input. The generation of harmonics is from nonlinearities in the elastic constants associated with the material (Zarembo and Krasil'nikov 1971). The second harmonic is of particular interest, and the resulting non-linear material parameter is represented by β (Kyung-Young 2000). A schematic of a typical single-sided measurement setup for non-linear acoustics measurements is shown in Figure B.2. Alternative setups use a transmitting probe to transmit acoustic energy through the specimen and a receiving probe on the opposite side of the specimen (through-transmission mode), or rely on the generation of Rayleigh surface waves.

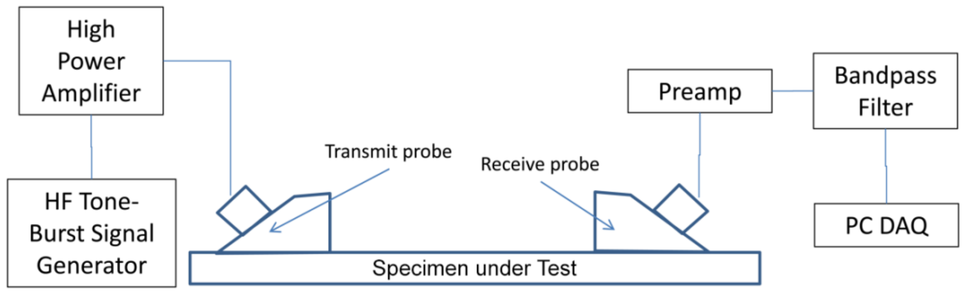

Figure B.2. Schematic of NLU Measurement System

NLU has been applied to the characterization of a range of damage mechanisms, including fatigue (Kyung-Young 2000; Cantrell and Yost 2001), irradiation embrittlement (Matlack et al. 2012b), SCC (Matlack et al. 2012a; Shintaku et al. 2010), and corrosion pitting (De et al. 2010). Sposito et al. (2010) indicate that the non-linear parameter exhibits greater sensitivity to creep damage accumulation than ultrasonic velocity measurements.

B.3 Eddy Currents

Eddy currents are generated in a conducting material by the principle of electromagnetic induction. A coil of wire produces a varying magnetic field when an alternating current is applied to it. The magnetic field of the coil (the primary magnetic field) induces eddy currents in the conducting specimen, which creates a secondary magnetic field in opposition to the primary magnetic field. Because the coil and the conducting specimen are a magnetically coupled system, the electrical impedance of the coil is altered by the electrical properties of the conducting specimen and distance from the coil. The presence of discontinuities in the specimen alters the induced eddy current pattern, further changing the electrical impedance of the coil as measured by the eddy current instrument. Both electrical and magnetic characteristics of the test object are of importance (Libby 1971). Eddy current flow within the test object results in a skin effect, which is a concentration of the current toward the surfaces adjacent to the exciting test coils. The skin depth is a function of the frequency of the exciting field, and electrical conductivity and magnetic permeability of the test material (ASNT 2004), and also governs the measurement of magnetic Barkhausen noise (Section B.1).

Figure B.3 provides a graphical representation of a typical eddy current examination. There are many variations to both coil configurations and coil geometry (ASNT 2004). Probe parameters that influence the depth of penetration of the eddy currents and the impedance of the coil include the wire and coil diameter, number of turns in the coil, and the type of core and shielding material.

Eddy current measurements have been used extensively in the nuclear power industry to examine components such as SG tubing and reactor internals for cracking, corrosion, and other forms of degradation. Because the measurement is a function of test specimen conductivity, eddy current measurements have been applied to also determine the electrical conductivity of specimens. Sposito et al. (2010) discuss the application of eddy currents to assess creep damage and compare its performance with other nondestructive approaches to detecting and assessing creep damage.

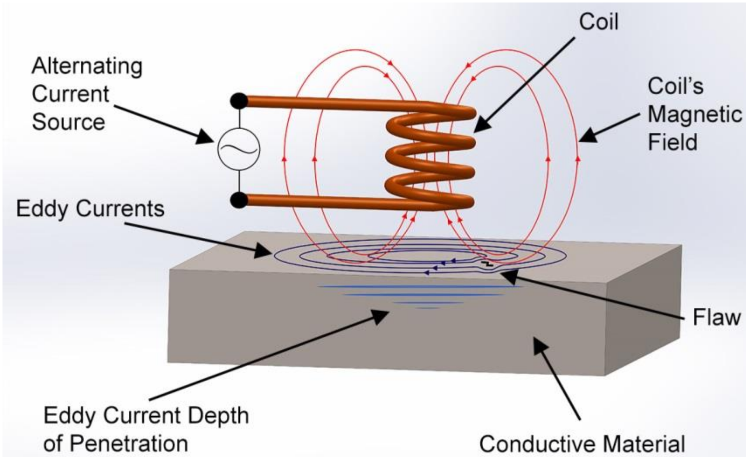

Figure B.3. Graphical Representation of a Typical Eddy Current Examination

B.4 Other NDE Methods

A number of other NDE measurements may be applicable to measure creep degradation (Sposito et al. 2010). These include potential drop measurements, digital image correlation, x-ray diffraction, small-angle neutron scattering, acoustic birefringence, acoustic backscatter, etc. Each of these approaches is sensitive to different aspects of material microstructural changes due to creep damage, although the level of sensitivity varies by technique.

B.5 Harsh-Environment Probes for NDE

Meyer et al. (2013a) discuss various probes that may be used for measurements in harsh environments. For ultrasonic NDE measurements, piezoelectric and electromagnetic acoustic transducer probes are the most common form, with piezoelectric sensing used to measure vibration, acoustic emission, guided ultrasonic waves, non-linear ultrasonic, ultrasonic velocity and attenuation, ultrasonic backscatter, diffuse fields ultrasonic testing, etc. However, the most common piezoelectric material used in ultrasonic probes (lead-zirconate-titanate or PZT) has limited applicability in high-temperature and irradiation environments. Materials considered more suitable for high-temperature transducers include bismuth titanate, modified bismuth titanate, and lead metaniobate (Ensminger and Bond 2011; Daw et al. 2012).

In general, probes used for magnetic measurement are limited by the choice of the magnet material (if any). As with piezoelectric materials, high-temperature applicability may be limited if the Curie temperature of the magnet (at which the magnet loses the ability to be magnetic) is lower than the operational temperature. This impacts measurements such as the magnetic Barkhausen noise measurement, as well as magnetostrictive probes that are used for measuring temperature. In irradiation environments, the activation of elements in typical magnets is a concern. Materials such as cobalt and samarium are readily activated by neutron irradiation and can result in difficulties in handling post-irradiation (such as during probe change-out).

In this research, we assume the availability of harsh-environment probes for online and/or in-situ measurement of the environmental conditions (temperature, flow, pressures, radiation fluence), and nondestructive measurement of material condition. In making this assumption, we expect to leverage ongoing research in this area (Parks and Tittmann 2011; Parks et al. 2010; Zhang et al. 2010; Veilleux et al. 2013; Daw et al. 2013). As a result, the focus of measurements in this research is on using readily available probes and probe materials for laboratory-scale NDE and process measurements.

Appendix C

Bayesian Prognostics Framework

Appendix C

Bayesian Prognostics Framework

C.1 Tracking Filters for Prognostics

Define x_k as the material state at time k. The material state is a numeric quantity that describes the condition of the material in the early stages of damage. Let z_k be the measurement at time k. Further, let $f(\cdot)$ be a state transition (or process) model that defines the relationship between x_k and x_j ($k > j$), and is a mathematical representation of the evolution of damage in the material with time:

$$x_k = f\left(x_j, \sigma_k, \sigma_{k-1}, ... \sigma_j, \eta_k\right) \tag{C.1}$$

where $\sigma_k, \sigma_{k-1}, ..., \sigma_j$ are the stressor values at times k, k–1, … j, with $j < k$, and η_k represents the uncertainty in the state transition model (random process noise). Also, let

$$z_k = h\left(x_k, \nu_k\right) \tag{C.2}$$

relate the material state to the measurements, where the quantity ν_k is used to represent the level of uncertainty in the measurement (again, using random measurement noise).

With this problem setup, the particle filter approach is derived as follows. Given the measurement z_k, the probability density function (PDF) $p(x_k, z_{1:k})$ of the material state x_k conditioned on all measurements up to (and including) z_k, may be obtained recursively using prediction and update stages. The prediction stage uses the system model (Eq. C.1) to predict the PDF forward from one measurement time step to the next. Suppose that the required PDF $p(x_{k-1}|z_{1:k-1})$ at time step $k-1$ is available. The prediction stage obtains the prediction density of the state at k, conditioned on the measurements up to (and including) z_{k-1}, (Ristic et al. 2004) as:

$$p(x_k \mid z_{1:k-1}) = \int p(x_k \mid x_{k-1}) p(x_{k-1} \mid z_{1:k-1}) dx_{k-1} \, . \tag{C.3}$$

For a Markov process of order-one, $p(x_k|x_{k-1}, z_{1:k-1}) = p(x_k|x_{k-1})$. Because the state is usually subject to unknown disturbances (modeled as random process noise η_k), the prediction step translates and distorts the PDF. The update operation uses the latest measurement to modify the prediction PDF, using Bayes' theorem as follows:

$$\begin{aligned} p(x_k \mid z_k) = p(x_k \mid z_k, z_{1:k-1}) &= \frac{p(z_k \mid x_k, z_{1:k-1}) p(x_k \mid z_{1:k-1})}{\int p(z_k \mid \vec{X}) p(\vec{X} \mid z_{1:k-1}) dx_k} \\ &= \frac{p(z_k \mid x_k) p(x_k \mid z_{1:k-1})}{\int p(z_k \mid \vec{X}) p(\vec{X} \mid z_{1:k-1}) dx_k} . \end{aligned} \tag{C.4}$$

In order to apply particle filtering, the posterior PDF $p(x_k|z_k)$ is represented in terms of samples and associated weights w_k^i at each state $x_k = x_k^i$:

$$p(x_k \mid z_k) \approx \sum_{i=1}^{N_s} w_k^i \delta(x_k - x_k^i) \tag{C.5}$$

Here, x_k^i are the samples (or particles) used to represent the posterior density, $i = 1{:}N_s$, where N_s is the total number of samples used and w_k^i is the weight associated with sample x_k^i. The samples are drawn from the prior distribution $p(x_k^i \mid x_{k-1}^i)$. Normalized weights are chosen using the principle of importance sampling (Doucet et al. 2000). If the samples x_k^i were drawn from an importance density, $q(x_{1:k} \mid z_{1:k})$, the weights are given by

$$w_k^i \propto \frac{p(x_{1:k}^i \mid z_{1:k})}{q(x_{1:k}^i \mid z_{1:k})} \tag{C.6}$$

With the reception of measurement z_k at time k, we wish to approximate $p(x_{1:k} \mid z_{1:k})$ with a new set of samples and weights. Given the set of weights w_{k-1} at time $k-1$, the weights at time k may be computed recursively using the weight update equation derived from the principle of importance sampling as

$$w_k^i \propto w_{k-1}^i \frac{p(z_k \mid x_k^i)\, p(x_k^i \mid x_{k-1}^i)}{q(x_k^i \mid x_{k-1}^i, z_k)}. \tag{C.7}$$

The most commonly used variant the of particle filter, known as the sampling-important resampling (SIR) algorithm (Ristic et al. 2004), is used in this study. The importance density in the SIR algorithm is the transitional prior:

$$q(x_k^i \mid x_{k-1}^i, z_k) = p(x_k^i \mid x_{k-1}^i) \tag{C.8}$$

Therefore from Eqs. (C.7) and (C.8),

$$w_k^i \propto w_{k-1}^i p(z_k \mid x_k^i) \tag{C.9}$$

C.2 Model Selection in a Bayesian Prognostics Framework

Mathematically, the Degradation Rate model defines the relationship between degradation levels x_k and x_j ($k > j$) and is a representation of the evolution of damage in the material with time. The model may also include information on stressor history; that is,

$$x_k = f\left(x_j, \sigma_k, \sigma_{k-1}, \ldots \sigma_j, \eta_{k-1}\right) \tag{C.10}$$

where σ_k, $\sigma_{k\text{-}1}, \ldots \sigma_j$, are stressor values at times $k, k\text{–}1, \ldots j$ with $j < k$. In Eq. (C.10), $\eta_{k\text{-}1}$ represents the uncertainty in the state transition model and is typically represented by a PDF. The Measurement Physics model relates the degradation level to the measurements z_k at the present time instant:

$$z_k = h\left(x_k, v_k\right) \tag{C.11}$$

with the quantity v_k representing the level of uncertainty in the relationship between the material condition and the measurement. As with $\eta_{k\text{-}1}$, v_k is generally represented by means of a PDF. Given the measurement z_k, the posterior PDF $p\left(x_k \mid z_{1:k}\right)$ of the material state x_k conditioned on all measurements up to (and including) z_k may be obtained recursively in two stages (Ristic et al. 2004): prediction and update. In particle filtering, the posterior PDF $p\left(x_k \mid z_{1:k}\right)$ is represented in terms of samples and associated weights at each location as:

$$p\left(x_k|z_{1:k}\right) = p\left(x_k|z_k\right) \approx \sum_{i=1}^{N_S} w_k^i \delta(x_k - x_k^i) \tag{C.12}$$

Here, x_k^i $(i = 1, \ldots, N_S)$ are the samples (or particles) used to represent the posterior density of the state, assumed to depend only on the current measurement z_k. N_S is the total number of samples used and w_k^i is the weight associated with sample x_k^i. Normalized weights are chosen using the principle of importance sampling (Doucet et al. 2000). The most commonly used variant of particle filter, SIR algorithm uses transitional prior $p\left(x_k^i|x_{k-1}^i\right)$, as the importance density function. This allows recursive update of the sample weights from time step k–1 to k as (Doucet et al. 2000):

$$w_k^i = w_{k-1}^i p(z_k \mid x_k^i) \tag{C.13}$$

The knowledge of statistical distribution of process uncertainty η_{k-1}, and measurement noise ν_k enables transitional prior $p\left(x_k^i|x_{k-1}^i\right)$, and the likelihood term $p(z_k \mid x_k^i)$ to be deduced from Eqs. (C.10) and (C.11), respectively. For the problem of prognostics, measurements may not be available at all instants. This can be accomplished by simply running the prediction step (using transitional prior) forward for several time steps without the corresponding weight update step. The generic steps for particle filtering-based state estimation or material degradation as implemented in this study can be enumerated as:

1) Generate x_0^i $(i = 1, \ldots, N_S)$ uniformly from known prior P_0, Initialize $w_0^i = 1/N_S; k = 0$.

2) Calculate $\bar{x}_{mean,0} = \frac{1}{N_S}\sum_{i=1}^{N_S} x_0^i$.

3) While $\bar{x}_{mean,k} < Failure\_threshold$ or $k < Max\_time\_steps$, Do:
   - $k = k + 1$.
   - For i taking values between 1 and N_s, Do:
     - Draw a particle $x_k^i \sim p\left(x_k^i|x_{k-1}^i\right)$
     - If measurement update z_k, is available at time instant k:
       - Evaluate importance weights w_k^i using Eq. (C.13).
       - Normalize importance weights for each particle, $w_{k,normalized}^i = w_k^i / \sum_{i=1}^{N_S} w_k^i$.
       - Implement resampling scheme using systematic resampling procedure as described in (Ristic et al. 2004).

$$\overline{x}_{mean,k} = \frac{1}{N_S}\sum_{i=1}^{N_S} x_k^i \tag{C.14}$$

Material state estimation framework, as described hitherto, can be implemented in practice if the material degradation phenomenon is well understood and the degradation rate model is explicitly defined. Quite often it is difficult to characterize, as well as quantify, all the stressors that exist in real operating conditions such as variation in environmental temperatures, loading conditions, pressure profiles, residual stresses, amount of radiation a material is being subjected to, and so on. Material degradation under these unknown stressors can be highly non-linear, which can make it even harder for a single degradation model to track evolution of damage in a material with time. Thus, a combination of different material degradation models that capture changes in different physical properties of the material may inevitably have to be used for accurate and reliable prognostics or material state estimation. In the presence of different material degradation models, it will be imperative for any prognostics algorithm to calculate model posterior probabilities based on the evidence (likelihood) at each measurement update. A wrapper algorithm that provides model posterior probabilities, based on Bayesian framework, will now be developed that can be used in conjunction with the particle filtering algorithm steps as described earlier.

Let $\mathrm{M}_\mathrm{I}^{(k)}$ represents I-th model being considered at time index *k* from a finite set of material degradation models $\boldsymbol{M}:\{M_1, M_2, \ldots M_{Nmodels}\}$ (Guan et al. 2011). Nmodels is the total number of models under consideration. Let $\theta_\mathrm{I}^{(k)}$ represent the model parameters for the I-th model at time index *k*. Let $\mathrm{p}\left(\mathrm{z_k}, \theta_\mathrm{I}^{(k)}, \mathrm{M}_\mathrm{I}^{(k)}\right)$ be defined as the joint probability distribution of model $\mathrm{M}_\mathrm{I}^{(k)}$, model parameters $\theta_\mathrm{I}^{(k)}$, and observed state z_k at time index *k* which can be expressed as

$$p\left(z_k, \theta_\mathrm{I}^{(k)}, M_I^{(k)}\right) = P\left(M_I^{(k)}\right) p\left(\theta_\mathrm{I}^{(k)} | M_I^{(k)}\right) p(z_k | \theta_\mathrm{I}^{(k)}, M_I^{(k)}) \tag{C.15}$$

where $\mathrm{P}\left(\mathrm{M}_\mathrm{i}^{(k)}\right)$ is the probability of $\mathrm{M}_\mathrm{I}^{(k)}$; $\mathrm{p}\left(\theta_\mathrm{I}^{(k)} \mid \mathrm{M}_\mathrm{i}^{(k)}\right)$ is the prior density for the parameter set for $\mathrm{M}_\mathrm{i}^{(k)}$; and $\mathrm{p}\left(\mathrm{z_k} | \theta_\mathrm{I}^{(k)}, \mathrm{M}_\mathrm{I}^{(k)}\right)$ is the posterior distribution of observed state z_k given model $M_I^{(k)}$, and model parameters $\theta_\mathrm{I}^{(k)}$, at time *k*.

$$p\left(z_k, \theta_\mathrm{I}^{(k)}, M_I^{(k)}\right) = P\left(M_I^{(k)}\right) p\left(\theta_\mathrm{I}^{(k)} | M_I^{(k)}\right) p(z_k | \theta_\mathrm{I}^{(k)}, M_I^{(k)}) \tag{C.16}$$

where $\mathrm{P}\left(\mathrm{M}_\mathrm{i}^{(k)}\right)$ is the probability of $\mathrm{M}_\mathrm{I}^{(k)}$; $\mathrm{p}\left(\theta_\mathrm{I}^{(k)} \mid \mathrm{M}_\mathrm{i}^{(k)}\right)$ is the parameter prior for the $\mathrm{M}_\mathrm{i}^{(k)}$; and $\mathrm{p}\left(\mathrm{z_k} | \theta_\mathrm{I}^{(k)}, \mathrm{M}_\mathrm{I}^{(k)}\right)$ is the posterior distribution of observed state z_k given model $M_I^{(k)}$, and model parameters $\theta_\mathrm{I}^{(k)}$, at time index *k*. As discussed in Newton and Raftery (1994b) and Guan et al. (2011), marginal likelihood of observed data z_k under model $M_I^{(k)}$ can be obtained as:

$$P\left(z_k | M_I^{(k)}\right) = \int p\left(z_k | \theta_\mathrm{I}^{(k)}, M_I^{(k)}\right) p\left(\theta_\mathrm{I}^{(k)} | M_I^{(k)}\right) d\theta_i \tag{C.17}$$

According to Bayes theorem, posterior probability of $M_I^{(k)}$ at time index *k* given observed data z_k is defined as:

$$P\left(M_I^{(k)} \mid z_k\right)=\frac{P\left(z_k \mid M_I^{(k)}\right)P(M_I^{(k)})}{P\left(z_k\right)} \tag{C.18}$$

The ratio of posterior probabilities of model $M_I^{(k)}$ and $M_J^{(k)}$ can be used to infer the preference of one model over another based on the measurement update at time index *k* as

$$\frac{P\left(M_I^{(k)} \mid z_k\right)}{P\left(M_J^{(k)} \mid z_k\right)}=\frac{P\left(z_k \mid M_I^{(k)}\right)P(M_I^{(k)})}{P\left(z_k \mid M_J^{(k)}\right)P(M_J^{(k)})} \tag{C.19}$$

Considering an additive normal distribution for $\eta_{k\text{-}1}$, ν_k, and a linear *h* (one-to-one mapping of the measurements with the states) in Eq. (C.11), the probabilistic description of the measurements z_k, given model $M_I^{(k)}$ can be expressed as

$$p\left(z_k \mid \theta_{\mathrm{I}}^{(\mathrm{k})}, M_I^{(k)}\right)=\mathrm{N}\left(f(x_j,\sigma_k,\sigma_{k-1},\ldots,\sigma_j),\eta_{k-1}^2+\nu_k^2\right) \tag{C.20}$$

Eq. (C.20) can be used to evaluate the marginal likelihood integral specified in Eq. (C.17) using Monte Carlo-based importance sampling schemes. As mentioned in Newton and Raftery (1994a), the following two estimates of marginal likelihood are possible based on the nature of importance sampling distributions.

$$\hat{P}_{Prior}\left(z_k \mid M_I^{(k)}\right)=\frac{1}{m}\sum_{j=1}^{m}p\left(z_k \mid \theta_{I,J}^{(k)}, M_I^{(k)}\right) \tag{C.21}$$

$$\hat{P}_{Posterior}\left(z_k \mid M_I^{(k)}\right)=\left[\frac{1}{m}\sum_{j=1}^{m}\left\{p\left(z_k \mid \theta_{I,J}^{(k)}, M_I^{(k)}\right)\right\}^{-1}\right]^{-1} \tag{C.22}$$

where $\hat{P}_{Prior}\left(z_k \mid M_I^{(k)}\right)$ is the estimate of the marginal likelihood using samples $\theta_{I,J}^{(k)}:(J=1,2,\ldots,m)$ from the prior distribution $p\left(\theta_{\mathrm{I}}^{(\mathrm{k})} \mid M_I^{(k)}\right)$, whereas $\hat{P}_{Posterior}\left(z_k \mid M_I^{(k)}\right)$ is the marginal likelihood estimate using the samples from the posterior distribution $p\left(\theta_{\mathrm{I}}^{(\mathrm{k})} \mid M_I^{(k)}, z_k\right)$. Both estimates approach to the true $P\left(z_k \mid M_I^{(k)}\right)$ as $m \to \infty$. It should be noted, however, that the marginal likelihood estimate has to be obtained for each model in the finite model set $\mathscr{M}$ to calculate the preference of one model over another, at each measurement update. This may become computationally expensive as size of $\mathscr{M}$ increases (*Nmodels* $\gg$ 1). An alternate approach to calculate posterior model probabilities is to consider model itself as a variable (Guan et al. 2011). Eq. (C.16) can be re-expressed as:

$$p\left(\theta_{\mathrm{I}}^{(\mathrm{k})}, M_I^{(k)} \mid z_k\right)=\frac{p\left(z_k \mid \theta_{\mathrm{I}}^{(\mathrm{k})}, M_I^{(k)}\right)p\left(\theta_{\mathrm{I}}^{(\mathrm{k})} \mid M_I^{(k)}\right)}{P\left(z_k\right)} \tag{C.23}$$

A standard MCMC simulation using Metropolis-Hastings (M-H) algorithm (Hastings 1970) can be used to obtain samples of $p\left(\theta_I^{(k)}, M_I^{(k)} \mid z_k\right)$ if all models in set $\mathcal{M}$ have their parameters belonging to the same dimensional space. Green (1995) had proposed a reversible jump MCMC (RJMCMC) approach, which removes the restriction on the dimensional space of the model parameters. Basically, it allows trans-dimensional moves (move across models with varying dimensional parameters) within the standard MCMC simulation and simplifies the evaluation of model posterior probabilities to a great extent by using only one simulation instance for the entire model set $\mathcal{M}$.

In this study, a specific implementation of automatic RJMCMC, as described in Guan et al. (2011) and , is used to evaluate posterior model probabilities at each measurement update. Material state estimation is obtained using particle filtering algorithm as discussed earlier. Furthermore, a model averaging procedure is incorporated wherein the state trajectory estimation is obtained using the weighted average of each model in the set $\mathcal{M}$, the weights are the model posterior probabilities obtained using the automatic RJMCMC algorithm at the latest measurement update. Thus a wrapper code is developed to calculate posterior model probabilities at each measurement update, and the results are used in the previously discussed particle filtering-based state estimation or material degradation algorithm to obtain damage evolution over time. A schematic representation of this approach is shown in Figure C.1.

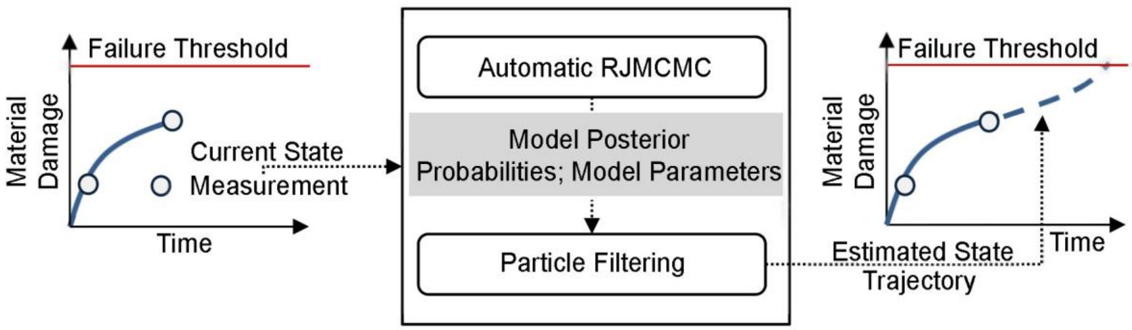

Figure C.1. Schematic of Material State Estimation Using Automatic RJMCMC and Particle Filtering Method

The implementation steps of the wrapper code to calculate model posterior probabilities at each measurement update z_k are enumerated as follows

1. Initialize burn-in samples N_{burn}, and total number of samples N_{total} for the RJMCMC chain.
2. Initialize model transition probabilities $T_{Nmodels \times Nmodels}$ wherein T_{IJ} refers to the probability of moving from model I to model J; $I,J = 1,2,\ldots,Nmodels$.
3. Initialize model prior probability $P\left(M_I^{(k)}\right)$, and model parameters $\theta_I^{(k)}$ for $k = 0$.
4. Begin with $count = 1$; $I = 1$; $Model\_Index(count) = I$.
5. While $count \leq N_{burn} + N_{total}$, Do
   - $count = count + 1$;
   - Generate a random number from uniform distribution $u_{model} \sim U(0,1)$. Construct a CDF vector using I-th row of model transition probability matrix $T_{Nmodels \times Nmodels}$ such that $\mathrm{CDF}(\mathrm{p}) = \sum_{a=1}^{p} T_{Ia}; p = 1,2,\ldots,Nmodels$. Select model index J such that $u_{model} < \mathrm{CDF(J)}$.

- If $I = J$
  - *Model_Index(count) = I.*
  - Perform within-model MCMC move by generating a sample from the posterior distribution $p\left(\theta_{\mathrm{I}}^{(\mathrm{k})}, M_I^{(k)} | z_k\right)$ as shown in Eq. (C.23) using standard M-H algorithm.

Else
  - Perform pilot MCMC runs for each model using $N_{burn}^{'} = 0.5 N_{burn}$ and $N_{total}^{'} = 0.5 N_{total}$, and construct $1 \times n_I$-dimensional mean vector μ_I and covariance matrix Σ_I from the resulting MCMC samples. Obtain B_I such that $B_I B_I^T = \Sigma_I$
  - Generate $u \sim p(u) = \aleph\left(0, \sigma_u^2\right)$; u is a random quantity used for dimensional matching such that $u = | n_J - n_I |$.
  - Calculate: $\theta_{\mathrm{J}}^{(\mathrm{k})} = \begin{Bmatrix} \mu_J + [(\theta_{\mathrm{I}}^{(\mathrm{k})} - \mu_I) B_I^{-1}]_{n_J} B_J; \quad n_J < n_I \\ \mu_J + [(\theta_{\mathrm{I}}^{(\mathrm{k})} - \mu_I) B_I^{-1}] B_J; \quad n_J = n_I \\ \mu_J + \left[(\theta_{\mathrm{I}}^{(\mathrm{k})} - \mu_I\right) B_I^{-1}, u] B_J; \quad n_J > n_I \end{Bmatrix}$
  - Calculate acceptance probability as: $\alpha_{IJ} = min\left\{1, \frac{p\left(\theta_{\mathrm{I}}^{(\mathrm{k})}, M_I^{(k)} | z_k\right) T_{JI}\, p(u) |\mathrm{B}_J|}{p\left(\theta_{\mathrm{J}}^{(\mathrm{k})}, M_J^{(k)} | z_k\right) T_{IJ} |\mathrm{B}_I|}\right\}$ if $n_J > n_I$, else $\alpha_{IJ} = min\left\{1, \frac{p\left(\theta_{\mathrm{I}}^{(\mathrm{k})}, M_I^{(k)} | z_k\right) T_{JI} |\mathrm{B}_J|}{p\left(\theta_{\mathrm{J}}^{(\mathrm{k})}, M_J^{(k)} | z_k\right) T_{IJ}\, p(u) |\mathrm{B}_I|}\right\}$; $|B_I|$ and $|B_J|$ are the determinants of matrices B_I and B_J, respectively.
  - Generate a random number from uniform distribution $u_{test} \sim U(0,1)$.
  - If $\alpha_{IJ} > u_{test}$; *Model_Index(count) = J*, else *Model_Index(count) = I.*

End If

6. Discard the starting N_{burn} samples of the vector *Model_Index*.

At the end of the single simulation instance of the RJMCMC chain, posterior model probabilities can be calculated as (Guan et al. 2011):

$$P\left(M_I^{(k)} | z_k\right) = \frac{N_I}{N_{total} - N_{burn}} \tag{C.24}$$

where N_I is the number of samples in the RJMCMC chain under I-th model. Once the posterior model probabilities are obtained at a specific measurement update, the mean state trajectory estimation at time k is calculated by taking the weighted average of the trajectories obtained under each model

$$\bar{x}_{mean,k} = \frac{1}{N_S} \sum_{I=1}^{Nmodels} P\left(M_I^{(k)} | z_k\right) \sum_{i=1}^{N_S} x_k^i \tag{C.25}$$

Appendix D

Passive Component Ex-situ Testbed for Demonstrating Prognostics

Appendix D

Passive Component Testbed for Demonstrating Prognostics

Prognostic Health Management (PHM) is a proactive maintenance philosophy in which maintenance or repairs to systems or components are performed prior to failure based on models that predict when failure is likely to occur. To predict failure, PHM systems require some type of input about the state of the component(s) of interest. These inputs could be in the form of information on stressors to which the system or component is exposed, or information on the condition of a specific system or component. Thus, measurements and diagnostics, in addition to prognostics, are key elements to a PHM system.

As described in previous reports (Meyer et al. 2013a; Meyer et al. 2013d), PHM for prototypical advanced reactor (AR) passive components will require measurements of component condition in addition to measurements of stressors. In order to evaluate the algorithms at each level of the hierarchy described earlier in this document, testbeds are required to be able to generate relevant data sets (unless such data sets are available through other sources). Given the sequential progression of R&D beginning at the localized level, a laboratory-scale testbed that can be scaled with the different stages of R&D is preferable. A set of requirements for such a testbed are described next.

D.1 Preliminary Requirements for Laboratory-scale Testbed

The laboratory-scale testbed concept must address the need to measure nondestructive evaluation (NDE) data from a representative passive component at multiple length scales—localized, component level, and potentially at a global level. A number of potential requirements for the testbed may be identified based on the need to use the testbed to validate the PHM algorithms, including:

- <u>Materials and degradation</u>: The testbed should be capable of incorporating components made of materials relevant to AR. In addition, as the objective is to evaluate prognostics for degradation accumulation in passive components, the testbed should include degradation modes of relevance to AR.
- <u>Accelerated aging</u>. The time taken to age a specimen should be accelerated when compared to the time taken to field-age specimens. While there is an open question about the applicability of accelerated aging tests to understanding mechanisms of degradation under non-accelerated conditions (i.e., under field-use conditions), the use of accelerated aging tests is expected to provide relevant data applicable for demonstrating prognostic algorithms.
- <u>Simulate operational conditions</u>. The testbed should be capable of simulating operational conditions likely to be seen in AR concepts (such as varying the temperature or load on a component over time).
- <u>Measurements</u>: The testbed should enable periodic or continuous measurements using one or more NDE methods. In addition, measurements of the stressors (temperature, load, etc.) on the materials or components should be enabled. Continuous measurements (of condition or stressors) should be performed synchronously. The measurements may be performed in-situ or ex-situ.
- <u>Scalability</u>. To increase efficiency and reduce costs, the testbed must be capable of addressing PHM evaluation needs at component and global scales with potentially modest changes to the testbed.

D.2 Testbed Concept

D.2.1 Localized Degradation and Measurements

To provide an initial context for the development of prognostics algorithms, high-temperature creep (effect of loads below the yield point for long periods of time, especially at elevated temperatures) was selected as the prototypical degradation mechanism for initial evaluation of prognostics for passive components.

A laboratory-scale creep-test machine was designed as the ex-situ testbed for the first phase of measurements and prognostics. Figure D.1 shows a design schematic for this machine, with the major components highlighted, while Figure D.2 shows a picture of the fabricated creep-test machine. Figure D.3 shows the interface used for control of this testbed. The creep-test machine consists of a mechanical load frame, furnace, 5-ton actuator, power supply enclosure, and control system enclosure. The control system enclosure houses the electronics that run the system, including the motor drive for the stepper motor that is used in conjunction with the 5-ton actuator. The load frame is the base that all components are mounted to, and is based off a 20-ton shop press. The furnace, actuator, and both electrical boxes mount to the load frame. The machine allows the user to specify a force to be applied to the specimen, as well as a temperature for testing. During a test, the machine logs the date, stepper position, sensor position, temperatures, and force applied to a file for future analysis.

A programmable logic controller is used to control the operation of the testbed, and enables independent control of temperature and load. Heating is controlled by means of three control circuits for the heater, with a 5-point thermocouple to control the heat independently in each of the three heater circuits. The load is controlled by means of a 5-ton actuator with a 24:1 gear reduction ball screw, which allows the system to apply a force of 5 tons to the specimen. A stepper motor with a 100:1 gear reduction allows for very precise control of the actuator. A separate position sensor is mounted to the actuator to monitor the position of the actuator.

<u>Materials and Degradation</u>: High-temperature creep is relevant to several of the AR concepts that are being considered, including the liquid-metal and HTGR concepts. The mechanism also enables the verification and validation of several concepts unique to proposed ARs, including multiple phases of degradation that require monitoring, variable loading, and long-term effects in harsh environments. Initial studies are being conducted using austenitic stainless steel, though the testbed may be used with other structural materials of relevance to ARs.

<u>Accelerated Aging and Simulation of Operational Conditions</u>: The ability to independently control temperature and load on a specimen enables the application of different stressor profiles on the test specimen to perform accelerated aging tests as well as simulate stressor profiles for different operational conditions in AR.

ITEM NO.	PART NUMBER	DESCRIPTION	QTY.
1	Press Upright	X	2
2	Foot	X	2
3	Press Top Mount	X	1
4	Universal Mockup	eel Take-Apart Pin & Block Universal Joint 2" Joint Diameter, 5-7/16" Overall Length	1
5	Load Cell	X	1
6	Cold Block	X	2
7	Ball Screw Actuator	X	1
8	Nema 56 Bell Housing	X	1
9	Gearhead	X	1
10	Gearbox Coupling Plate	X	1
11	Shaft Coupler	FLEXIBLE SPIDER COUPLING	1
12	Plate, Actuator	X	1
13	Heater Main Swival Block	X	2
14	Shaft Main Pivot	X	1
15	Heater Pivot Block	X	2
16	Heater	X	1
17	2380K28	Zinc-Plated Steel Two-Piece Clamp-on Collar 1-1/8" Bore, 1-7/8" Outside Diameter, 1/2" Width	6
18	Shaft Heater Pivot	X	1
19	Press Lower Mount	X	1
20	91247A739		4
21	50785K115		1
22	Electrical Box Mount Block	X	4
23	Electrical Box Mount Plate	X	2
24	Electrical SmallBox Mount Plate	X	2
25	Duff Norton Anti Rotation Block	X	1

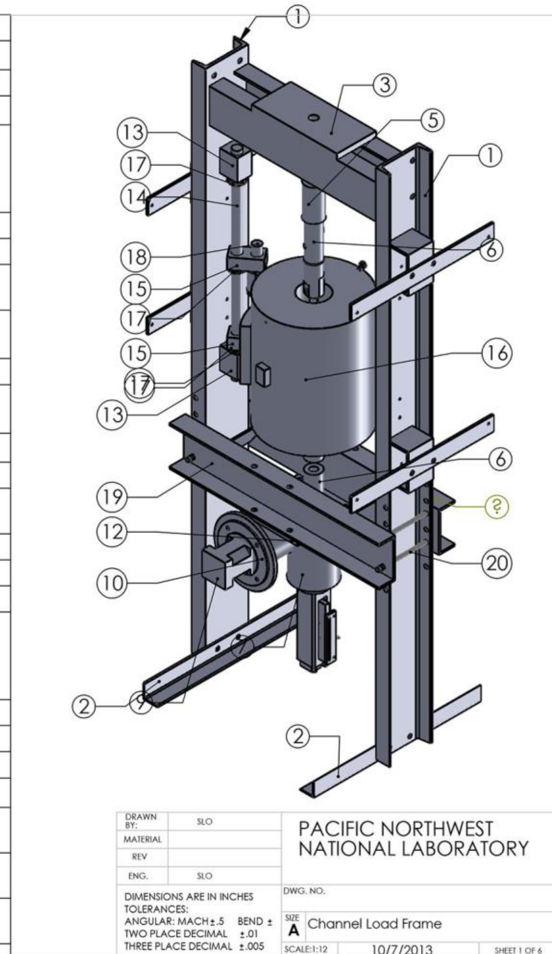

Figure D.1. Design Schematic of Creep-Test Frame

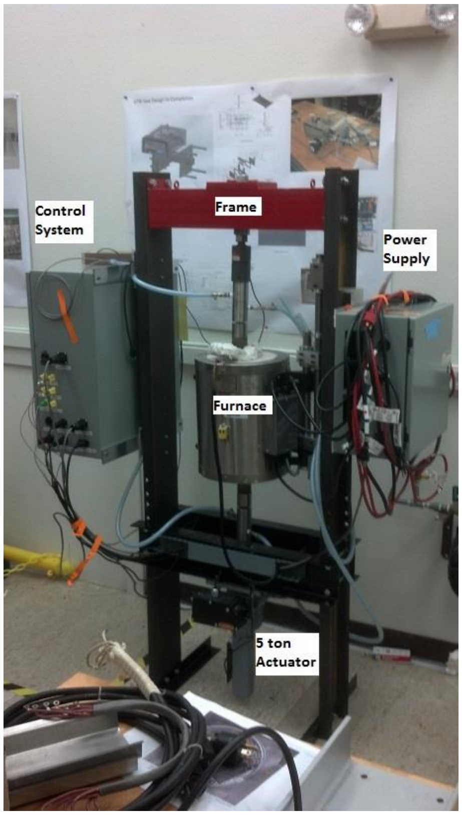

Figure D.2. Laboratory-scale High-temperature Creep-Test Machine

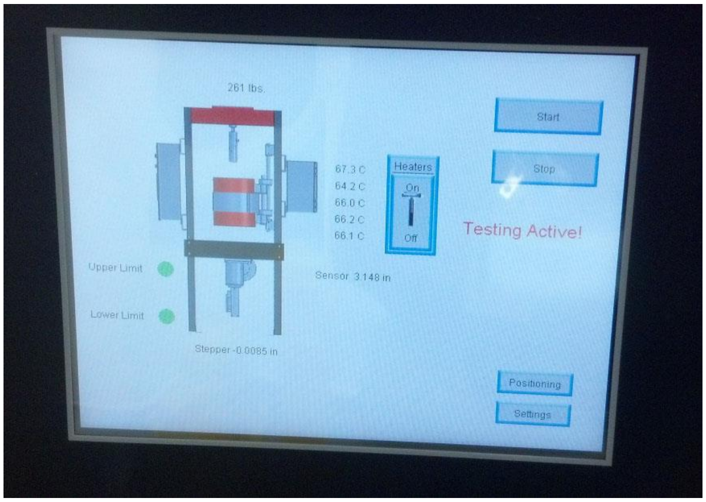

Figure D.3. Main Screen of the User Control Interface for Creep System to Validate Prognostic Algorithms

D.2.2 Ex-situ and In-situ Measurements

Two sets of measurement protocols have been developed. The first of these enables periodic ex-situ condition measurements on specimens in the creep testbed. Each specimen is placed in the testbed and subjected to elevated temperatures and loading for a prescribed time period. After this time, the specimen is unloaded, allowed to cool, and NDE measurements are performed. The specimen may be either re-inserted into the ex-situ testbed after the measurements (for an additional cycle of creep testing, followed by more measurements), or set aside for future destructive testing. NDE measurements that are currently being evaluated include:

1) Non-linear ultrasonic testing
2) Ultrasonic through-transmission testing
3) Eddy current
4) Magnetic Barkhausen emission
5) Digital measurements of thickness and width
6) Linear strain assessment using a Smartscope

The second protocol enables periodic in-situ condition measurements on specimens in the creep testbed using ultrasonic methods. Each specimen has two ultrasonic probes attached on either end. Each specimen is placed in the testbed and subjected to elevated temperatures and loading for a prescribed time period. During this process, ultrasonic measurements are collected at specified intervals using pre-determined parameters by pulsing one of the ultrasonic probes and receiving the resulting response on the second probe. After this time, the specimen is unloaded, and allowed to cool. The specimen may be either re-inserted into the in-situ testbed after the measurements (for an additional cycle of creep testing, followed by more measurements), or set aside for future destructive testing.

As described earlier, measurements of the stressor variables (temperature, load, position) are also recorded and time-stamped.

D.2.3 Component-scale and Global-scale Measurements

The creep testbed is flexible enough to be modified for future component-scale and system-scale measurements. Specifically, we plan to augment the system to eventually incorporate a small-scale flow-loop that includes the ability to change (and monitor) temperature, loading, and chemistry. Figure D.4 presents a simplified concept diagram for such an extension, and shows a tube-within-a-tube arrangement that may be used for inducing localized degradation (such as corrosion or creep) while studying its effects on component- or system-level measurements (such as flow-induced vibration). The diagram does not show a furnace or heat source; however, such a source may be included through the use of induction or resistance heating, or a conventional furnace.

As the testbed grows to include component- or system-level features, additional measurements will be needed to evaluate the ability to measure and monitor the growth of degradation in larger-scale test specimens. For this purpose, accelerometers and acoustic emission sensors will be used to augment the periodic localized measurements listed above. In the example of concentric tubes, the sensors may be placed inside the inner tube to protect them from a corrosive environment in the space between the tubes. Other measurement techniques (and sensor locations) will be evaluated as needed.

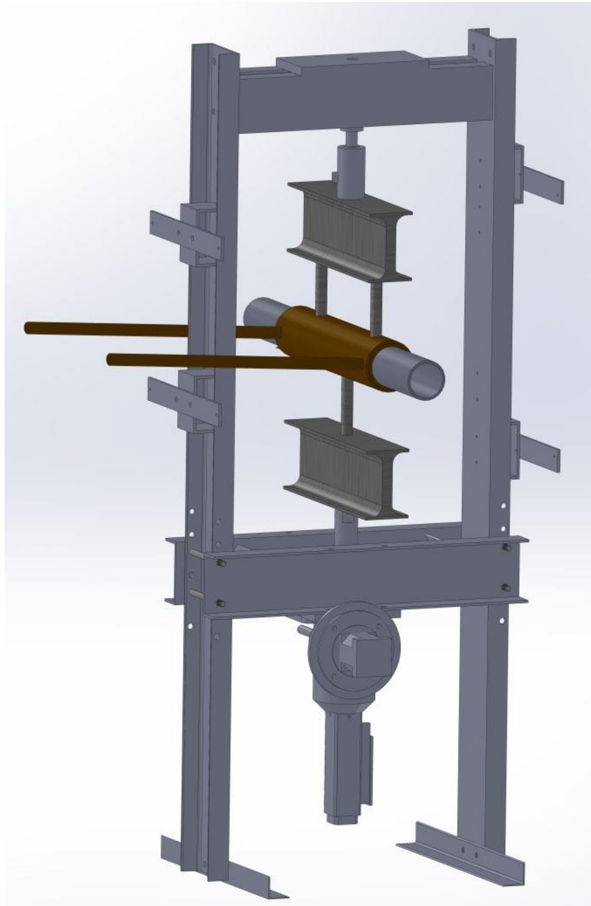

Figure D.4. Concept Drawing, Showing A Potential Modification to Creep Testbed, to Enable Testing of Scaled Versions of Components

D.3 Summary

A testbed concept has been developed to acquire condition and process measurements for evaluating the proposed hierarchical PHM system and associated prognostics algorithms. Two versions of this testbed, one allowing ex-situ measurements and the second enabling in-situ measurements, for evaluating prognostics based on localized measurements has been built and are currently in use. Future modifications to this testbed are envisioned to address measurement needs at component- and global-system levels.

www.pnnl.gov

Pacific Northwest
NATIONAL LABORATORY

Proudly Operated by **Battelle** *Since 1965*

U.S. DEPARTMENT OF
ENERGY

902 Battelle Boulevard
P.O. Box 999
Richland, WA 99352
1-888-375-PNNL (7665)